Doctoral Thesis

Projective-Symmetry-Group Analysis of Majorana-Spinon-Mediated Raman Scattering in Kitaev Spin Balls

(Kitaev スピン・ボールにおける Majorana スピノン媒介 Raman 散乱の拡張対称操作群による解析)

Taku Kimura

Department of Physics, Graduate School of Science, Hokkaido University

March, 2021

Contents

1 Introduction **4**

2 Kitaev Spin Balls **6**

2.1 Fermionization 6

2.2 Projection operators 10

2.3 Gauge transformation 12

3 Projective Symmetry Group for Gauge-Ground Kitaev Spin Balls **13**

3.1 Projective symmetry operation 13

3.2 Irreducible representations of double groups 17

3.3 Direct-product representations of double groups 23

3.4 PSG characterization of Majorana excitation spectra 28

4 Majorana-Spinon-Mediated Raman Scattering **31**

4.1 Raman response of the Kitaev quantum spin liquid 31

4.2 Raman intensity at absolute zero: Point-symmetry argument 33

4.3 Raman intensity at absolute zero: projective-symmetry argument 42

4.4 Raman intensity at finite temperatures 43

5 Summary and Discussion **46**

Appendix A Time Reversal Symmetry for Kitaev Model **49**

Appendix B Projection Operator Eliminating Unphysical States **50**

Acknowledgement

I would like to express my sincere gratitude to Professor Shoji Yamamoto for his many valuable ideas, critical discussions and helpful suggestions. I have learnt almost all my knowledge about physics from his papers, lectures and many pieces of discussion. I would like to acknowledge Professor Hiroshi Amitsuka, Professor Hiroyuki Yamase and Dr. Jun Ohara for many valuable comments in the review process of this thesis. I would like to thank all members of Mathematical Physics for their encouragements. In particular, I thank Dr. Yusaku Noriki and Mr. Kosuke Suzuki for their collaboration and useful discussions. Finally, I would like to appreciate my family and all my friends for warm encouragements.

Abstract

Projective symmetry groups are applied to Raman observations of the Kitaev quantum spin liquids in spherical lattice geometries realized by Platonic and Archimedean polyhedra. Parton single excitations in Kitaev spin polyhedra are characterized by double-valued irreducible representations of their belonging projective symmetry groups, whereas parton geminate excitations relevant to Raman scattering are decomposed into single-valued irreducible representations of the corresponding point symmetry groups. We combine a standard point-symmetry-group analysis of the Loudon-Fleury vertices and an elaborate projective-symmetry-group analysis of itinerant spinons against the ground gauge fields to reveal *hidden selection rules* for Raman scattering in $\mathbb{Z}_2$ spin liquids.

1 Introduction

The Kitaev honeycomb model [1] sparked a brandnew interest in quantum spin liquids (QSLs) [2–5]. It is exactly solvable to have a QSL ground state accompanied by $\mathbb{Z}_2$ gauge fields, whose excitations are fractional, decomposing into itinerant “spinons" and local gapped “visons". Jackeli and Khaliullin [6] designed Mott insulators in the strong spin-orbit coupling limit for the Kitaev model [see. Fig. 1], leading to many candidate materials such as Na_2IrO_3 [7], α-Li_2IrO_3 [8], $H_3LiIr_2O_6$ [9], and α-$RuCl_3$ [10]. The pure Kitaev model is hard to realize but often accompanied by not only usual Heisenberg interactions, whether intralayer [11, 12] or interlayer [13–16], but also off-diagonal exchanges referred to as the Γ term [17–19]. Since fractional excitations remain possible in such “effective" Kitaev models [4, 5, 20–29], inelastic-neutron-scattering [30–33], x-ray-absorption [10], and Raman-scattering [34] measurements have been performed on them in an attempt to diagnose QSLs. Raman spectroscopy is particularly useful in detecting spinons separately from visons [24, 25, 35].

The Kitaev QSL is realizable with any lattice of coordination number three. β-Li_2IrO_3 [36] and γ-Li_2IrO_3 [37], consisting of “hyperhoneycomb" [38, 39] and “stripyhoneycomb" [40] lattices, respectively, are such candidates in three dimensions. While they both exhibit gapless spinon excitations coming from nodal rings, the degeneracy of the Fermi level strongly depends on the lattice geometry in general. A normal Fermi surface is emergent in a “hyperoctagon" lattice [41, 42], whereas it reduces to what they call Weyl points in “hypernonagon" [42, 43] and “hyperhexagon" [42, 44] lattices.

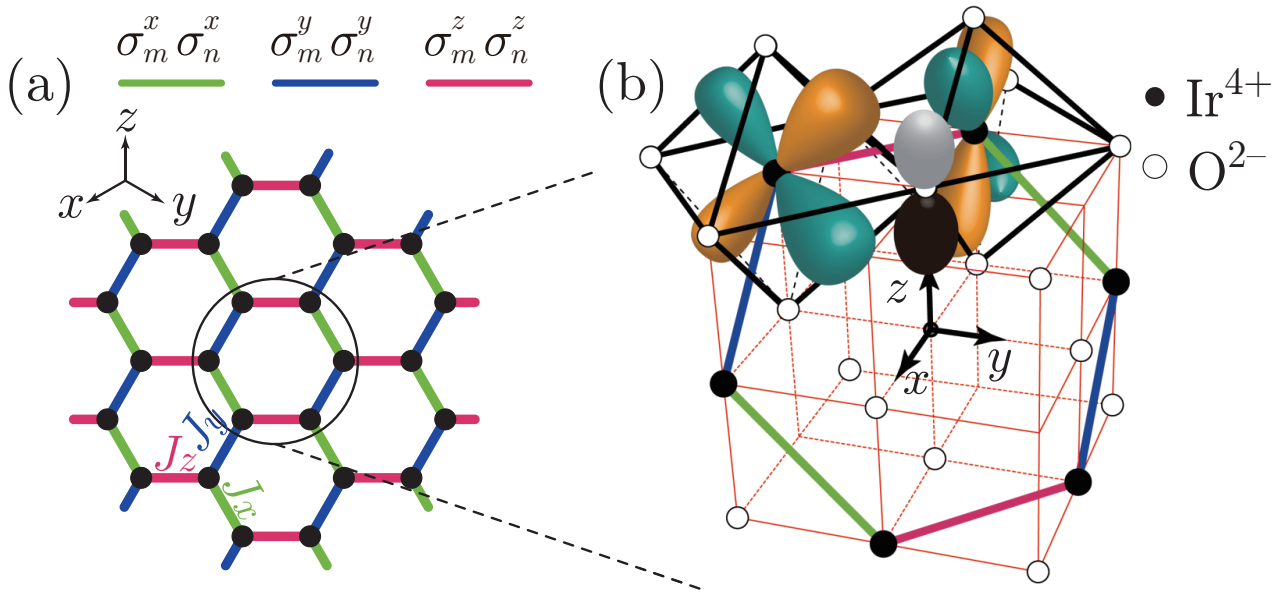

Fig. 1: (a) Kitaev honeycomb model. Green, blue, and red bonds denote $\sigma^x_m\sigma^x_n$, $\sigma^y_m\sigma^y_n$, and $\sigma^z_m\sigma^z_n$ interactions, respectively. (b) The schematic picture of the mechanism for realizing Kitaev-type interaction in iridates [6].

Spinon excitations may be gapped from the ground state [42]. Kitaev models in lower than two dimensions also attract much interest. Kitaev honeycomb nanoribbons with both zigzag and armchair edges are discussed in an attempt to optically distinguish between different topological phases [45] and investigated with particular interest in a bulk-edge correspondence [46], i.e. a possible relation between gapped states in the bulk and gapless states in the boundary. A Kitaev spin ladder maps onto a one-dimensional p-wave superconductor in terms of Dirac fermions to reveal the equivalence between spontaneous global $\mathbb{Z}_2$ symmetry breaking and emergent isolated Majorana modes [47], while that with inhomogeneous exchange interactions exhibits coexistent different topological phases with Majorana end states inbetween [48].

In such circumstances, Mellado, Petrova, and Tchernyshyov (MPT) [49] discuss the Kitaev spin model in a spherical lattice geometry realized by Archimedean solids. Analyzing the projective symmetry [50, 51] of the gauge-ground Majorana fermionic Hamiltonian (cf. Sec. 3) rather than the point symmetry of the background lattice, they claim that a parton behaves like an electrically charged particle in a radial (monopole) magnetic field within the continuum—in the sense of a perfect sphere—approximation. This parton has a *half-odd-integral* orbital angular momentum due to the magnetic monopole located at the center of the cluster.

Motivated by the MPT theory, we present a symmetry argument of optical observations of "Kitaev spin balls"—QSLs in a spherical lattice geometry realized by Platonic and Archimedean polyhedra (cf. Fig. 2). Since Raman scattering within the Loudon-Fleury (LF) scheme [52–54] is mediated by spinons in pair, we make direct-product representations out of irreducible representations of the corresponding projective symmetry group and then decompose them into irreducible representations again. In order to reveal how each spinon geminate excitation behaves under spatial inversion, which is vitally important in the context of Raman scattering, we go so far as to take *gauged inversion*, if any, as well as gauged rotations, into the projective symmetry. *Kitaev spin balls made only of* $2l$*-sided polygons* ($l \in \mathbb{N}$) require such an elaborate formulation, namely, making direct-product representations of the *extended* binary polyhedral group, i.e. the double cover of the *full* icosahedral or octahedral group, to obtain *inversion-symmetry-definite* single-valued irreducible representations.

2 Kitaev Spin Balls

2.1 Fermionization

The Kitaev Hamiltonian (Fig. 2) reads

$$\mathscr{H} = -\sum_{\lambda=x,y,z}\sum_{<m,n>_\lambda} J_\lambda \sigma_m^\lambda \sigma_n^\lambda, \tag{2.1}$$

where $(\sigma_l^x, \sigma_l^y, \sigma_l^z)$ $(l = 1, \cdots, L)$ are the Pauli matrices and $< m, n >_\lambda$ $(\lambda = x, y, z)$ each run over a different set of $L/2$ nearest-neighbor bonds between the λ components. We set this model in various polyhedral geometries, i.e. on dodecahedral, truncated-tetrahedral, and truncated-octahedral lattices, whose point symmetry groups are given by $\mathbf{I}_\mathrm{h} = \mathbf{I} \times \mathbf{C}_\mathrm{i}$, $\mathbf{T}_\mathrm{d} = \mathbf{T} + IC_4\mathbf{T}$, and $\mathbf{O}_\mathrm{h} = \mathbf{O} \times \mathbf{C}_\mathrm{i} = \mathbf{T}_\mathrm{d} \times \mathbf{C}_\mathrm{i}$, respectively. J_x, J_y, and J_z are all set to $J > 0$ in the following.

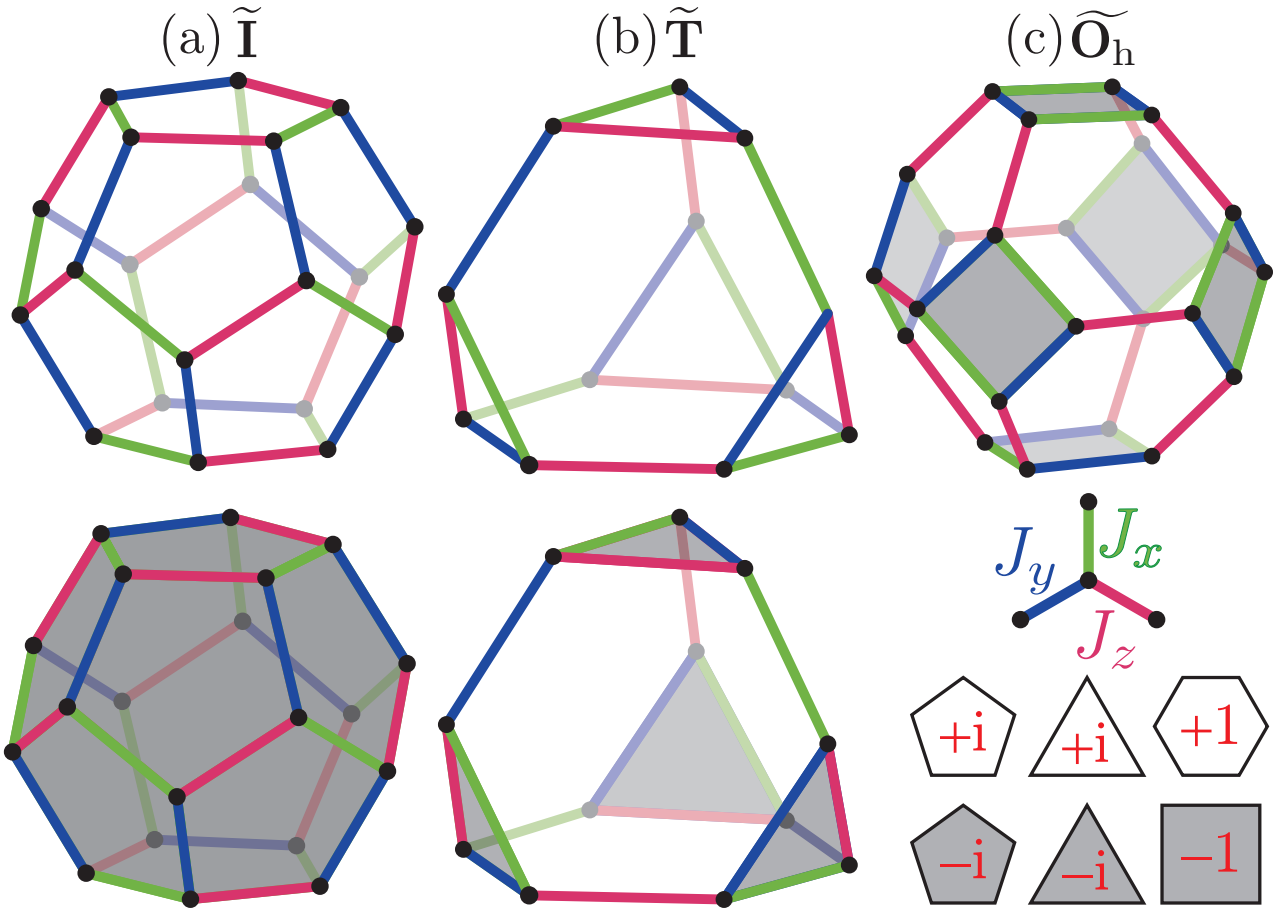

Fig. 2: Kitaev spin balls consisting of dodecahedral (a), truncated tetrahedral (b), and truncated octahedral (c) lattices in their ground flux configurations. The ground state of the truncated octahedron is unique, whereas those of the dodecahedron and truncated tetrahedron are both degenerate [55] with their constituent pentagons arrangeable into either $\{W_p = +i;\, p = 1, \cdots, 12\}$ or $\{W_p = -i;\, p = 1, \cdots, 12\}$ and triangles arrangeable into either $\{W_p = +i;\, p = 1, \cdots, 4\}$ or $\{W_p = -i;\, p = 1, \cdots, 4\}$.

By representing the spin operators in terms of four Majorana fermions, $\sigma_l^\lambda = i\eta_l^\lambda c_l$, with anticommutation relations between them, $\{\eta_m^\mu, \eta_n^\nu\} = 2\delta_{mn}\delta_{\mu\nu}$, $\{c_m, c_n\} = 2\delta_{mn}$, and $\{\eta_m^\lambda, c_n\} = 0$, and then introducing bond operators,

$$\hat{u}_{<m,n>_\lambda} \equiv i\eta_m^\lambda \eta_n^\lambda = \hat{u}^\dagger_{<m,n>_\lambda} = -\hat{u}_{<n,m>_\lambda}, \tag{2.2}$$

the spin Hamiltonian (2.1) is rewritten into

$$\mathscr{H} = iJ \sum_{\lambda=x,y,z} \sum_{<m,n>_\lambda} \hat{u}_{<m,n>_\lambda} c_m c_n. \tag{2.3}$$

Since $[\hat{u}_{<m,n>_\lambda}, \mathscr{H}] = 0$ and $\hat{u}^2_{<m,n>_\lambda} = 1$, $\hat{u}_{<m,n>_\lambda}$ reads a $\mathbb{Z}_2$ classical variable, $u_{<m,n>_\lambda} = \pm 1$. Numbering the constituent polygons of a polyhedra, $p = 1, \cdots, \frac{L}{2}+2$, we define a flux operator [1,56] for each by multiplying its N_p spin operators in the anticlockwise manner viewed from the outside of the polyhedron,

$$\begin{aligned} \hat{W}_p \equiv e^{i\hat{\Phi}_p} &= \prod_{<m,n>_\lambda \in \partial p} \sigma_m^\lambda \sigma_n^\lambda \\ &= (-i)^{N_p} \prod_{<m,n>_\lambda \in \partial p} \hat{u}_{<m,n>_\lambda}. \end{aligned} \tag{2.4}$$

$\hat{W}_p$ also commutes with (2.3) and thus behaves as a classical variable, $W_p = \pm 1$ or $\pm i$ according as N_p is even or odd. A U(1) gauge flux, $W_p \equiv e^{i\Phi_p}$ $(-\pi < \Phi_p \leq \pi)$, pierces the constituent polygon p. Every Kitaev spin ball consists of $\frac{L}{2}+2$ gauged polygons with their flux variables satisfying $\prod_{p=1}^{\frac{L}{2}+2} W_p = 1$. The Hilbert space of the spin Hamiltonian (2.1) is block-diagonal with respect to flux configurations $\{W_p\}$, consisting of $2^{\frac{L}{2}+1}$ blocks of dimension $2^{\frac{L}{2}-1} \times 2^{\frac{L}{2}-1}$, while that of the augmented Majorana Hamiltonian (2.3) is block-diagonal with respect to bond configurations $\{u_{<m,n>_\lambda}\}$ as well as $\{W_p\}$, consisting of $2^{\frac{3L}{2}}$ blocks of dimension $2^{\frac{L}{2}} \times 2^{\frac{L}{2}}$. Four Majorana fermions at each site have 2^{2L} degrees of freedom, containing "unphysical states" [57, 58] to be projected out by the operator [57–60]

$$\mathscr{P} = \prod_{l=1}^{L} \frac{1}{2}(1 + \eta_l^x \eta_l^y \eta_l^z c_l). \tag{2.5}$$

We explain the projection operation and its effect on calculation of physical quantity in Sec. 2.2 and Appendix B.

Once a set of the $3L/2$ gauge fields $\{u_{<m,n>_\lambda}\}$ is given, we have a Majorana quadratic Hamiltonian to be solved,

$$\begin{aligned} \mathscr{H} &= \frac{i}{2} \sum_{m=1}^{L} \sum_{n=1}^{L} \mathcal{H}_{mn} c_m c_n; \\ \mathcal{H}_{mn} &= -\mathcal{H}_{nm} \equiv J u_{<m,n>_\lambda}. \end{aligned} \tag{2.6}$$

The real skew-symmetric matrix $\mathcal{H}$ can be block-diagonalized by a real orthogonal matrix $\mathbf{\Psi}$,

$$\begin{aligned}
&\mathscr{H} = \frac{i}{2}{}^{\mathrm{t}}\boldsymbol{c}\mathbf{\Psi}{}^{\mathrm{t}}\mathbf{\Psi}\mathcal{H}\mathbf{\Psi}{}^{\mathrm{t}}\mathbf{\Psi}\boldsymbol{c} = \frac{i}{2}{}^{\mathrm{t}}\tilde{\boldsymbol{c}}\mathcal{E}\tilde{\boldsymbol{c}} = i\sum_{k=1}^{L/2}\frac{\varepsilon_k}{2}\tilde{c}_{2k-1}\tilde{c}_{2k};\\
&\boldsymbol{c} \equiv \begin{bmatrix} c_1 \\ \vdots \\ c_L \end{bmatrix} = \begin{bmatrix} \psi_{1,1} & \cdots & \psi_{1,L} \\ \vdots & \ddots & \vdots \\ \psi_{L,1} & \cdots & \psi_{L,L} \end{bmatrix}\begin{bmatrix} \tilde{c}_1 \\ \vdots \\ \tilde{c}_L \end{bmatrix} \equiv \mathbf{\Psi}\tilde{\boldsymbol{c}},\\
&\tilde{\boldsymbol{c}} = {}^{\mathrm{t}}\mathbf{\Psi}\boldsymbol{c},\ \mathcal{E} \equiv \frac{1}{2}\begin{bmatrix} 0 & \varepsilon_1 & & & & \\ -\varepsilon_1 & 0 & & & & \\ & & \ddots & & & \\ & & & 0 & \varepsilon_{\frac{L}{2}} \\ & & & -\varepsilon_{\frac{L}{2}} & 0 \end{bmatrix}.
\end{aligned} \tag{2.7}$$

We recomplexify Majorana fermions,

$$\begin{aligned}
&\tilde{c}_{2k-1} = \alpha_k^\dagger + \alpha_k,\ \tilde{c}_{2k} = i\big(\alpha_k^\dagger - \alpha_k\big),\\
&c_l = \sum_{k=1}^{L/2}(\psi_{l,2k-1}\tilde{c}_{2k-1} + \psi_{l,2k}\tilde{c}_{2k})\\
&\quad = \sum_{k=1}^{L/2}\big[(\psi_{l,2k-1} + i\psi_{l,2k})\alpha_k^\dagger + (\psi_{l,2k-1} - i\psi_{l,2k})\alpha_k\big],\\
&\alpha_k = \frac{1}{2}(\tilde{c}_{2k-1} + i\tilde{c}_{2k}) = \frac{1}{2}\sum_{l=1}^{L}(\psi_{l,2k-1} + i\psi_{l,2k})c_l,\\
&\alpha_k^\dagger = \frac{1}{2}(\tilde{c}_{2k-1} - i\tilde{c}_{2k}) = \frac{1}{2}\sum_{l=1}^{L}(\psi_{l,2k-1} - i\psi_{l,2k})c_l,
\end{aligned} \tag{2.8}$$

so as to obtain a diagonal Hamiltonian,

$$\mathscr{H} = \sum_{k=1}^{L/2}\frac{\varepsilon_k}{2}\big(\alpha_k^\dagger\alpha_k - \alpha_k\alpha_k^\dagger\big) = \sum_{k=1}^{L/2}\varepsilon_k\left(\alpha_k^\dagger\alpha_k - \frac{1}{2}\right), \tag{2.9}$$

with nonnegative eigenvalues $\varepsilon_k \geq 0$. Note that all sets of the gauge fields $\{u_{<m,n>_\lambda};\ <m,n>_x, <m,n>_y, <m,n>_z = 1, \cdots, \frac{L}{2}\}$ yielding the same flux configuration $\{W_p;\ p = 1, \cdots, \frac{L}{2}+2\}$ give the same set of eigenvalues $\{\varepsilon_k;\ k = 1, \cdots, \frac{L}{2}\}$ (cf. Sec. 2.2). $\mathscr{P}$ can be expressed in terms of the bond variables $u_{<m,n>_\lambda}$, mixing coefficients $\psi_{l,l'}$, and quasiparticle occupation operators $\alpha_k^\dagger\alpha_k$ to act on quasiparticle (spinon) states labeled background gauge fields $\{u_{<m,n>_\lambda}\}$. Physical (unphysical) spinon states in the ground (lowest-energy) gauge sector consist of even (odd) numbers of emergent spinons $\alpha_k^\dagger\alpha_k$. All the $2^{\frac{3L}{2}}$ gauge sectors each contain $2^{\frac{L}{2}-1}$ physical and $2^{\frac{L}{2}-1}$ unphysical states, each consisting of either only even or only odd numbers of spinons.

The ground flux configurations of Kitaev spin balls (Fig. 2) are such that W_p of every constituent N_p-sided polygon is $+1$, -1, or either of $+i$ and $-i$ according as N_p is $4l+2$, $4l$, or $2l+1$ with $l \in \mathbb{N}$ [49, 56]. With the time-reversal-invariant Hamiltonian (cf. Appendix A), the ground state

is at least doubly degenerate unless all N_p's are even [55]. Considering that the eigenspectrum of (2.3) depends on $\{u_{<m,n>_\lambda}\}$ only through $\{W_p\}$ and W_p's each commute with (2.1) as well as (2.3), we describe the ground state, unless otherwise noted, as the spinon vacuum against a ground flux configuration

$$|\{n_k\}\rangle_0 \otimes |\{W_p\}\rangle_0 \equiv |0\rangle, \tag{2.10}$$

where we denote the κth spinon state against the qth flux configuration by $|\{n_k\}\rangle_\kappa \otimes |\{W_p\}\rangle_q$ ($\kappa = 0, \cdots, 2^{\frac{L}{2}-1} - 1$; $q = 0, \cdots, 2^{\frac{L}{2}+1} - 1$), allowing it to run over physical states only.

2.2 Projection operators

We define a local gauge operator $\hat{D}_l$

$$\hat{D}_l \equiv -i\sigma_l^x\sigma_l^y\sigma_l^z. \tag{2.11}$$

Although $\hat{D}_l$ satisfies

$$\hat{D}_l = -i\underbrace{\sigma_l^x\sigma_l^y}_{=i\sigma_l^z}\sigma_l^z = 1 \tag{2.12}$$

in original spin space, $\hat{D}_l$ has $\mathbb{Z}_2$ eignevalues in enlarged Majorana space:

$$\hat{D}_l \equiv -i\sigma_l^x\sigma_l^y\sigma_l^z = \eta_l^x\eta_l^y\eta_l^z c_l; \quad \hat{D}_l^2 = 1,\ D_l = \pm 1, \tag{2.13}$$

$$\hat{D}_l|\psi\rangle_{\text{phys}} = |\psi\rangle_{\text{phys}}, \qquad \hat{D}_l|\psi\rangle_{\text{unphys}} = -|\psi\rangle_{\text{unphys}}, \tag{2.14}$$

$$|\psi\rangle_{\text{phys}} : \text{physical states}, \quad |\psi\rangle_{\text{unphys}} : \text{unphysical states}.$$

Using $\hat{D}_l$, we can define projection operator from Majorana space to spin space

$$\mathscr{P} = \prod_{l=1}^{L}\left(\frac{1+\hat{D}_l}{2}\right). \tag{2.15}$$

Moreover, $\mathscr{P}$ can be factorized as

$$\mathscr{P} = \left(\frac{1}{2^{L-1}}\sum_{\{l\}}{}' \prod_{l\in\{l\}}\hat{D}_l\right)\left(\frac{1+\prod_{l=1}^{L}\hat{D}_l}{2}\right) \equiv \mathscr{S}\cdot\mathscr{P}_0; \tag{2.16}$$

$$\mathscr{S} \equiv \left(\frac{1}{2^{L-1}}\sum_{\{l\}}{}' \prod_{l\in\{l\}}\hat{D}_l\right), \quad \mathscr{P}_0 \equiv \left(\frac{1+\prod_{l=1}^{L}\hat{D}_l}{2}\right),$$

where $\sum'_{\{l\}}$ indicates that the summation is restricted to half of all possible subset of site indices [57,58,61]. $\mathscr{S}$ is a gage symmetrization operator; $[\hat{W}_p, \mathscr{S}] = 0$, and $\mathscr{P}_0$ is a projection operator that excludes completely unphysical states (cf. Appendix B).

Two states, we denote $|\psi\rangle$ and $|\psi'\rangle$, with the same flux configuration but different bond configuration are connected by the gauge transformations:

$$|\psi'\rangle = \left(\prod_{\{l\}}\hat{D}_l\right)|\psi\rangle. \tag{2.17}$$

Since $\hat{W}_p$ is gage invariant, $[\hat{D}_l, \hat{W}_p] = 0$, $\mathscr{S}$ superimposes wavefunctions with all unequivalent bond configurations with the same $\hat{W}_p$ configurations. Therefore, two states with different bond configurations are connected by the following relation:

$$\mathscr{S}|\psi'\rangle = \mathscr{S}|\psi\rangle. \tag{2.18}$$

Having in mind $[\hat{D}_l, \mathscr{P}] = 0$, all the different bond configurations are mapped to the same physical space.

We consider expected value of the operator $\hat{\mathcal{O}}$ that does not change the $\hat{u}_{<m,n>_\lambda}$ or $\hat{W}_p$. Let $|\widetilde{\psi}\rangle$ and $\widetilde{\psi'}\rangle$ be the states in which the complete unphysical states are excluded from Let $|\psi\rangle$ and $\psi'\rangle$, respectively. The expected value of $\hat{\mathcal{O}}$ can be expressed as

$$\frac{\langle\psi|\mathscr{P}\hat{\mathcal{O}}\mathscr{P}|\psi\rangle}{\langle\psi|\mathscr{P}\mathscr{P}|\psi\rangle} = \frac{\langle\widetilde{\psi}|\mathscr{S}\hat{\mathcal{O}}\mathscr{S}|\widetilde{\psi}\rangle}{\langle\widetilde{\psi}|\mathscr{S}\mathscr{S}|\widetilde{\psi}\rangle} = \frac{\langle\widetilde{\psi'}|\mathscr{S}\hat{\mathcal{O}}\mathscr{S}|\widetilde{\psi'}\rangle}{\langle\widetilde{\psi'}|\mathscr{S}\mathscr{S}|\widetilde{\psi'}\rangle} = \frac{\langle\psi'|\mathscr{P}\hat{\mathcal{O}}\mathscr{P}|\psi'\rangle}{\langle\psi'|\mathscr{P}\mathscr{P}|\psi'\rangle}. \tag{2.19}$$

Having in mind $[\mathscr{S}, \hat{\mathcal{O}}] = 0$,

$$\begin{aligned}
\frac{\langle\widetilde{\psi}|\mathscr{S}\hat{\mathcal{O}}\mathscr{S}|\widetilde{\psi}\rangle}{\langle\widetilde{\psi}|\mathscr{S}\mathscr{S}|\widetilde{\psi}\rangle} &= \frac{\langle\widetilde{\psi}|\hat{\mathcal{O}}\mathscr{S}\mathscr{S}|\widetilde{\psi}\rangle}{\langle\widetilde{\psi}|\mathscr{S}\mathscr{S}|\widetilde{\psi}\rangle} = \frac{\langle\widetilde{\psi}|\hat{\mathcal{O}}\mathscr{S}|\widetilde{\psi}\rangle}{\langle\widetilde{\psi}|\mathscr{S}|\widetilde{\psi}\rangle} = \frac{\langle\widetilde{\psi}|\hat{\mathcal{O}}\left(\sum_{i\in\{W_p\}}|\widetilde{\psi}_i\rangle\right)}{\langle\widetilde{\psi}|\left(\sum_{i\in\{W_p\}}|\widetilde{\psi}_i\rangle\right)} \\
&= \frac{\langle\widetilde{\psi}|\hat{\mathcal{O}}|\widetilde{\psi}\rangle}{\langle\widetilde{\psi}|\widetilde{\psi}\rangle}, \qquad (2.20) \\
\frac{\langle\widetilde{\psi'}|\mathscr{S}\hat{\mathcal{O}}\mathscr{S}|\widetilde{\psi'}\rangle}{\langle\widetilde{\psi'}|\mathscr{S}\mathscr{S}|\widetilde{\psi'}\rangle} &= \frac{\langle\widetilde{\psi'}|\hat{\mathcal{O}}\mathscr{S}|\widetilde{\psi'}\rangle}{\langle\widetilde{\psi'}|\mathscr{S}|\widetilde{\psi'}\rangle} = \frac{\langle\widetilde{\psi'}|\hat{\mathcal{O}}\left(\sum_{i\in\{W_p\}}|\widetilde{\psi}_i\rangle\right)}{\langle\widetilde{\psi'}|\left(\sum_{i\in\{W_p\}}|\widetilde{\psi}_i\rangle\right)} \\
&= \frac{\langle\widetilde{\psi'}|\hat{\mathcal{O}}|\widetilde{\psi'}\rangle}{\langle\widetilde{\psi'}|\widetilde{\psi'}\rangle}, \qquad (2.21) \\
\therefore \frac{\langle\widetilde{\psi}|\hat{\mathcal{O}}|\widetilde{\psi}\rangle}{\langle\widetilde{\psi}|\widetilde{\psi}\rangle} &= \frac{\langle\widetilde{\psi'}|\hat{\mathcal{O}}|\widetilde{\psi'}\rangle}{\langle\widetilde{\psi'}|\widetilde{\psi'}\rangle}. \qquad (2.22)
\end{aligned}$$

That is, *the expected value is independent on the bond configurations unless an operator $\hat{\mathcal{O}}$ changes $\hat{W}_p$ or $\hat{u}_{<m,n>_\lambda}$ configurations.*

2.3 Gauge transformation

As a preliminary step to the analysis of the symmetry group of Majorana Hamiltonian, we discuss the gauge degree of freedom of the Hamiltonian (2.3).

The gauge transformation $\hat{D}_l$, which inverse the sign of $\hat{u}_{<l,l'>_\lambda}$ is complementary expressed by local gauge transformation Λ_l:

$$\begin{aligned} &\Lambda_l = \pm 1, \\ &\begin{cases} \eta_l^x \to \Lambda_l \eta_l^x, \\ \eta_l^y \to \Lambda_l \eta_l^y, \\ \eta_l^z \to \Lambda_l \eta_l^z, \end{cases} \quad c_l \to c_l' \equiv \Lambda_l c_l, \end{aligned} \tag{2.23}$$

$$\hat{u}_{<l,l'>_\lambda} \to \hat{u}'_{<l,l'>_\lambda} \equiv \Lambda_l \hat{u}_{<l,l'>_\lambda} \Lambda_{l'}. \tag{2.24}$$

The spin Hamiltonian in enlarged Majorana space is invariant under the local gauge transformation:

$$\begin{aligned} \mathscr{H} =& iJ_x \sum_{<l,l'>_x} \hat{u}_{<l,l'>_x} c_l c_{l'} + iJ_y \sum_{<l,l'>_y} \hat{u}_{<l,l'>_y} c_l c_{l'} + iJ_z \sum_{<l,l'>_z} \hat{u}_{<l,l'>_z} c_l c_{l'} \\ \overset{\text{Gauge Transformation}}{\longrightarrow}& iJ_x \sum_{<l,l'>_x} \hat{u}'_{<l,l'>_x} c_i' c_{l'}' + iJ_y \sum_{<l,l'>_y} \hat{u}'_{<l,l'>_y} c_i' c_{l'}' + iJ_z \sum_{<l,l'>_z} \hat{u}'_{<l,l'>_z} c_i' c_{l'}' \\ =& iJ_x \sum_{<l,l'>_x} \Lambda_l \hat{u}_{<l,l'>_x} \Lambda_{l'} \Lambda_l c_l \Lambda_{l'} c_{l'} + iJ_y \sum_{<l,l'>_y} \Lambda_l \hat{u}_{<l,l'>_y} \Lambda_{l'} \Lambda_l c_l \Lambda_{l'} c_{l'} \\ &+ iJ_z \sum_{<l,l'>_z} \Lambda_l \hat{u}_{<l,l'>_z} \Lambda_{l'} \Lambda_l c_l \Lambda_{l'} c_{l'} \\ =& iJ_x \sum_{<l,l'>_x} \hat{u}_{<l,l'>_x} c_l c_{l'} + iJ_y \sum_{<l,l'>_y} \hat{u}_{<l,l'>_y} c_l c_{l'} + iJ_z \sum_{<l,l'>_z} \hat{u}_{<l,l'>_z} c_l c_{l'} = \mathscr{H}. \end{aligned} \tag{2.25}$$

When we fix the gauge configuration $\{\hat{u}_{<m,n>_\lambda}\}$, the local-gauge transformation reads $c_l \to \Lambda_l c_l$. This local gauge transformation for itinerant Majorana fermions reads the local gauge transformation for bond operators:

$$\begin{aligned} \mathscr{H} &= iJ_x \sum_{<l,l'>_x} u_{<l,l'>_x} c_l c_{l'} + iJ_y \sum_{<l,l'>_y} u_{<l,l'>_y} c_l c_{l'} + iJ_z \sum_{<l,l'>_z} u_{<l,l'>_z} c_l c_{l'} \\ &\longrightarrow iJ_x \sum_{<l,l'>_x} u_{<l,l'>_x} c_l' c_{l'}' + iJ_y \sum_{<l,l'>_y} u_{<l,l'>_y} c_l' c_{l'}' + iJ_z \sum_{<l,l'>_z} u_{<l,l'>_z} c_l' c_{l'}' \\ &= iJ_x \sum_{<l,l'>_x} (\Lambda_l u_{<l,l'>_x} \Lambda_{l'}) c_l c_{l'} + iJ_y \sum_{<l,l'>_y} (\Lambda_l u_{<l,l'>_y} \Lambda_{l'}) c_l c_{l'} \\ &\quad + iJ_z \sum_{<l,l'>_z} (\Lambda_l u_{<l,l'>_z} \Lambda_{l'}) c_l c_{l'}. \end{aligned} \tag{2.26}$$

That is, the gauge transformation $c_l \to -c_l$ corresponds to inverting all the bonds associated with the l site:

$$u_{<l,l'>_x} \to -u_{<l,l'>_x}, \quad u_{<l,l'>_y} \to -u_{<l,l'>_y}, \quad u_{<l,l'>_z} \to -u_{<l,l'>_z}. \tag{2.27}$$

3 Projective Symmetry Group for Gauge-Ground Kitaev Spin Balls

3.1 Projective symmetry operation

Characterizing Raman scattering mediated by Majorana spinons emergent in the gauge-ground Kitaev truncated octahedron in terms of its projective symmetry group is essentially twofold: first we go further than MPT [49] in obtaining a projective symmetry group for single Majorana eigenmodes, i.e., construct the double cover of the $\mathrm{O}(3)$ superset of a pure rotation group, and then analyze direct-product representations made of its double-valued irreducible representations.

Dodecahedral, truncated-tetrahedral, and truncated-octahedral lattices belong to the point symmetry groups $\mathbf{I}_\mathrm{h}$, $\mathbf{T}_\mathrm{d}$, and $\mathbf{O}_\mathrm{h}$, respectively. We illustrate their symmetry operations with Fig. 3. When we consider Kitaev models on these lattices, their free Majorana fermionic Hamiltonians with given gauge fields are not generally invariant under the point group actions of their belonging lattices. Let us find gauged point symmetry operations of the ground gauge sectors of these Hamiltonians. We illustrate symmetry operations of gauge-ground polyhedra with Fig. 4. Every gauge-ground Kitaev spin ball is such that all W_p's of $N_p = 0 \bmod 4$ are -1, all W_p's of $N_p = 2 \bmod 4$ are $+1$, and all W_p's of odd N_p are either of $+i$ and $-i$ [49]. Since the Kitaev spin Hamiltonian is time reversal invariant, its ground state is at least doubly degenerate unless all N_p's are even [55].

Figure 4(a) illustrates a gauged rotation of the gauge-ground Kitaev dodecahedron. Suppose we rotate it by $\frac{2\pi}{3}$ about one of the threefold axes $\boldsymbol{n}$, which we shall denote by $R(\frac{2\pi}{3}, \boldsymbol{n})$, and then gauge some Majorana fermions as $c_l \to -c_l$, or equivalently, change the signs of their relevant

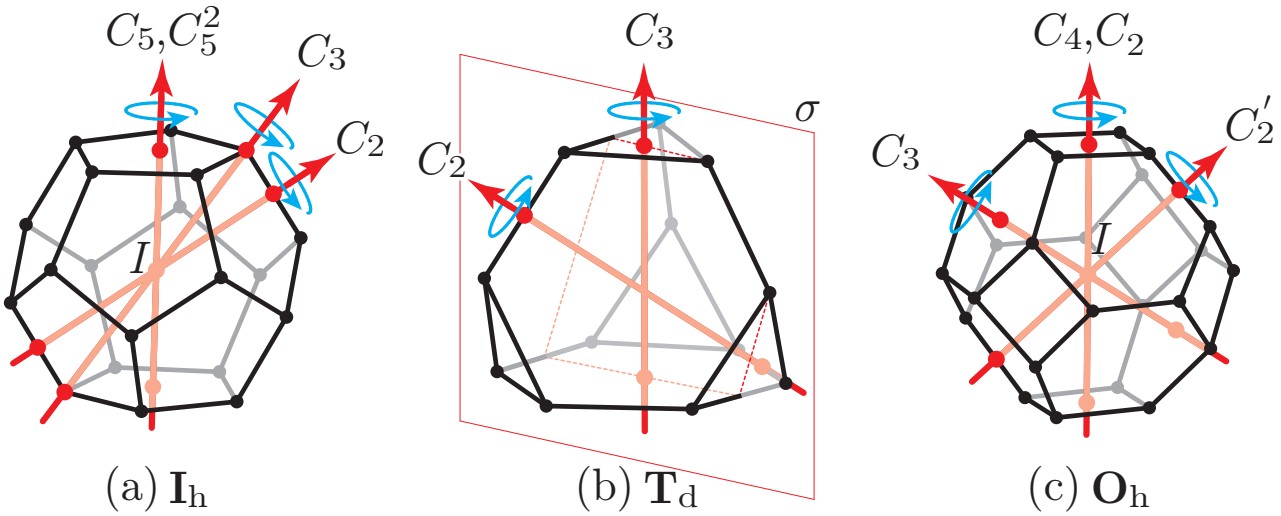

Fig. 3: Point symmetry operations on dodecahedral (a), truncated-tetrahedral (b), and truncated-octahedral (c) lattices belonging to the full icosahedral ($\mathbf{I}_\mathrm{h}$), tetrahedral ($\mathbf{T}_\mathrm{d}$), and octahedral ($\mathbf{O}_\mathrm{h}$) groups, respectively.

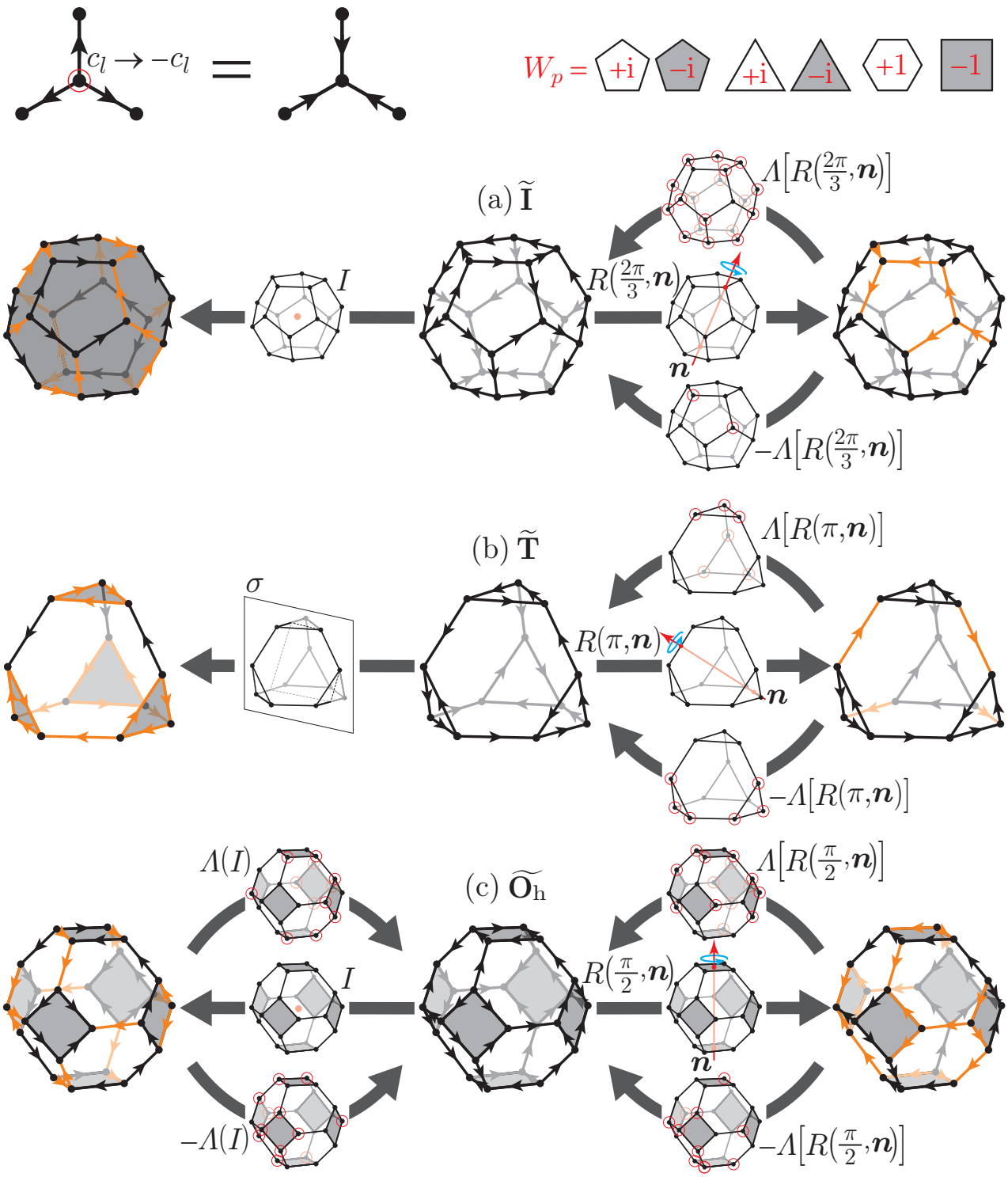

Fig. 4: Gauged rotations, (gauged) inversion, and mirror operations of gauge-ground Kitaev spin balls consisting of dodecahedral (a), truncated-tetrahedral (b), and truncated-octahedral (c) lattices, whose symmetry groups read $\widetilde{\mathbf{I}}$, $\widetilde{\mathbf{T}}$, and $\widetilde{\mathbf{O}_\mathrm{h}}$, respectively. Inversion $I \in \mathbf{I}_\mathrm{h}$ of the gauged dodecahedron and mirror operations $\sigma \in \mathbf{T}_\mathrm{d}$ of the gauged truncated tetrahedron can be followed by no such gauge operation as to recover the initial bond configuration.

bonds as $u_{<l,l'>_\lambda} \to -u_{<l,l'>_\lambda}$ ($\lambda = x, y, z$) (cf. Sec. 2.3), so as to recover the initial bond configuration. When a rotational symmetry operation $R(\varphi, \boldsymbol{n})$ ($0 \le \varphi < 2\pi$) is performed, there exist two such local gauge operations, which we shall denote by $\pm\Lambda\left[R(\varphi, \boldsymbol{n})\right]$ with a reminiscence of the double-valued nature of rotation operators acting on half-integral spin states. In the example of Fig. 4(a), $-\Lambda\left[R(\frac{2\pi}{3}, \boldsymbol{n})\right]$ acts on two sites, while $+\Lambda\left[R(\frac{2\pi}{3}, \boldsymbol{n})\right]$ on all the rest, where we make site assignment to $\pm\Lambda\left[R(\varphi, \boldsymbol{n})\right]$ in accordance with $\mathrm{SU}(2)$ rotations. How many and which sites to operate depend not only on the rotation axis $\boldsymbol{n}$ and angle φ but also the initial bond configuration. We have $2^{\frac{L}{2}+1}$ flux configurations $\{W_p\}$ including the ground two, each available from a set of $2^{\frac{3L}{2}}/2^{\frac{L}{2}+1} = 2^{L-1}$ different bond configurations $\{u_{<m,n>_\lambda}\}$. We denote a couple of these serial transformations as $+\Lambda\left[R(\frac{2\pi}{3}, \boldsymbol{n})\right] R(\frac{2\pi}{3}, \boldsymbol{n}) \equiv \overline{R(\frac{2\pi}{3}, \boldsymbol{n})}$ and $-\Lambda\left[R(\frac{2\pi}{3}, \boldsymbol{n})\right] R(\frac{2\pi}{3}, \boldsymbol{n}) \equiv \underline{R(\frac{2\pi}{3}, \boldsymbol{n})}$. Note that $\left[\overline{R(\frac{2\pi}{3}, \boldsymbol{n})}\right]^3 \{u_{<m,n>_\lambda}\} = -\{u_{<m,n>_\lambda}\}$, while $\left[\underline{R(\frac{2\pi}{3}, \boldsymbol{n})}\right]^3 \{u_{<m,n>_\lambda}\} = \{u_{<m,n>_\lambda}\}$. In the following, we generally denote a couple of gauged point symmetry operations $\pm\Lambda(P)P$ unifiedly as $\widetilde{P}$ and distinguishably by $\overline{P}$ and $\underline{P}$.

Figure 4(a) illustrates inversion of the gauge-ground Kitaev dodecahedron as well, resulting in all W_p's being reversed, $\{W_p = +i;\, p = 1, \cdots, 12\} \to \{W_p = -i;\, p = 1, \cdots, 12\}$. The constituent pentagons each initially have a flux of $\frac{\pi}{2}$ and all their fluxes Φ_p are reversed into $-\Phi_p$ by inversion. The flux variables $W_p \equiv e^{i\Phi_p}$ are also all reversed. Any local gauge transformation $c_l \to -c_l$ results in reversing the signs of bonds in pair in the three surrounding polygons and therefore causes no change in their W_p's. We find that the symmetry group of the gauge-ground Kitaev dodecahedron is not the double cover of the full point symmetry group, $\widetilde{\mathbf{I}}_\mathrm{h}$, but that of an $\mathrm{SO}(3)$ subgroup, $\widetilde{\mathbf{I}}$. This is the case with the gauge-ground Kitaev truncated tetrahedron as well [Fig. 4(b)]. Since a mirror operation $\sigma \in \mathbf{T}_\mathrm{d}$ reverses W_p's of its four constituent triangles, its symmetry group is not $\widetilde{\mathbf{T}_\mathrm{d}}$ but $\widetilde{\mathbf{T}}$. On the other hand, inversion causes no change in W_p's of the gauge-ground truncated octahedron [Fig. 4(c)]. This is because the truncated octahedron consists only of $2l$-sided polygons ($l \in \mathbb{N}$), whose fluxes are either 0 or π. Even though inversion reverses such fluxes as $\Phi_p \to -\Phi_p$, the corresponding flux variables $W_p \equiv e^{i\Phi_p}$ remain unchanged. Any two bond configurations $\{u_{<m,n>_\lambda}\}$ yielding the same set of fluxes $\{W_p\}$ can be converted to each other by local gauge operations. Inversion of the gauge-ground truncated octahedron can be followed by two such local gauge operations as to recover the initial bond configuration, which we shall denote by $\pm\Lambda(I)$, each to act on different halves of the lattice sites. Therefore, the symmetry groups of the gauge-ground Kitaev truncated octahedron is the $\mathbb{Z}_2$-gauge extension of its *full* point symmetry group, $\widetilde{\mathbf{O}_\mathrm{h}}$.

While gauged rotations $\widetilde{R}$ with $R \in \mathbf{O}$ and gauged inversions $\widetilde{I}$ with $I \in \mathbf{C}_\mathrm{i}$ are all symmetry operations of the gauge-ground Kitaev truncated octahedron, they are not necessarily commutable because every gauge transformation $\Lambda(P)$ is obedient to the preceding point symmetry operation P. All the $g^{\widetilde{\mathbf{O}}} \times g^{\widetilde{\mathbf{C}_\mathrm{i}}} + g^{\widetilde{\mathbf{C}_\mathrm{i}}} \times g^{\widetilde{\mathbf{O}}} = 384$ products between the $g^{\widetilde{\mathbf{O}}}$ elements of $\widetilde{\mathbf{O}}$ and the $g^{\widetilde{\mathbf{C}_\mathrm{i}}}$ elements of $\widetilde{\mathbf{C}_\mathrm{i}}$ are indeed symmetry operations of the gauge-ground Kitaev truncated octahedron, but they quadruply count the $g^{\widetilde{\mathbf{O}_\mathrm{h}}} = 96$ elements of $\widetilde{\mathbf{O}_\mathrm{h}} = \widetilde{\mathbf{O}} + \overline{I}\widetilde{\mathbf{O}}$. Note further that the symmetry group of the gauge-ground Kitaev truncated octahedron is different from that of half-integral spins in an

octahedral environment, $\widetilde{\mathbf{O}} \times \mathbf{C}_{\mathrm{i}}$ (cf. Sec. 3.2), where $\widetilde{\mathbf{O}} \subset \mathrm{SU}(2)$, being a double covering group for the pure rotation group $\mathbf{O} \subset \mathrm{SO}(3)$, commutes with $\mathbf{C}_{\mathrm{i}}$ because inversion has no effect on any angular momentum [62]. Therefore, we are now in position to construct the double group $\widetilde{\mathbf{O}_{\mathrm{h}}}$.

3.2 Irreducible representations of double groups

We denote the orders of a point symmetry group $\mathbf{P}$ and its double covering group $\widetilde{\mathbf{P}}$ by $g^{\mathbf{P}}$ and $g^{\widetilde{\mathbf{P}}}$, respectively. Suppose the double cover $\widetilde{\mathbf{P}}$ to be the $\mathbb{Z}_2$-gauge extension of $\mathbf{P} \subset \mathrm{O}(3)$. Two group elements $\widetilde{P}_1 \in \widetilde{\mathbf{P}}$ and $\widetilde{P}_2 \in \widetilde{\mathbf{P}}$ are conjugate when we find such an element $\widetilde{P} \in \widetilde{\mathbf{P}}$ as to satisfy

$$\widetilde{P}_2 = \widetilde{P}\widetilde{P}_1\widetilde{P}^{-1}. \tag{3.1}$$

Every set of conjugate elements forms a class. The classes of the double groups of our interest read

$$\begin{aligned}
\widetilde{\mathbf{I}} :&\{\overline{E}\}, \{\underline{E}\}, \{12\overline{C_5}\}, \{12\underline{C_5}\}, \{12\overline{C_5^2}\}, \{12\underline{C_5^2}\}, \{20\overline{C_3}\}, \{20\underline{C_3}\}, \{15\overline{C_2}, 15\underline{C_2}\};\\
\widetilde{\mathbf{T}} :&\{\overline{E}\}, \{\underline{E}\}, \{3\overline{C_2}, 3\underline{C_2}\}, \{4\overline{C_3}\}, \{4\underline{C_3}\}, \{4\overline{C_3^2}\}, \{4\underline{C_3^2}\};\\
\widetilde{\mathbf{O}} :&\{\overline{E}\}, \{\underline{E}\}, \{6\overline{C_4}\}, \{6\underline{C_4}\}, \{3\overline{C_2}, 3\underline{C_2}\}, \{6\overline{C_2'}, 6\underline{C_2'}\}, \{8\overline{C_3}\}, \{8\underline{C_3}\};\\
\widetilde{\mathbf{O}_{\mathrm{h}}} :&\begin{array}{l}\{\overline{E}\}, \{\underline{E}\}, \{6\overline{C_4}, 6\underline{C_4}\}, \{3\overline{C_2}, 3\underline{C_2}\}, \{6\overline{C_2'}, 6\underline{C_2'}\}, \{8\overline{C_3}\}, \{8\underline{C_3}\},\\ \{\overline{I}, \underline{I}\}, \{6\overline{IC_4}, 6\underline{IC_4}\}, \{3\overline{IC_2}, 3\underline{IC_2}\}, \{6\overline{IC_2'}, 6\underline{IC_2'}\}, \{8\overline{IC_3}\}, \{8\underline{IC_3}\}.\end{array}
\end{aligned}$$

Supposing the qth class $\mathcal{C}_q$ ($q = 1, \cdots, n_{\mathcal{C}}^{\widetilde{\mathbf{P}}}$) of $\widetilde{\mathbf{P}}$ to consist of h_q elements, it reads $\{h_q\overline{P}_q\}$, $\{h_q\underline{P}_q\}$, or $\{\frac{h_q}{2}\overline{P}_q, \frac{h_q}{2}\underline{P}_q\}$.

The number of (complex) irreducible representations equals how many classes are in the group. Since all the single-valued (complex) irreducible representations of $\mathbf{P}$, amounting to $n_{\mathcal{C}}^{\mathbf{P}}$, remain unchanged in $\widetilde{\mathbf{P}}$, we find $n_{\mathcal{C}}^{\widetilde{\mathbf{P}}} - n_{\mathcal{C}}^{\mathbf{P}}$ double-valued (complex) irreducible representations in $\widetilde{\mathbf{P}}$. When we denote the ith (complex) irreducible representation of $\mathbf{P}$ ($\widetilde{\mathbf{P}}$) by Ξ_i ($\widetilde{\Xi}_i$) and its dimensionality by $d_{\Xi_i}^{\mathbf{P}}$ ($d_{\widetilde{\Xi}_i}^{\widetilde{\mathbf{P}}}$), we have

$$\sum_{i=1}^{n_{\mathcal{C}}^{\mathbf{I}}\equiv 5} \left(d_{\Xi_i}^{\mathbf{I}}\right)^2 = g^{\mathbf{I}} = 60, \qquad \sum_{i=1}^{n_{\mathcal{C}}^{\widetilde{\mathbf{I}}}\equiv 9} \left(d_{\widetilde{\Xi}_i}^{\widetilde{\mathbf{I}}}\right)^2 = g^{\mathbf{I}} + \sum_{i=n_{\mathcal{C}}^{\mathbf{I}}+1}^{n_{\mathcal{C}}^{\widetilde{\mathbf{I}}}\equiv 9} \left(d_{\widetilde{\Xi}_i}^{\widetilde{\mathbf{I}}}\right)^2 = g^{\widetilde{\mathbf{I}}} = 120; \tag{3.2}$$

$$\sum_{i=1}^{n_{\mathcal{C}}^{\mathbf{T}}\equiv 4} \left(d_{\Xi_i}^{\mathbf{T}}\right)^2 = g^{\mathbf{T}} = 12, \qquad \sum_{i=1}^{n_{\mathcal{C}}^{\widetilde{\mathbf{T}}}\equiv 7} \left(d_{\widetilde{\Xi}_i}^{\widetilde{\mathbf{T}}}\right)^2 = g^{\mathbf{T}} + \sum_{i=n_{\mathcal{C}}^{\mathbf{T}}+1}^{n_{\mathcal{C}}^{\widetilde{\mathbf{T}}}\equiv 7} \left(d_{\widetilde{\Xi}_i}^{\widetilde{\mathbf{T}}}\right)^2 = g^{\widetilde{\mathbf{T}}} = 24; \tag{3.3}$$

$$\sum_{i=1}^{n_{\mathcal{C}}^{\mathbf{O}}\equiv 5} \left(d_{\Xi_i}^{\mathbf{O}}\right)^2 = g^{\mathbf{O}} = 24, \qquad \sum_{i=1}^{n_{\mathcal{C}}^{\widetilde{\mathbf{O}}}\equiv 8} \left(d_{\widetilde{\Xi}_i}^{\widetilde{\mathbf{O}}}\right)^2 = g^{\mathbf{O}} + \sum_{i=n_{\mathcal{C}}^{\mathbf{O}}+1}^{n_{\mathcal{C}}^{\widetilde{\mathbf{O}}}\equiv 8} \left(d_{\widetilde{\Xi}_i}^{\widetilde{\mathbf{O}}}\right)^2 = g^{\widetilde{\mathbf{O}}} = 48; \tag{3.4}$$

$$\sum_{i=1}^{n_{\mathcal{C}}^{\mathbf{O}_{\mathrm{h}}}\equiv 10} \left(d_{\Xi_i}^{\mathbf{O}_{\mathrm{h}}}\right)^2 = g^{\mathbf{O}_{\mathrm{h}}} = 48, \sum_{i=1}^{n_{\mathcal{C}}^{\widetilde{\mathbf{O}_{\mathrm{h}}}}\equiv 13} \left(d_{\widetilde{\Xi}_i}^{\widetilde{\mathbf{O}_{\mathrm{h}}}}\right)^2 = g^{\mathbf{O}_{\mathrm{h}}} + \sum_{i=n_{\mathcal{C}}^{\mathbf{O}_{\mathrm{h}}}+1}^{n_{\mathcal{C}}^{\widetilde{\mathbf{O}_{\mathrm{h}}}}\equiv 13} \left(d_{\widetilde{\Xi}_i}^{\widetilde{\mathbf{O}_{\mathrm{h}}}}\right)^2 = g^{\widetilde{\mathbf{O}_{\mathrm{h}}}} = 96 \tag{3.5}$$

in an attempt to determine the dimensionalities of the double-valued (complex) irreducible representations $d_{\widetilde{\Xi}_i}^{\widetilde{\mathbf{P}}}$ ($i = n_{\mathcal{C}}^{\mathbf{P}} + 1, \cdots, n_{\mathcal{C}}^{\widetilde{\mathbf{P}}}$). The characters of $\widetilde{\Xi}_i$ are such that

$$\chi_{\widetilde{\Xi}_i}^{\widetilde{\mathbf{P}}}(\overline{P}) = \chi_{\widetilde{\Xi}_i}^{\widetilde{\mathbf{P}}}(\underline{P}) \ (i = 1, \cdots, n_{\mathcal{C}}^{\mathbf{P}}), \tag{3.6}$$

$$\chi_{\widetilde{\Xi}_i}^{\widetilde{\mathbf{P}}}(\overline{P}) = -\chi_{\widetilde{\Xi}_i}^{\widetilde{\mathbf{P}}}(\underline{P}) \ (i = n_{\mathcal{C}}^{\mathbf{P}} + 1, \cdots, n_{\mathcal{C}}^{\widetilde{\mathbf{P}}}). \tag{3.7}$$

When $\overline{P}$ and $\underline{P}$ belong to the same class, i.e., $\chi^{\widetilde{\mathbf{P}}}_{\widetilde{\Xi}_i}(\overline{P}) = \chi^{\widetilde{\mathbf{P}}}_{\widetilde{\Xi}_i}(\underline{P})$, we immediately find

$$\chi^{\widetilde{\mathbf{P}}}_{\widetilde{\Xi}_i}(\overline{P}) = \chi^{\widetilde{\mathbf{P}}}_{\widetilde{\Xi}_i}(\underline{P}) = 0 \; (i = n^{\mathbf{P}}_{\mathcal{C}} + 1, \cdots, n^{\widetilde{\mathbf{P}}}_{\mathcal{C}}). \tag{3.8}$$

The character orthogonality theorems of the first and second kinds read [62]

$$\sum_{q=1}^{n^{\widetilde{\mathbf{P}}}_{\mathcal{C}}} h_q \chi^{\widetilde{\mathbf{P}}}_{\widetilde{\Xi}_i}(\mathcal{C}_q)^* \chi^{\widetilde{\mathbf{P}}}_{\widetilde{\Xi}_j}(\mathcal{C}_q) = g^{\widetilde{\mathbf{P}}} \delta_{ij}, \tag{3.9}$$

$$\sum_{i=1}^{n^{\widetilde{\mathbf{P}}}_{\mathcal{C}}} \chi^{\widetilde{\mathbf{P}}}_{\widetilde{\Xi}_i}(\mathcal{C}_q)^* \chi^{\widetilde{\mathbf{P}}}_{\widetilde{\Xi}_i}(\mathcal{C}_r) = \frac{g^{\widetilde{\mathbf{P}}}}{h_q} \delta_{qr}. \tag{3.10}$$

When we denote the h_q elements of $\mathcal{C}_q$ distinguishably as $\{\widetilde{P}^{(1)}_q, \cdots, \widetilde{P}^{(h_q)}_q\}$, we can define structure constants as

$$\sum_{i=1}^{h_q} \widetilde{P}^{(i)}_q \sum_{j=1}^{h_r} \widetilde{P}^{(j)}_r = \sum_{s=1}^{n^{\widetilde{\mathbf{P}}}_{\mathcal{C}}} c_{qr:s} \sum_{k=1}^{h_k} \widetilde{P}^{(k)}_s \tag{3.11}$$

to have another relation,

$$h_q h_r \chi^{\widetilde{\mathbf{P}}}_{\widetilde{\Xi}_i}(\mathcal{C}_q) \chi^{\widetilde{\mathbf{P}}}_{\widetilde{\Xi}_i}(\mathcal{C}_r) = d^{\widetilde{\mathbf{P}}}_{\widetilde{\Xi}_i} \sum_{s=1}^{n^{\widetilde{\mathbf{P}}}_{\mathcal{C}}} h_s c_{qr:s} \chi^{\widetilde{\mathbf{P}}}_{\widetilde{\Xi}_i}(\mathcal{C}_s). \tag{3.12}$$

With Eqs. (3.8), (3.9), (3.10), and (3.12) in mind, we can obtain characters of both single- and double-valued (complex) irreducible representations of any double group $\widetilde{\mathbf{P}}$, which are listed in Tables 1–4 with particular emphasis on the relation between $\widetilde{\mathbf{P}}$ and $\mathbf{P}$. In the case of Kitaev truncated octahedron, we name the double-valued irreducible representations $\mathrm{G}^{\mathrm{g}}_{\frac{3}{2}}$, $\mathrm{G}^{\mathrm{u}}_{\frac{3}{2}}$, and $\mathrm{G}_{\frac{1}{2}+\frac{5}{2}}$ so that they signify the gerade- or ungerade-like response to a gauged point symmetry operation as well as suggest the compatibility relations between $\widetilde{\mathbf{O}_{\mathrm{h}}}$ and its subgroup $\widetilde{\mathbf{O}}$, $\mathrm{G}_{\frac{1}{2}+\frac{5}{2}} \downarrow \widetilde{\mathbf{O}} = \mathrm{E}_{\frac{1}{2}} \oplus \mathrm{E}_{\frac{5}{2}}$ and $\mathrm{G}^{\mathrm{g}}_{\frac{3}{2}} \downarrow \widetilde{\mathbf{O}} = \mathrm{G}^{\mathrm{u}}_{\frac{3}{2}} \downarrow \widetilde{\mathbf{O}} = \mathrm{G}_{\frac{3}{2}}$, i.e.,

$$\chi^{\widetilde{\mathbf{O}_{\mathrm{h}}}}_{\mathrm{G}_{\frac{1}{2}+\frac{5}{2}}}(\widetilde{P}) = \chi^{\widetilde{\mathbf{O}}}_{\mathrm{E}_{\frac{1}{2}}}(\widetilde{P}) + \chi^{\widetilde{\mathbf{O}}}_{\mathrm{E}_{\frac{5}{2}}}(\widetilde{P}); \tag{3.13}$$

$$\chi^{\widetilde{\mathbf{O}_{\mathrm{h}}}}_{\mathrm{G}^{\mathrm{g}}_{\frac{3}{2}}}(\widetilde{P}) = \chi^{\widetilde{\mathbf{O}}}_{\mathrm{G}_{\frac{3}{2}}}(\widetilde{P}); \; \chi^{\widetilde{\mathbf{O}_{\mathrm{h}}}}_{\mathrm{G}^{\mathrm{g}}_{\frac{3}{2}}}(\widetilde{IC_3}) = \sqrt{3}\chi^{\widetilde{\mathbf{O}_{\mathrm{h}}}}_{\mathrm{G}^{\mathrm{g}}_{\frac{3}{2}}}(\widetilde{C_3}), \tag{3.14}$$

$$\chi^{\widetilde{\mathbf{O}_{\mathrm{h}}}}_{\mathrm{G}^{\mathrm{u}}_{\frac{3}{2}}}(\widetilde{P}) = \chi^{\widetilde{\mathbf{O}}}_{\mathrm{G}_{\frac{3}{2}}}(\widetilde{P}); \; \chi^{\widetilde{\mathbf{O}_{\mathrm{h}}}}_{\mathrm{G}^{\mathrm{u}}_{\frac{3}{2}}}(\widetilde{IC_3}) = -\sqrt{3}\chi^{\widetilde{\mathbf{O}_{\mathrm{h}}}}_{\mathrm{G}^{\mathrm{u}}_{\frac{3}{2}}}(\widetilde{C_3}). \tag{3.15}$$

Table. 1: Irreducible representations of the double group $\widetilde{\mathbf{I}}$ and their characters.

$\widetilde{\mathbf{I}}$	$\mathbf{I}$		$\{\overline{E}\}$	$\{\underline{E}\}$	$\{12\overline{C_5}\}$	$\{12\underline{C_5}\}$	$\{12\overline{C_5^2}\}$	$\{12\underline{C_5^2}\}$	$\{20\overline{C_3}\}$	$\{20\underline{C_3}\}$	$\{15\overline{C_2}, 15\underline{C_2}\}$
		A	1		1		1		1		1
		T_1	3		$\frac{1+\sqrt{5}}{2}$		$\frac{1-\sqrt{5}}{2}$		0		-1
		T_2	3		$\frac{1-\sqrt{5}}{2}$		$\frac{1+\sqrt{5}}{2}$		0		-1
		G	4		-1		-1		1		0
		H	5		0		0		-1		1
		$E_{\frac{1}{2}}$	2	-2	$\frac{1+\sqrt{5}}{2}$	$-\frac{1+\sqrt{5}}{2}$	$-\frac{1-\sqrt{5}}{2}$	$\frac{1-\sqrt{5}}{2}$	1	-1	0
		$E_{\frac{7}{2}}$	2	-2	$\frac{1-\sqrt{5}}{2}$	$-\frac{1-\sqrt{5}}{2}$	$-\frac{1+\sqrt{5}}{2}$	$\frac{1+\sqrt{5}}{2}$	1	-1	0
		$G_{\frac{3}{2}}$	4	-4	1	-1	-1	1	-1	1	0
		$I_{\frac{5}{2}}$	6	-6	-1	1	1	-1	0	0	0

Table. 2: Irreducible representations of the double group $\widetilde{\mathbf{T}}$ and their characters.

$\widetilde{\mathbf{T}}$		$\{\overline{E}\}$	$\{\underline{E}\}$	$\{3\overline{C_2},$ $3\underline{C_2}\}$	$\{4\overline{C_3}\}$	$\{4\underline{C_3}\}$	$\{4\overline{C_3^2}\}$	$\{4\underline{C_3^2}\}$
$\mathbf{T}$	A	1	1	1	1	1	1	1
	E	2	2	2	-1	-1	-1	-1
	$\mathrm{E}^{(1)}$		1	1		$e^{-i\frac{2\pi}{3}}$		$e^{-i\frac{4\pi}{3}}$
	$\mathrm{E}^{(2)}$		1	1		$e^{i\frac{2\pi}{3}}$		$e^{i\frac{4\pi}{3}}$
	T	3	3	-1	0	0	0	0
	$\mathrm{E}_{\frac{1}{2}}$	2	-2	0	1	-1	-1	1
	$\mathrm{G}_{\frac{3}{2}}$	4	-4	0	-1	1	1	-1
	$\mathrm{G}_{\frac{3}{2}}^{(1)}$	2	-2	0	$e^{-i\frac{2\pi}{3}}$	$-e^{-i\frac{2\pi}{3}}$	$-e^{-i\frac{4\pi}{3}}$	$e^{-i\frac{4\pi}{3}}$
	$\mathrm{G}_{\frac{3}{2}}^{(2)}$	2	-2	0	$e^{i\frac{2\pi}{3}}$	$-e^{i\frac{2\pi}{3}}$	$-e^{i\frac{4\pi}{3}}$	$e^{i\frac{4\pi}{3}}$

Table. 3: Irreducible representations of the double group $\widetilde{\mathbf{O}}$ and their characters.

$\widetilde{\mathbf{O}}$		$\{\overline{E}\}$	$\{\underline{E}\}$	$\{6\overline{C_4}\}$	$\{6\underline{C_4}\}$	$\{3\overline{C_2},$ $3\underline{C_2}\}$	$\{6\overline{C_2'},$ $6\underline{C_2'}\}$	$\{8\overline{C_3}\}$	$\{8\underline{C_3}\}$
$\mathbf{O}$	A_1	1	1	1	1	1	1	1	1
	A_2	1	1	-1	-1	1	-1	1	1
	E	2	2	0	0	2	0	-1	-1
	T_1	3	3	1	-1	-1	-1	0	0
	T_2	3	3	-1	1	-1	1	0	0
	$\mathrm{E}_{\frac{1}{2}}$	2	-2	$\sqrt{2}$	$-\sqrt{2}$	0	0	1	-1
	$\mathrm{E}_{\frac{5}{2}}$	2	-2	$-\sqrt{2}$	$\sqrt{2}$	0	0	1	-1
	$\mathrm{G}_{\frac{3}{2}}$	4	-4	0	0	0	0	-1	1

Table. 4: Irreducible representations of the double group $\widetilde{\mathbf{O}_\mathrm{h}}$ and their characters. Those of the direct-product group $\widetilde{\mathbf{O}} \times \mathbf{C}_\mathrm{i}$ are also presented.

		$\{\overline{E}\}$	$\{\underline{E}\}$	$\{6\overline{C_4}, 6\underline{C_4}\}$		$\{3\overline{C_2}, 3\underline{C_2}\}$	$\{6\overline{C_2'}, 6\underline{C_2'}\}$	$\{8\overline{C_3}\}$	$\{8\underline{C_3}\}$	
$\widetilde{\mathbf{O}_\mathrm{h}}$	$\mathbf{O}_\mathrm{h}$	$\mathrm{A_{1g}}$	1		1		1	1	1	$\widetilde{\mathbf{O}}\times\mathbf{C}_\mathrm{i}$
		$\mathrm{A_{2g}}$	1		-1		1	-1	1	
		$\mathrm{E_g}$	2		0		2	0	-1	
		$\mathrm{T_{1g}}$	3		1		-1	-1	0	
		$\mathrm{T_{2g}}$	3		-1		-1	1	0	
		$\mathrm{A_{1u}}$	-1		-1		-1	-1	-1	
		$\mathrm{A_{2u}}$	-1		1		-1	1	-1	
		$\mathrm{E_u}$	-2		0		-2	0	1	
		$\mathrm{T_{1u}}$	-3		-1		1	1	0	
		$\mathrm{T_{2u}}$	-3		1		1	-1	0	
		$\mathrm{G}_{\frac{1}{2}+\frac{5}{2}}$	4	-4	0		0	0	2	-2
		$\mathrm{G}^{\mathrm{g}}_{\frac{3}{2}}$	4	-4	0		0	0	-1	1
		$\mathrm{G}^{\mathrm{u}}_{\frac{3}{2}}$	4	-4	0		0	0	-1	1
			$\{\overline{E}\}$	$\{\underline{E}\}$	$\{6\overline{C_4}\}$	$\{6\underline{C_4}\}$	$\{3\overline{C_2}, 3\underline{C_2}\}$	$\{6\overline{C_2'}, 6\underline{C_2'}\}$	$\{8\overline{C_3}\}$	$\{8\underline{C_3}\}$	
		$\mathrm{E}_{\frac{1}{2}\mathrm{g}}$	2	-2	$\sqrt{2}$	$-\sqrt{2}$	0	0	1	-1	$\widetilde{\mathbf{O}}\times\mathbf{C}_\mathrm{i}$
		$\mathrm{E}_{\frac{5}{2}\mathrm{g}}$	2	-2	$-\sqrt{2}$	$\sqrt{2}$	0	0	1	-1	
		$\mathrm{G}_{\frac{3}{2}\mathrm{g}}$	4	-4	0	0	0	0	-1	1	
		$\mathrm{E}_{\frac{1}{2}\mathrm{u}}$	2	-2	$\sqrt{2}$	$-\sqrt{2}$	0	0	1	-1	
		$\mathrm{E}_{\frac{5}{2}\mathrm{u}}$	2	-2	$-\sqrt{2}$	$\sqrt{2}$	0	0	1	-1	
		$\mathrm{G}_{\frac{3}{2}\mathrm{u}}$	4	-4	0	0	0	0	-1	1	

		$\{\overline{I},\ \underline{I}\}$	$\{6\overline{IC_4},\ 6\underline{IC_4}\}$	$\{3\overline{IC_2},\ 3\underline{IC_2}\}$	$\{6\overline{IC_2'},\ 6\underline{IC_2'}\}$	$\{8\overline{IC_3}\}$	$\{8\underline{IC_3}\}$	
$\widetilde{\mathbf{O}}_{\mathrm{h}}$	$\mathbf{O}_{\mathrm{h}}$							
	$\mathrm{A_{1g}}$	1	1	1	1	1	1	$\widetilde{\mathbf{O}}\times\mathbf{C}_{\mathrm{i}}$
	$\mathrm{A_{2g}}$	1	−1	1	−1	1	1	
	$\mathrm{E_g}$	2	0	2	0	−1	−1	
	$\mathrm{T_{1g}}$	3	1	−1	−1	0	0	
	$\mathrm{T_{2g}}$	3	−1	−1	1	0	0	
	$\mathrm{A_{1u}}$	−1	−1	−1	−1	−1	−1	
	$\mathrm{A_{2u}}$	−1	1	−1	1	−1	−1	
	$\mathrm{E_u}$	−2	0	−2	0	1	1	
	$\mathrm{T_{1u}}$	−3	−1	1	1	0	0	
	$\mathrm{T_{2u}}$	−3	1	1	−1	0	0	
	$\mathrm{G}_{\frac{1}{2}+\frac{5}{2}}$	0	0	0	0	0	0	
	$\mathrm{G}^{\mathrm{g}}_{\frac{3}{2}}$	0	0	0	0	$-\sqrt{3}$	$\sqrt{3}$	
	$\mathrm{G}^{\mathrm{u}}_{\frac{3}{2}}$	0	0	0	0	$\sqrt{3}$	$-\sqrt{3}$	

	$\{\overline{I}\}$	$\{\underline{I}\}$	$\{6\overline{IC_4}\}$	$\{6\underline{IC_4}\}$	$\{3\overline{IC_2},\ 3\underline{IC_2}\}$	$\{6\overline{IC_2'},\ 6\underline{IC_2'}\}$	$\{8\overline{IC_3}\}$	$\{8\underline{IC_3}\}$	
$\mathrm{E}_{\frac{1}{2}\mathrm{g}}$	2	−2	$\sqrt{2}$	$-\sqrt{2}$	0	0	1	−1	$\widetilde{\mathbf{O}}\times\mathbf{C}_{\mathrm{i}}$
$\mathrm{E}_{\frac{5}{2}\mathrm{g}}$	2	−2	$-\sqrt{2}$	$\sqrt{2}$	0	0	1	−1	
$\mathrm{G}_{\frac{3}{2}\mathrm{g}}$	4	−4	0	0	0	0	−1	1	
$\mathrm{E}_{\frac{1}{2}\mathrm{u}}$	−2	2	$-\sqrt{2}$	$\sqrt{2}$	0	0	−1	1	
$\mathrm{E}_{\frac{5}{2}\mathrm{u}}$	−2	2	$\sqrt{2}$	$-\sqrt{2}$	0	0	−1	1	
$\mathrm{G}_{\frac{3}{2}\mathrm{u}}$	−4	4	0	0	0	0	1	−1	

3.3 Direct-product representations of double groups

Since Raman scattering within the LF scheme [24, 52–54] is caused by spinons in pair, we make direct-product representations out of double-valued irreducible representations of double covers $\widetilde{\mathbf{P}}$ of the corresponding point symmetry groups $\mathbf{P} \subset \mathrm{O}(3)$. Direct-product representations of a nonabelian group are not necessarily irreducible even though the constituent representations are irreducible. We take interest in spinon-geminate-excitation-relevant direct-product representations $\widetilde{\Xi}_i \otimes \widetilde{\Xi}_j \, (i,j = n_{\mathcal{C}}^{\mathbf{P}} + 1, \cdots, n_{\mathcal{C}}^{\widetilde{\mathbf{P}}})$ of $\widetilde{\mathbf{P}}$, which are decomposed into single-valued irreducible representations of the corresponding point symmetry group $\mathbf{P}$,

$$\widetilde{\Xi}_i \otimes \widetilde{\Xi}_j = \bigoplus_{k=1}^{n_{\mathcal{C}}^{\widetilde{\mathbf{P}}}} \widetilde{\Xi}_k \sum_{q=1}^{n_{\mathcal{C}}^{\widetilde{\mathbf{P}}}} \frac{h_q}{g^{\widetilde{\mathbf{P}}}} \chi^{\widetilde{\mathbf{P}}}_{\widetilde{\Xi}_k}(\mathcal{C}_q)^* \chi^{\widetilde{\mathbf{P}}}_{\widetilde{\Xi}_i \otimes \widetilde{\Xi}_j}(\mathcal{C}_q) = \bigoplus_{k=1}^{n_{\mathcal{C}}^{\mathbf{P}}} \Xi_k \sum_{q=1}^{n_{\mathcal{C}}^{\widetilde{\mathbf{P}}}} \frac{h_q}{g^{\widetilde{\mathbf{P}}}} \chi^{\mathbf{P}}_{\Xi_k}(\mathcal{C}_q)^* \chi^{\widetilde{\mathbf{P}}}_{\widetilde{\Xi}_i \otimes \widetilde{\Xi}_j}(\mathcal{C}_q), \quad (3.16)$$

having in mind that

$$\chi^{\widetilde{\mathbf{P}}}_{\widetilde{\Xi}_i \otimes \widetilde{\Xi}_j}(\overline{P}) = \chi^{\widetilde{\mathbf{P}}}_{\widetilde{\Xi}_i}(\overline{P}) \chi^{\widetilde{\mathbf{P}}}_{\widetilde{\Xi}_j}(\overline{P}) = \chi^{\widetilde{\mathbf{P}}}_{\widetilde{\Xi}_i}(\underline{P}) \chi^{\widetilde{\mathbf{P}}}_{\widetilde{\Xi}_j}(\underline{P}) = \chi^{\widetilde{\mathbf{P}}}_{\widetilde{\Xi}_i \otimes \widetilde{\Xi}_j}(\underline{P}) \; (i,j = n_{\mathcal{C}}^{\mathbf{P}} + 1, \cdots, n_{\mathcal{C}}^{\widetilde{\mathbf{P}}}). \quad (3.17)$$

Direct-product representations made of the two same irreducible representations consist of symmetric (bosonic) and antisymmetric (fermionic) parts,

$$\widetilde{\Xi}_i \otimes \widetilde{\Xi}_i = [\widetilde{\Xi}_i \otimes \widetilde{\Xi}_i] \oplus \{\widetilde{\Xi}_i \otimes \widetilde{\Xi}_i\}, \quad (3.18)$$

which are decomposed into symmetric and antisymmetric single-valued irreducible representations of the corresponding point symmetry group $\mathbf{P}$, respectively,

$$[\widetilde{\Xi}_i \otimes \widetilde{\Xi}_i] = \bigoplus_{k=1}^{n_{\mathcal{C}}^{\mathbf{P}}} [\Xi_k] \sum_{q=1}^{n_{\mathcal{C}}^{\widetilde{\mathbf{P}}}} \frac{h_q}{g^{\widetilde{\mathbf{P}}}} \chi^{\mathbf{P}}_{\Xi_k}(\mathcal{C}_q)^* \chi^{\widetilde{\mathbf{P}}}_{[\widetilde{\Xi}_i \otimes \widetilde{\Xi}_i]}(\mathcal{C}_q), \quad (3.19)$$

$$\{\widetilde{\Xi}_i \otimes \widetilde{\Xi}_i\} = \bigoplus_{k=1}^{n_{\mathcal{C}}^{\mathbf{P}}} \{\Xi_k\} \sum_{q=1}^{n_{\mathcal{C}}^{\widetilde{\mathbf{P}}}} \frac{h_q}{g^{\widetilde{\mathbf{P}}}} \chi^{\mathbf{P}}_{\Xi_k}(\mathcal{C}_q)^* \chi^{\widetilde{\mathbf{P}}}_{\{\widetilde{\Xi}_i \otimes \widetilde{\Xi}_i\}}(\mathcal{C}_q). \quad (3.20)$$

Note that characters of symmetric and antisymmetric direct-product representations are given by

$$\chi^{\widetilde{\mathbf{P}}}_{[\widetilde{\Xi}_i \otimes \widetilde{\Xi}_i]}(\widetilde{P}) = \frac{1}{2} \left[\chi^{\widetilde{\mathbf{P}}}_{\widetilde{\Xi}_i}(\widetilde{P})^2 + \chi^{\widetilde{\mathbf{P}}}_{\widetilde{\Xi}_i}(\widetilde{P}^2) \right], \quad (3.21)$$

$$\chi^{\widetilde{\mathbf{P}}}_{\{\Xi_i \otimes \Xi_i\}}(\widetilde{P}) = \frac{1}{2} \left[\chi^{\widetilde{\mathbf{P}}}_{\widetilde{\Xi}_i}(\widetilde{P})^2 - \chi^{\widetilde{\mathbf{P}}}_{\widetilde{\Xi}_i}(\widetilde{P}^2) \right]. \quad (3.22)$$

We can obtain characters of any direct-product representation using Eqs. (3.21) and (3.22) as well as (3.17), which of our interest are listed in Tables 5–8. Direct-product representations for geminate excitations of different Majorana spinon eigenmodes are not necessarily made of different irreducible representations but may be made of the same ones. Those made of different irreducible representations can be decomposed into irreducible representations by Eq. (3.16), while those made of the same ones by Eqs. (3.19) and (3.20). Direct-product representations for geminate excitations of degenerate Majorana spinon eigenmodes are also the latter case. The thus-obtained decompositions into irreducible representations are all listed in Table 9.

Table. 5: Direct-product representations made of double-valued irreducible representations of the double group $\widetilde{\mathbf{I}}$ and their characters.

$\widetilde{\Xi}_i \otimes \widetilde{\Xi}_j$	$\{\overline{E}\}$ $\{\underline{E}\}$	$\{12\overline{C_5}\}$ $\{12\underline{C_5}\}$	$\{12\overline{C_5^2}\}$ $\{12\underline{C_5^2}\}$	$\{20\overline{C_3}\}$ $\{20\underline{C_3}\}$	$\{15\overline{C_2}, 15\underline{C_2}\}$
$[\mathrm{I}_{\frac{5}{2}} \otimes \mathrm{I}_{\frac{5}{2}}]$	21	1	1	0	-3
$\{\mathrm{I}_{\frac{5}{2}} \otimes \mathrm{I}_{\frac{5}{2}}\}$	15	0	0	0	3
$\mathrm{I}_{\frac{5}{2}} \otimes \mathrm{G}_{\frac{3}{2}}$	24	-1	-1	0	0
$[\mathrm{G}_{\frac{3}{2}} \otimes \mathrm{G}_{\frac{3}{2}}]$	10	0	0	1	-2
$\{\mathrm{G}_{\frac{3}{2}} \otimes \mathrm{G}_{\frac{3}{2}}\}$	6	1	1	0	2
$[\mathrm{E}_{\frac{1}{2}} \otimes \mathrm{E}_{\frac{1}{2}}]$	3	$\frac{1+\sqrt{5}}{2}$	$\frac{1-\sqrt{5}}{2}$	0	-1
$\{\mathrm{E}_{\frac{1}{2}} \otimes \mathrm{E}_{\frac{1}{2}}\}$	1	1	1	1	1
$\mathrm{E}_{\frac{1}{2}} \otimes \mathrm{E}_{\frac{7}{2}}$	4	-1	-1	1	0
$\mathrm{E}_{\frac{1}{2}} \otimes \mathrm{G}_{\frac{3}{2}}$	8	$\frac{1+\sqrt{5}}{2}$	$\frac{1-\sqrt{5}}{2}$	-1	0
$\mathrm{E}_{\frac{1}{2}} \otimes \mathrm{I}_{\frac{5}{2}}$	12	$-\frac{1+\sqrt{5}}{2}$	$-\frac{1-\sqrt{5}}{2}$	0	0
$[\mathrm{E}_{\frac{7}{2}} \otimes \mathrm{E}_{\frac{7}{2}}]$	3	$\frac{1-\sqrt{5}}{2}$	$\frac{1+\sqrt{5}}{2}$	0	-1
$\{\mathrm{E}_{\frac{7}{2}} \otimes \mathrm{E}_{\frac{7}{2}}\}$	1	1	1	1	1
$\mathrm{E}_{\frac{7}{2}} \otimes \mathrm{G}_{\frac{3}{2}}$	8	$\frac{1-\sqrt{5}}{2}$	$\frac{1+\sqrt{5}}{2}$	-1	0
$\mathrm{E}_{\frac{7}{2}} \otimes \mathrm{I}_{\frac{5}{2}}$	12	$-\frac{1-\sqrt{5}}{2}$	$-\frac{1+\sqrt{5}}{2}$	0	0

Table. 6: Direct-product representations made of double-valued irreducible representations of the double group $\widetilde{\mathbf{T}}$ and their characters.

$\widetilde{\Xi}_i \otimes \widetilde{\Xi}_j$	$\{\overline{E}\}$	$\{\underline{E}\}$	$\{3\overline{C_2}, 3\underline{C_2}\}$	$\{4\overline{C_3}\}$	$\{4\underline{C_3}\}$	$\{4\overline{C_3^2}\}$	$\{4\underline{C_3^2}\}$
$[\mathrm{G}^{(2)}_{\frac{3}{2}} \otimes \mathrm{G}^{(2)}_{\frac{3}{2}}]$	3		-1	0		0	
$\{\mathrm{G}^{(2)}_{\frac{3}{2}} \otimes \mathrm{G}^{(2)}_{\frac{3}{2}}\}$	1		1	$e^{-i\frac{2}{3}\pi}$		$e^{-i\frac{4}{3}\pi}$	
$\mathrm{G}^{(2)}_{\frac{3}{2}} \otimes \mathrm{E}_{\frac{1}{2}}$	4		0	$e^{-i\frac{4}{3}\pi}$		$e^{-i\frac{2}{3}\pi}$	
$[\mathrm{E}_{\frac{1}{2}} \otimes \mathrm{E}_{\frac{1}{2}}]$	3		-1	0		0	
$\{\mathrm{E}_{\frac{1}{2}} \otimes \mathrm{E}_{\frac{1}{2}}\}$	1		1	1		1	
$\mathrm{G}^{(1)}_{\frac{3}{2}} \otimes \mathrm{G}^{(2)}_{\frac{3}{2}}$	4		0	1		1	
$\mathrm{G}^{(1)}_{\frac{3}{2}} \otimes \mathrm{E}_{\frac{1}{2}}$	4		0	$e^{-i\frac{2}{3}\pi}$		$e^{-i\frac{4}{3}\pi}$	
$[\mathrm{G}^{(1)}_{\frac{3}{2}} \otimes \mathrm{G}^{(1)}_{\frac{3}{2}}]$	3		-1	0		0	
$\{\mathrm{G}^{(1)}_{\frac{3}{2}} \otimes \mathrm{G}^{(1)}_{\frac{3}{2}}\}$	1		1	$e^{-i\frac{4}{3}\pi}$		$e^{-i\frac{2}{3}\pi}$	

Table. 7: Direct-product representations made of double-valued irreducible representations of the double group $\widetilde{\mathbf{O}}$ and their characters.

$\widetilde{\Xi}_i \otimes \widetilde{\Xi}_j$	$\{\overline{E}\}$	$\{\underline{E}\}$	$\{6\overline{C_4}\}$	$\{6\underline{C_4}\}$	$\{3\overline{C_2}, 3\underline{C_2}\}$	$\{6\overline{C_2'}, 6\underline{C_2'}\}$	$\{8\overline{C_3}\}$	$\{8\underline{C_3}\}$
$[\mathrm{E}_{\frac{1}{2}} \otimes \mathrm{E}_{\frac{1}{2}}]$	3		1		-1	-1	0	
$\{\mathrm{E}_{\frac{1}{2}} \otimes \mathrm{E}_{\frac{1}{2}}\}$	1		1		1	1	1	
$\mathrm{E}_{\frac{1}{2}} \otimes \mathrm{E}_{\frac{5}{2}}$	4		-2		0	0	1	
$[\mathrm{E}_{\frac{5}{2}} \otimes \mathrm{E}_{\frac{5}{2}}]$	3		1		-1	-1	0	
$\{\mathrm{E}_{\frac{5}{2}} \otimes \mathrm{E}_{\frac{5}{2}}\}$	1		1		1	1	1	
$\mathrm{G}_{\frac{3}{2}} \otimes \mathrm{E}_{\frac{1}{2}}$	8		0		0	0	-1	
$\mathrm{G}_{\frac{3}{2}} \otimes \mathrm{E}_{\frac{5}{2}}$	8		0		0	0	-1	
$[\mathrm{G}_{\frac{3}{2}} \otimes \mathrm{G}_{\frac{3}{2}}]$	10		0		-2	-2	1	
$\{\mathrm{G}_{\frac{3}{2}} \otimes \mathrm{G}_{\frac{3}{2}}\}$	6		0		2	2	0	

Table. 8: Direct-product representations made of double-valued irreducible representations of the double group $\widetilde{\mathbf{O}_{\mathrm{h}}}$ and their characters.

$\widetilde{\Xi}_i \otimes \widetilde{\Xi}_j$	$\{\overline{E}\}$	$\{\underline{E}\}$	$\{6\overline{C_4}, 6\underline{C_4}\}$	$\{3\overline{C_2}, 3\underline{C_2}\}$	$\{6\overline{C_2'}, 6\underline{C_2'}\}$	$\{8\overline{C_3}\}$	$\{8\underline{C_3}\}$
$[\mathrm{G}_{\frac{1}{2}+\frac{5}{2}} \otimes \mathrm{G}_{\frac{1}{2}+\frac{5}{2}}]$	10		0	−2	−2		1
$\{\mathrm{G}_{\frac{1}{2}+\frac{5}{2}} \otimes \mathrm{G}_{\frac{1}{2}+\frac{5}{2}}\}$	6		0	2	2		3
$\mathrm{G}^{\mathrm{g}}_{\frac{3}{2}} \otimes \mathrm{G}_{\frac{1}{2}+\frac{5}{2}}$	16		0	0	0		−2
$[\mathrm{G}^{\mathrm{g}}_{\frac{3}{2}} \otimes \mathrm{G}^{\mathrm{g}}_{\frac{3}{2}}]$	10		0	−2	−2		1
$\{\mathrm{G}^{\mathrm{g}}_{\frac{3}{2}} \otimes \mathrm{G}^{\mathrm{g}}_{\frac{3}{2}}\}$	6		0	2	2		0
$\mathrm{G}^{\mathrm{u}}_{\frac{3}{2}} \otimes \mathrm{G}_{\frac{1}{2}+\frac{5}{2}}$	16		0	0	0		−2
$\mathrm{G}^{\mathrm{g}}_{\frac{3}{2}} \otimes \mathrm{G}^{\mathrm{u}}_{\frac{3}{2}}$	16		0	0	0		1
$[\mathrm{G}^{\mathrm{u}}_{\frac{3}{2}} \otimes \mathrm{G}^{\mathrm{u}}_{\frac{3}{2}}]$	10		0	−2	−2		1
$\{\mathrm{G}^{\mathrm{u}}_{\frac{3}{2}} \otimes \mathrm{G}^{\mathrm{u}}_{\frac{3}{2}}\}$	6		0	2	2		0

$\widetilde{\Xi}_i \otimes \widetilde{\Xi}_j$	$\{\overline{I}, \underline{I}\}$	$\{6\overline{IC_4}, 6\underline{IC_4}\}$	$\{3\overline{IC_2}, 3\underline{IC_2}\}$	$\{6\overline{IC_2'}, 6\underline{IC_2'}\}$	$\{8\overline{IC_3}\}$	$\{8\underline{IC_3}\}$
$[\mathrm{G}_{\frac{1}{2}+\frac{5}{2}} \otimes \mathrm{G}_{\frac{1}{2}+\frac{5}{2}}]$	−2	0	2	−2		1
$\{\mathrm{G}_{\frac{1}{2}+\frac{5}{2}} \otimes \mathrm{G}_{\frac{1}{2}+\frac{5}{2}}\}$	2	0	−2	2		−1
$\mathrm{G}^{\mathrm{g}}_{\frac{3}{2}} \otimes \mathrm{G}_{\frac{1}{2}+\frac{5}{2}}$	0	0	0	0		0
$[\mathrm{G}^{\mathrm{g}}_{\frac{3}{2}} \otimes \mathrm{G}^{\mathrm{g}}_{\frac{3}{2}}]$	−2	0	2	−2		1
$\{\mathrm{G}^{\mathrm{g}}_{\frac{3}{2}} \otimes \mathrm{G}^{\mathrm{g}}_{\frac{3}{2}}\}$	2	0	−2	2		2
$\mathrm{G}^{\mathrm{u}}_{\frac{3}{2}} \otimes \mathrm{G}_{\frac{1}{2}+\frac{5}{2}}$	0	0	0	0		0
$\mathrm{G}^{\mathrm{g}}_{\frac{3}{2}} \otimes \mathrm{G}^{\mathrm{u}}_{\frac{3}{2}}$	0	0	0	0		−3
$[\mathrm{G}^{\mathrm{u}}_{\frac{3}{2}} \otimes \mathrm{G}^{\mathrm{u}}_{\frac{3}{2}}]$	−2	0	2	−2		1
$\{\mathrm{G}^{\mathrm{u}}_{\frac{3}{2}} \otimes \mathrm{G}^{\mathrm{u}}_{\frac{3}{2}}\}$	2	0	−2	2		2

Table. 9: Direct-product representations made of double-valued irreducible representations $\widetilde{\Xi}_i \otimes \widetilde{\Xi}_j$ $(i, j = n_{\mathcal{C}}^{\mathbf{P}} + 1, \cdots, n_{\mathcal{C}}^{\widetilde{\mathbf{P}}})$ and their decompositions into single-valued irreducible representations $\widetilde{\Xi}_k$ $(k = 1, \cdots, n_{\mathcal{C}}^{\mathbf{P}})$, which are doubly or singly underlined when they are relevant to inelastic (Raman) or elastic (Rayleigh) light scatterings, for various double groups $\widetilde{\mathbf{P}}$. Note that $\widetilde{\Xi}_k$ of $\widetilde{\mathbf{P}}$ is nothing but Ξ_k of $\mathbf{P}$.

$\widetilde{\mathbf{P}}$	$\widetilde{\Xi}_i \otimes \widetilde{\Xi}_j$	$\bigoplus_k \widetilde{\Xi}_k = \bigoplus_k \Xi_k$
$\widetilde{\mathbf{I}}$	$\mathrm{I}_{\frac{5}{2}} \otimes \mathrm{I}_{\frac{5}{2}}$	$\{\underline{\mathrm{A}}\}\oplus 2[\mathrm{T}_1]\oplus 2[\mathrm{T}_2]\oplus[\mathrm{G}]\oplus\{\mathrm{G}\}\oplus[\underline{\underline{\mathrm{H}}}]\oplus 2\{\underline{\underline{\mathrm{H}}}\}$
	$\mathrm{I}_{\frac{5}{2}} \otimes \mathrm{G}_{\frac{3}{2}}$	$\mathrm{T}_1\oplus\mathrm{T}_2\oplus 2\mathrm{G}\oplus 2\underline{\underline{\mathrm{H}}}$
	$\mathrm{G}_{\frac{3}{2}} \otimes \mathrm{G}_{\frac{3}{2}}$	$\{\underline{\mathrm{A}}\}\oplus[\mathrm{T}_1]\oplus[\mathrm{T}_2]\oplus[\mathrm{G}]\oplus\{\underline{\underline{\mathrm{H}}}\}$
	$\mathrm{E}_{\frac{1}{2}} \otimes \mathrm{E}_{\frac{1}{2}}$	$\{\underline{\mathrm{A}}\}\oplus[\mathrm{T}_1]$
	$\mathrm{E}_{\frac{1}{2}} \otimes \mathrm{E}_{\frac{7}{2}}$	G
	$\mathrm{E}_{\frac{1}{2}} \otimes \mathrm{G}_{\frac{3}{2}}$	$\mathrm{T}_1\oplus\underline{\underline{\mathrm{H}}}$
	$\mathrm{E}_{\frac{1}{2}} \otimes \mathrm{I}_{\frac{5}{2}}$	$\mathrm{T}_2\oplus\mathrm{G}\oplus\underline{\underline{\mathrm{H}}}$
	$\mathrm{E}_{\frac{7}{2}} \otimes \mathrm{E}_{\frac{7}{2}}$	$\{\underline{\mathrm{A}}\}\oplus[\mathrm{T}_2]$
	$\mathrm{E}_{\frac{7}{2}} \otimes \mathrm{G}_{\frac{3}{2}}$	$\mathrm{T}_2\oplus\underline{\underline{\mathrm{H}}}$
	$\mathrm{E}_{\frac{7}{2}} \otimes \mathrm{I}_{\frac{5}{2}}$	$\mathrm{T}_1\oplus\mathrm{G}\oplus\underline{\underline{\mathrm{H}}}$
$\widetilde{\mathbf{T}}$	$\mathrm{G}^{(2)}_{\frac{3}{2}} \otimes \mathrm{G}^{(2)}_{\frac{3}{2}}$	$\{\underline{\underline{\mathrm{E}^{(1)}}}\}\oplus[\underline{\mathrm{T}}]$
	$\mathrm{G}^{(2)}_{\frac{3}{2}} \otimes \mathrm{E}_{\frac{1}{2}}$	$\underline{\underline{\mathrm{E}^{(2)}}}\oplus\underline{\mathrm{T}}$
	$\mathrm{E}_{\frac{1}{2}} \otimes \mathrm{E}_{\frac{1}{2}}$	$\{\underline{\mathrm{A}}\}\oplus[\underline{\mathrm{T}}]$
	$\mathrm{G}^{(1)}_{\frac{3}{2}} \otimes \mathrm{G}^{(2)}_{\frac{3}{2}}$	$\underline{\mathrm{A}}\oplus\underline{\mathrm{T}}$
	$\mathrm{G}^{(1)}_{\frac{3}{2}} \otimes \mathrm{E}_{\frac{1}{2}}$	$\underline{\underline{\mathrm{E}^{(1)}}}\oplus\underline{\mathrm{T}}$
	$\mathrm{G}^{(1)}_{\frac{3}{2}} \otimes \mathrm{G}^{(1)}_{\frac{3}{2}}$	$\{\underline{\underline{\mathrm{E}^{(2)}}}\}\oplus[\underline{\mathrm{T}}]$
$\widetilde{\mathbf{O}}$	$\mathrm{E}_{\frac{1}{2}} \otimes \mathrm{E}_{\frac{1}{2}}$	$\{\underline{\mathrm{A}_1}\}\oplus[\mathrm{T}_1]$
	$\mathrm{E}_{\frac{1}{2}} \otimes \mathrm{E}_{\frac{5}{2}}$	$\mathrm{A}_2\oplus\underline{\underline{\mathrm{T}_2}}$
	$\mathrm{E}_{\frac{5}{2}} \otimes \mathrm{E}_{\frac{5}{2}}$	$\{\underline{\mathrm{A}_1}\}\oplus[\mathrm{T}_1]$
	$\mathrm{G}_{\frac{3}{2}} \otimes \mathrm{E}_{\frac{1}{2}}$	$\underline{\underline{\mathrm{E}}}\oplus\mathrm{T}_1\oplus\underline{\underline{\mathrm{T}_2}}$
	$\mathrm{G}_{\frac{3}{2}} \otimes \mathrm{E}_{\frac{5}{2}}$	$\underline{\underline{\mathrm{E}}}\oplus\mathrm{T}_1\oplus\underline{\underline{\mathrm{T}_2}}$
	$\mathrm{G}_{\frac{3}{2}} \otimes \mathrm{G}_{\frac{3}{2}}$	$\{\underline{\mathrm{A}_1}\}\oplus[\mathrm{A}_2]\oplus\{\underline{\underline{\mathrm{E}}}\}\oplus 2[\mathrm{T}_1]\oplus[\underline{\underline{\mathrm{T}_2}}]\oplus\{\underline{\underline{\mathrm{T}_2}}\}$
$\widetilde{\mathbf{O}_{\mathrm{h}}}$	$\mathrm{G}_{\frac{1}{2}+\frac{5}{2}} \otimes \mathrm{G}_{\frac{1}{2}+\frac{5}{2}}$	$\{\underline{\mathrm{A}_{1\mathrm{g}}}\}\oplus\{\mathrm{A}_{1\mathrm{u}}\}\oplus[\mathrm{A}_{2\mathrm{g}}]\oplus\{\mathrm{A}_{2\mathrm{u}}\}\oplus[\mathrm{T}_{1\mathrm{g}}]\oplus[\mathrm{T}_{1\mathrm{u}}]\oplus\{\underline{\underline{\mathrm{T}_{2\mathrm{g}}}}\}\oplus[\mathrm{T}_{2\mathrm{u}}]$
	$\mathrm{G}^{\mathrm{g}}_{\frac{3}{2}} \otimes \mathrm{G}_{\frac{1}{2}+\frac{5}{2}}$	$\underline{\underline{\mathrm{E}_{\mathrm{g}}}}\oplus\mathrm{E}_{\mathrm{u}}\oplus\mathrm{T}_{1\mathrm{g}}\oplus\mathrm{T}_{1\mathrm{u}}\oplus\underline{\underline{\mathrm{T}_{2\mathrm{g}}}}\oplus\mathrm{T}_{2\mathrm{u}}$
	$\mathrm{G}^{\mathrm{g}}_{\frac{3}{2}} \otimes \mathrm{G}^{\mathrm{g}}_{\frac{3}{2}}$	$\{\underline{\mathrm{A}_{1\mathrm{g}}}\}\oplus[\mathrm{A}_{2\mathrm{g}}]\oplus\{\mathrm{E}_{\mathrm{u}}\}\oplus[\mathrm{T}_{1\mathrm{g}}]\oplus[\mathrm{T}_{1\mathrm{u}}]\oplus\{\underline{\underline{\mathrm{T}_{2\mathrm{g}}}}\}\oplus[\mathrm{T}_{2\mathrm{u}}]$
	$\mathrm{G}^{\mathrm{u}}_{\frac{3}{2}} \otimes \mathrm{G}_{\frac{1}{2}+\frac{5}{2}}$	$\underline{\underline{\mathrm{E}_{\mathrm{g}}}}\oplus\mathrm{E}_{\mathrm{u}}\oplus\mathrm{T}_{1\mathrm{g}}\oplus\mathrm{T}_{1\mathrm{u}}\oplus\underline{\underline{\mathrm{T}_{2\mathrm{g}}}}\oplus\mathrm{T}_{2\mathrm{u}}$
	$\mathrm{G}^{\mathrm{g}}_{\frac{3}{2}} \otimes \mathrm{G}^{\mathrm{u}}_{\frac{3}{2}}$	$\mathrm{A}_{1\mathrm{u}}\oplus\mathrm{A}_{2\mathrm{u}}\oplus\underline{\underline{\mathrm{E}_{\mathrm{g}}}}\oplus\mathrm{T}_{1\mathrm{g}}\oplus\mathrm{T}_{1\mathrm{u}}\oplus\underline{\underline{\mathrm{T}_{2\mathrm{g}}}}\oplus\mathrm{T}_{2\mathrm{u}}$
	$\mathrm{G}^{\mathrm{u}}_{\frac{3}{2}} \otimes \mathrm{G}^{\mathrm{u}}_{\frac{3}{2}}$	$\{\underline{\mathrm{A}_{1\mathrm{g}}}\}\oplus[\mathrm{A}_{2\mathrm{g}}]\oplus\{\mathrm{E}_{\mathrm{u}}\}\oplus[\mathrm{T}_{1\mathrm{g}}]\oplus[\mathrm{T}_{1\mathrm{u}}]\oplus\{\underline{\underline{\mathrm{T}_{2\mathrm{g}}}}\}\oplus[\mathrm{T}_{2\mathrm{u}}]$

3.4 PSG characterization of Majorana excitation spectra

The projection operator that extracts the components of an irreducible representation $\widetilde{\Xi}_i$ from the arbitrary function is defined as follows:

$$\mathcal{P}^{\widetilde{\Xi}_i} = \frac{d^{\mathbf{P}}_{\widetilde{\Xi}_i}}{g^{\mathbf{P}}} \sum_{k=1}^{g^{\tilde{\mathbf{P}}}} [\chi^{\widetilde{\mathbf{P}}}_{\widetilde{\Xi}_i}(\widetilde{P}_k)]^* \widetilde{P}_k. \tag{3.23}$$

When the projection operator is applied to the Majorana fermion basis $\boldsymbol{c}$, we get a symmetry-definite Majorana fermion basis $\tilde{c}^{\widetilde{\Xi}_i}$ which is characterized by the irreducible representation $\widetilde{\Xi}_i$:

$$\mathcal{P}^{\Xi_i}\boldsymbol{c} = \mathcal{P}^{\Xi_i}\begin{bmatrix} c_1 \\ c_2 \\ c_3 \\ \vdots \\ c_L \end{bmatrix} = \begin{bmatrix} \widetilde{c}_1^{\widetilde{\Xi}_i} \\ \widetilde{c}_2^{\widetilde{\Xi}_i} \\ \widetilde{c}_3^{\widetilde{\Xi}_i} \\ \vdots \\ \widetilde{c}_L^{\widetilde{\Xi}_i} \end{bmatrix} = \widetilde{\boldsymbol{c}}^{\widetilde{\Xi}_i}, \qquad \widetilde{c}_i^{\widetilde{\Xi}_i} = \sum_{j=1}^{L} \psi_{i,j}^{\widetilde{\Xi}_i} c_j. \tag{3.24}$$

Using the result of the above projection operation, we can define a unitary transformation U that diagonalizes the Hamiltonian into irreducible representation blocks:

$$\begin{aligned} \mathscr{H} &= [c_1\ c_2\ c_3\ \cdots\ c_L]\,\mathcal{H}\begin{bmatrix} c_1 \\ c_2 \\ c_3 \\ \vdots \\ c_L \end{bmatrix} = [c_1\ c_2\ c_3\ \cdots\ c_L]\,U^\dagger U\mathcal{H}U^\dagger U\begin{bmatrix} c_1 \\ c_2 \\ c_3 \\ \vdots \\ c_L \end{bmatrix} \\ &= [c'_1\ c'_2\ c'_3\ \cdots\ c'_L]\begin{bmatrix} \boxed{\widetilde{\mathcal{H}}^{\widetilde{\Xi}_1}} & & & \\ & \boxed{\widetilde{\mathcal{H}}^{\widetilde{\Xi}_2}} & & \\ & & \ddots & \\ & & & \boxed{\widetilde{\mathcal{H}}^{\widetilde{\Xi}_k}} \end{bmatrix}\begin{bmatrix} c'_1 \\ c'_2 \\ c'_3 \\ \vdots \\ c'_L \end{bmatrix} \\ &\equiv {}^t\boldsymbol{c}'\widetilde{\mathcal{H}}\boldsymbol{c}'. \end{aligned} \tag{3.25}$$

Furthermore, when the unitary transformation $\widetilde{U}$, which makes each block completely diagonal, is applied,

$$\mathscr{H} = {}^t\boldsymbol{c}'\widetilde{\mathcal{H}}\boldsymbol{c}' = {}^t\boldsymbol{c}'\widetilde{U}^\dagger\widetilde{U}\widetilde{\mathcal{H}}\widetilde{U}^\dagger\widetilde{U}\boldsymbol{c}'$$

$$= \begin{bmatrix}\alpha_1^\dagger & \alpha_2^\dagger & \alpha_3^\dagger & \cdots & \alpha_{L/2}^\dagger\end{bmatrix} \begin{bmatrix} \boxed{\begin{matrix}\varepsilon_1^{\widetilde{\Xi}_i} & & \\ & \ddots & \\ & & \varepsilon_{l_{\widetilde{\Xi}_i}}^{\widetilde{\Xi}_i}\end{matrix}} & & & \\ & \boxed{\begin{matrix}\varepsilon_1^{\widetilde{\Xi}_j} & & \\ & \ddots & \\ & & \varepsilon_{l_{\widetilde{\Xi}_j}}^{\widetilde{\Xi}_j}\end{matrix}} & & \\ & & \ddots & \\ & & & \boxed{\begin{matrix}\varepsilon_1^{\widetilde{\Xi}_k} & & \\ & \ddots & \\ & & \varepsilon_{l_{\widetilde{\Xi}_k}}^{\widetilde{\Xi}_k}\end{matrix}} \end{bmatrix} \begin{bmatrix}\alpha_1 \\ \alpha_2 \\ \alpha_3 \\ \vdots \\ \alpha_{L/2}\end{bmatrix}. \quad (3.26)$$

Each matrix element of Eq. (3.26) is the eigenvalue of one-quasiparticle excited state. Therefore, the eigenvalues in each block are characterized by the irreducible representations of their block. Since

$$\overline{P} = -\underline{P} \quad (3.27)$$

and

$$\chi^{\widetilde{\mathbf{P}}}_{\widetilde{\Xi}_i}(\overline{P}) = \chi^{\widetilde{\mathbf{P}}}_{\widetilde{\Xi}_i}(\underline{P}) \quad (3.28)$$

for single-valued irreducible representations, every projection operator for single-valued irreducible representations is vanish,

$$\mathcal{P}^{\widetilde{\Xi}_i} = 0\,(i = 1, 2, \ldots, n^{\mathbf{P}}_{\mathcal{C}}), \quad (3.29)$$

and the gauge-ground Hamiltonian does not contain single-valued irreducible representations.

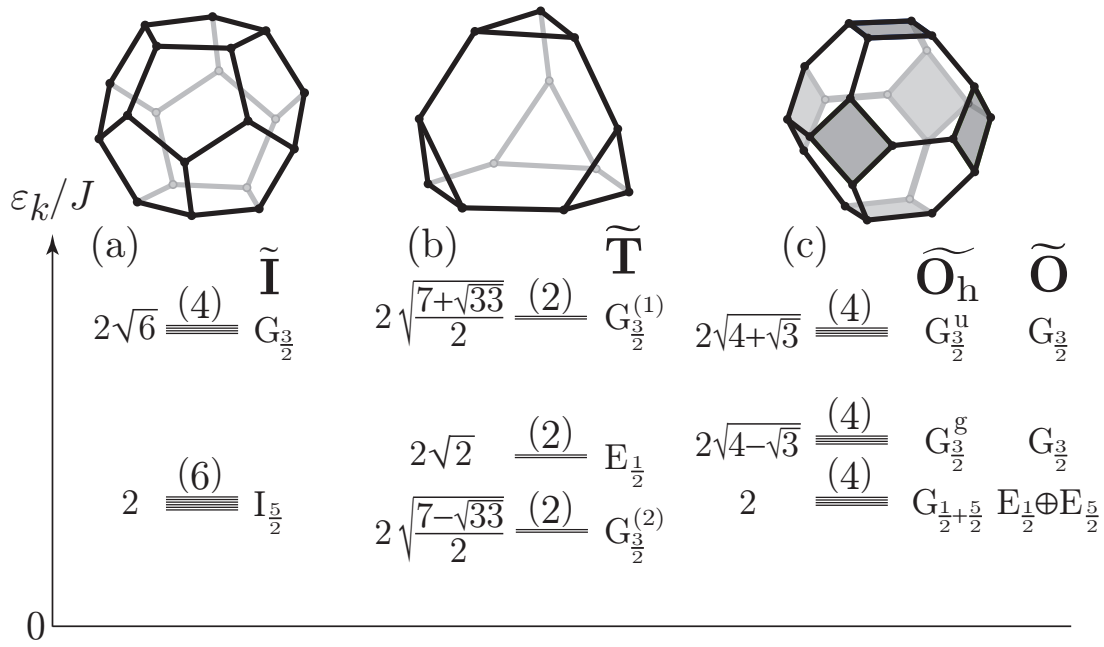

Fig. 5: Majorana excitation spectra of Kitaev spin balls consisting of dodecahedral (a), truncated-tetrahedral (b) and truncated-octahedral (c) lattices in their ground flux configurations. The eigenenergy, multiplicity, and irreducible representation are specified beside each eigenlevel.

Figure 5 shows Majorana excitation spectra of the Kitaev polyhedra. Each excitation spectrum are characterized by *double-valued* irreducible representations of its belonging double-covered group $\widetilde{\mathbf{P}}$. The Majorana spinon spectrum of the gauge-ground $\widetilde{\mathbf{O}_{\mathrm{h}}}$ Kitaev polyhedron thus consists of three quadruplets $3 \times 4 = L/2$ [see Fig. 5 together with Eq. (2.9)]. If we employ $\widetilde{\mathbf{O}}$ [49] in this context, we have two doublets, $\mathrm{E}_{\frac{1}{2}}$ and $\mathrm{E}_{\frac{5}{2}}$, instead of the quadruplet $\mathrm{G}_{\frac{1}{2}+\frac{5}{2}}$, and they look *accidentally* degenerate with each other. Only the full symmetry group $\widetilde{\mathbf{O}_{\mathrm{h}}}$ can reveal the necessary quadruplet. All the $L/2$ Majorana spinon eigenmodes of the gauge-ground $\widetilde{\mathbf{I}}$ and $\widetilde{\mathbf{T}}$ Kitaev polyhedra are also describable with double-valued irreducible representations of their projective symmetry groups [see Fig. 5 together with Eq. (2.9)]. The former consist of a sextuplet of $\mathrm{I}_{\frac{5}{2}}$ and a quadruplet of $\mathrm{G}_{\frac{3}{2}}$, while the latter consist of three doublets of $\mathrm{G}^{(1)}_{\frac{3}{2}}$, $\mathrm{G}^{(2)}_{\frac{3}{2}}$, and $\mathrm{E}_{\frac{1}{2}}$, where the 4-dimensional real irreducible representation $\mathrm{G}_{\frac{3}{2}}$ splits into the 2-dimensional complex ones $\mathrm{G}^{(1)}_{\frac{3}{2}}$ and $\mathrm{G}^{(2)}_{\frac{3}{2}}$ due to the pure imaginary Hamiltonian (2.9).

4 Majorana-Spinon-Mediated Raman Scattering

4.1 Raman response of the Kitaev quantum spin liquid

Raman scattering is inelastic light scattering probing magnetic correlations between photon absorption and emitting process [52,63]. In the Kitaev model, unlike the dynamical spin correlations, Raman scattering does not excite fluxes but pairs of Majorana fermions (cf. Sec. 4.2). We can calculate scattering intensity exactly and probe Majorana fermion excitation directly.

Raman scattering intensities of Kitaev models have been discussed from two perspectives in previous theoretical studies. The first point of view is polarization dependence. Just like the Kagome antiferromagnet [64], the Kitaev honeycomb model has no polarization dependence. The polarization dependence is weak even if the perturbative Heisenberg interaction is added to the Kitaev Hamiltonian [24]. Therefore, it has been speculated that the weak polarization dependence may be a feature of the quantum spin liquid state [24].

Another point of view is how fermionic spinon excitations appear in Raman scattering intensity. Since Raman scattering is a visible light scattering process, Raman scattering intensity at absolute zero reflects the Majorana pair excitations with zero momentum. Therefore, the Raman scattering spectrum indirectly reflects the Majorana excitation spectrum [24, 65]. On the other hand, Raman scattering intensity at finite temperatures can be fit to a fermionic thermal occupation function [25]. This thermal behavior is inconsistent with the bosonic excitation that reflects the magnon excitations in conventional magnetically ordered systems. Raman scattering experiment is conducted on the candidate of the Kitaev honeycomb model, α-$\mathrm{RuCl_3}$ [34]. Although this candidate material is magnetically ordered at absolute zero, it shows a fermionic temperature dependence in the scattering

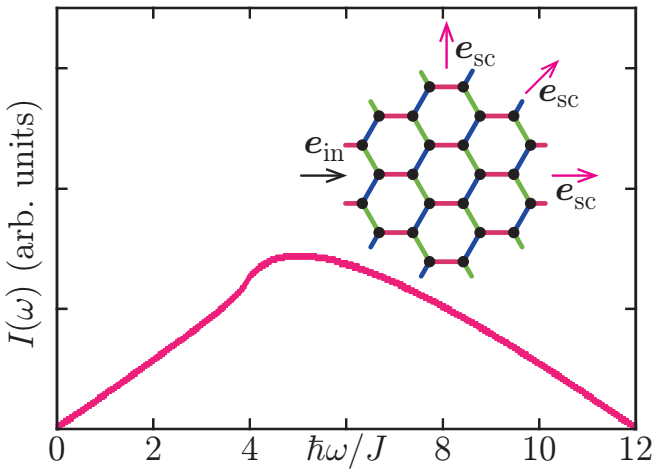

Fig. 6: Raman scattering intensity $I(\omega)$ of the Kitaev honeycomb model in the ground flux configuration. Raman scattering intensity is independent of the incident polarization vector $\boldsymbol{e}_{\mathrm{in}}$ and scattered polarization vectors $\boldsymbol{e}_{\mathrm{sc}}$.

intensity as well. This peculiar temperature dependence could be evidence of the Majorana spinons.

We analyze the features of the Raman intensity of the Kitaev spin liquids by two types of group analysis. We use point symmetry group analysis to discuss whether vanishing polarization dependence is *true* feature of quantum spin liquid states. Moreover, we use projective symmetry group analysis to discuss how projective symmetry of spinons appears in Raman scattering intensity.

4.2 Raman intensity at absolute zero: Point-symmetry argument

We first discuss the Raman scattering intensity at absolute zero. The ground-state Raman scattering intensity of a Kitaev gauged lattice within the LF scheme [24, 52–54, 65] reads

$$\begin{aligned} I(\omega) &= \frac{1}{2\pi\hbar L}\int_{-\infty}^{\infty}\langle 0|e^{\frac{i\mathscr{H}t}{\hbar}}\mathscr{R}e^{-\frac{i\mathscr{H}t}{\hbar}}\mathscr{R}|0\rangle e^{i\omega t}dt; \\ \mathscr{R} &\equiv -J\sum_{\lambda=x,y,z}\sum_{<m,n>_\lambda}(\boldsymbol{e}_{\rm in}\cdot\boldsymbol{d}_{mn})(\boldsymbol{e}_{\rm sc}\cdot\boldsymbol{d}_{mn})\sigma_m^\lambda\sigma_n^\lambda \\ &= iJ\sum_{\lambda=x,y,z}\sum_{<m,n>_\lambda}(\boldsymbol{e}_{\rm in}\cdot\boldsymbol{d}_{mn})(\boldsymbol{e}_{\rm sc}\cdot\boldsymbol{d}_{mn})\hat{u}_{<m,n>_\lambda}c_mc_n, \end{aligned} \tag{4.1}$$

where $\boldsymbol{e}_{\rm in}\equiv{}^{\rm t}[e_{\rm in}^x\ e_{\rm in}^y\ e_{\rm in}^z]=[\sin\vartheta_{\rm in}\cos\varphi_{\rm in},\sin\vartheta_{\rm in}\sin\varphi_{\rm in},\cos\vartheta_{\rm in}]$ and $\boldsymbol{e}_{\rm sc}\equiv{}^{\rm t}[e_{\rm sc}^x\ e_{\rm sc}^y\ e_{\rm sc}^z]=[\sin\vartheta_{\rm in}\cos\varphi_{\rm in},\sin\vartheta_{\rm in}\sin\varphi_{\rm in},\cos\vartheta_{\rm in}]$ are the polarization vectors of incident and scattered lights, respectively, while $\boldsymbol{d}_{mn}\equiv\boldsymbol{r}_m-\boldsymbol{r}_n$ are the lattice vectors with $\boldsymbol{r}_m$ and $\boldsymbol{r}_n$ being the positions of neighboring sites. For later analysis, we reexpress $\mathscr{R}$ in a Cartesian coordinate system as follows:

$$\mathscr{R}\equiv\sum_{\mu=x,y,z}\sum_{\nu=x,y,z}e_{\rm in}^\mu e_{\rm sc}^\nu\mathcal{R}^{\mu\nu}\equiv{}^{\rm t}\boldsymbol{e}_{\rm in}\mathcal{R}\boldsymbol{e}_{\rm sc}, \tag{4.2}$$

$$\begin{aligned} \mathcal{R}^{\mu\nu} &\equiv -J\sum_{\lambda=x,y,z}\sum_{<m,n>_\lambda}d_{mn}^\mu d_{mn}^\nu\sigma_m^\lambda\sigma_n^\lambda, \\ &= iJ\sum_{\lambda=x,y,z}\sum_{<m,n>_\lambda}d_{mn}^\mu d_{mn}^\nu\hat{u}_{<m,n>_\lambda}c_mc_n \\ &= iJ\sum_{\lambda=x,y,z}\sum_{<m,n>_\lambda}\sum_{k=1}^{L/2}\sum_{k'=1}^{L/2}d_{mn}^\mu d_{mn}^\nu\hat{u}_{<m,n>_\lambda} \\ &\quad\times\left[(\psi_{m,2k-1}+i\psi_{m,2k})\alpha_k^\dagger+(\psi_{m,2k-1}-i\psi_{m,2k})\alpha_k\right] \\ &\quad\times\left[(\psi_{n,2k'-1}+i\psi_{n,2k'})\alpha_{k'}^\dagger+(\psi_{n,2k'-1}-i\psi_{n,2k'})\alpha_{k'}\right], \end{aligned} \tag{4.3}$$

where $\mathcal{R}\equiv[\mathcal{R}^{\mu\nu}]$ is the matrix representation of the Raman operator in Cartesian coordinates.

When we identify the ground state with Eq. (2.10) without specifying its gauge fields $|\{u_{<m,n>_\lambda}\}\rangle_{0(r)}$, it belongs to $\mathbf{P}$ rather than $\widetilde{\mathbf{P}}$. If we recognize the ground state by its gauge fields, $|0\rangle\equiv|\{n_k\}\rangle_0\otimes|\{u_{<m,n>_\lambda}\}\rangle_{0(0)}$, for instance, with $|\{n_k\}\rangle_\kappa\otimes|\{u_{<m,n>_\lambda}\}\rangle_{q(r)}$ being the κth spinon state ($\kappa=0,\cdots,2^{\frac{L}{2}}-1$) against the $q(r)$th bond configuration [$q(r)=2^{L-1}q+r$; $q=0,\cdots,2^{\frac{L}{2}+1}-1$, $r=0,\cdots,2^{L-1}-1$], $|0\rangle$ chosen in the augmented Hilbert space is no longer invariant under every symmetry operation of $\mathbf{P}$ but belongs to its $\mathbb{Z}_2$-gauge extension $\widetilde{\mathbf{P}}$. Therefore, when the ground state belongs to the double group $\widetilde{\mathbf{P}}$, it is useful to write the Raman operator (4.1) as [63]

$$\mathscr{R}=\sum_i{}'\sum_{\mu=1}^{d_{\tilde{\Xi}_i}^{\tilde{\mathbf{P}}}}E_{\tilde{\Xi}_i:\mu}^{\tilde{\mathbf{P}}}\mathcal{R}_{\tilde{\Xi}_i:\mu}^{\tilde{\mathbf{P}}}=\sum_i{}'\sum_{\mu=1}^{d_{\Xi_i}^{\mathbf{P}}}E_{\Xi_i:\mu}^{\mathbf{P}}\mathcal{R}_{\Xi_i:\mu}^{\mathbf{P}}, \tag{4.4}$$

where $E^{\widetilde{\mathbf{P}}}_{\widetilde{\Xi}_i:\mu}$ ($E^{\mathbf{P}}_{\Xi_i:\mu}$) is the μth polarization-vector basis function for the $\widetilde{\Xi}_i$ (Ξ_i) irreducible representation of $\widetilde{\mathbf{P}}$ ($\mathbf{P}$), $\mathcal{R}^{\widetilde{\mathbf{P}}}_{\widetilde{\Xi}_i:\mu}$ ($\mathcal{R}^{\mathbf{P}}_{\Xi_i:\mu}$) is the symmetry-definite LF vertex accompanying it, and $\sum_i'$ runs over the *LF-active* irreducible representations. The LF-active irreducible representations $\widetilde{\Xi}_i$ of $\widetilde{\mathbf{P}}$, which are necessarily *real* and *single-valued* and therefore equal to the irreducible representations Ξ_i of the corresponding point symmetry group $\mathbf{P}$.

Within the LF formulation, the nonvanishing vertices and corresponding basis functions read

$$
\begin{aligned}
E^{\mathbf{I}}_{\mathrm{A}:1} &= E^{\mathbf{T}}_{\mathrm{A}:1} = E^{\mathbf{O}_\mathrm{h}}_{\mathrm{A_{1g}}:1} = \frac{e^x_\mathrm{in}e^x_\mathrm{sc} + e^y_\mathrm{in}e^y_\mathrm{sc} + e^z_\mathrm{in}e^z_\mathrm{sc}}{\sqrt{3}}, & \mathcal{R}^{\mathbf{I}}_{\mathrm{A}:1} &= \mathcal{R}^{\mathbf{T}}_{\mathrm{A}:1} = \mathcal{R}^{\mathbf{O}_\mathrm{h}}_{\mathrm{A_{1g}}:1} = \frac{\mathcal{R}^{xx} + \mathcal{R}^{yy} + \mathcal{R}^{zz}}{\sqrt{3}},\\
E^{\mathbf{I}}_{\mathrm{H}:1} &= E^{\mathbf{T}}_{\mathrm{E}:1} = E^{\mathbf{O}_\mathrm{h}}_{\mathrm{E_g}:1} = \frac{2e^z_\mathrm{in}e^z_\mathrm{sc} - e^x_\mathrm{in}e^x_\mathrm{sc} - e^y_\mathrm{in}e^y_\mathrm{sc}}{\sqrt{6}}, & \mathcal{R}^{\mathbf{I}}_{\mathrm{H}:1} &= \mathcal{R}^{\mathbf{T}}_{\mathrm{E}:1} = \mathcal{R}^{\mathbf{O}_\mathrm{h}}_{\mathrm{E_g}:1} = \frac{2\mathcal{R}^{zz} - \mathcal{R}^{xx} - \mathcal{R}^{yy}}{\sqrt{6}},\\
E^{\mathbf{I}}_{\mathrm{H}:2} &= E^{\mathbf{T}}_{\mathrm{E}:2} = E^{\mathbf{O}_\mathrm{h}}_{\mathrm{E_g}:2} = \frac{e^x_\mathrm{in}e^x_\mathrm{sc} - e^y_\mathrm{in}e^y_\mathrm{sc}}{\sqrt{2}}, & \mathcal{R}^{\mathbf{I}}_{\mathrm{H}:2} &= \mathcal{R}^{\mathbf{T}}_{\mathrm{E}:2} = \mathcal{R}^{\mathbf{O}_\mathrm{h}}_{\mathrm{E_g}:2} = \frac{\mathcal{R}^{xx} - \mathcal{R}^{yy}}{\sqrt{2}},\\
E^{\mathbf{I}}_{\mathrm{H}:3} &= E^{\mathbf{T}}_{\mathrm{T}:1} = E^{\mathbf{O}_\mathrm{h}}_{\mathrm{T_{2g}}:1} = \frac{e^x_\mathrm{in}e^y_\mathrm{sc} + e^y_\mathrm{in}e^x_\mathrm{sc}}{\sqrt{2}}, & \mathcal{R}^{\mathbf{I}}_{\mathrm{H}:3} &= \mathcal{R}^{\mathbf{T}}_{\mathrm{T}:1} = \mathcal{R}^{\mathbf{O}_\mathrm{h}}_{\mathrm{T_{2g}}:1} = \frac{\mathcal{R}^{xy} + \mathcal{R}^{yx}}{\sqrt{2}},\\
E^{\mathbf{I}}_{\mathrm{H}:4} &= E^{\mathbf{T}}_{\mathrm{T}:2} = E^{\mathbf{O}_\mathrm{h}}_{\mathrm{T_{2g}}:2} = \frac{e^y_\mathrm{in}e^z_\mathrm{sc} + e^z_\mathrm{in}e^y_\mathrm{sc}}{\sqrt{2}}, & \mathcal{R}^{\mathbf{I}}_{\mathrm{H}:4} &= \mathcal{R}^{\mathbf{T}}_{\mathrm{T}:2} = \mathcal{R}^{\mathbf{O}_\mathrm{h}}_{\mathrm{T_{2g}}:2} = \frac{\mathcal{R}^{yz} + \mathcal{R}^{zy}}{\sqrt{2}},\\
E^{\mathbf{I}}_{\mathrm{H}:5} &= E^{\mathbf{T}}_{\mathrm{T}:3} = E^{\mathbf{O}_\mathrm{h}}_{\mathrm{T_{2g}}:3} = \frac{e^z_\mathrm{in}e^x_\mathrm{sc} + e^x_\mathrm{in}e^z_\mathrm{sc}}{\sqrt{2}}, & \mathcal{R}^{\mathbf{I}}_{\mathrm{H}:5} &= \mathcal{R}^{\mathbf{T}}_{\mathrm{T}:3} = \mathcal{R}^{\mathbf{O}_\mathrm{h}}_{\mathrm{T_{2g}}:3} = \frac{\mathcal{R}^{zx} + \mathcal{R}^{xz}}{\sqrt{2}}
\end{aligned}
\tag{4.5}
$$

for the $\widetilde{\mathbf{I}}$, $\widetilde{\mathbf{T}}$, and $\widetilde{\mathbf{O}_\mathrm{h}}$ gauged polyhedra, and, for reference,

$$
\begin{aligned}
E^{\mathbf{C}_\mathrm{6v}}_{\mathrm{A_1}:1} &= \frac{e^x_\mathrm{in}e^x_\mathrm{sc} + e^y_\mathrm{in}e^y_\mathrm{sc}}{\sqrt{2}}, E^{\mathbf{C}_\mathrm{6v}}_{\mathrm{E_2}:1} = \frac{e^x_\mathrm{in}e^x_\mathrm{sc} - e^y_\mathrm{in}e^y_\mathrm{sc}}{\sqrt{2}}, E^{\mathbf{C}_\mathrm{6v}}_{\mathrm{E_2}:2} = \frac{e^x_\mathrm{in}e^y_\mathrm{sc} + e^y_\mathrm{in}e^x_\mathrm{sc}}{\sqrt{2}},\\
\mathcal{R}^{\mathbf{C}_\mathrm{6v}}_{\mathrm{A_1}:1} &= \frac{\mathcal{R}^{xx} + \mathcal{R}^{yy}}{\sqrt{2}}, \quad \mathcal{R}^{\mathbf{C}_\mathrm{6v}}_{\mathrm{E_2}:1} = \frac{\mathcal{R}^{xx} - \mathcal{R}^{yy}}{\sqrt{2}}, \quad \mathcal{R}^{\mathbf{C}_\mathrm{6v}}_{\mathrm{E_2}:2} = \frac{\mathcal{R}^{xy} + \mathcal{R}^{yx}}{\sqrt{2}}
\end{aligned}
\tag{4.6}
$$

for the two-dimensional $\widetilde{\mathbf{C}_\mathrm{6v}}$ gauged honeycomb of triangular geometry [64–67]. In the spherical lattice geometry realized by Platonic and Archimedean polyhedra, all the vertices of the identity representation, such as $\mathcal{R}^{\mathbf{I}}_{\mathrm{A}:\mu}$, $\mathcal{R}^{\mathbf{T}}_{\mathrm{A}:\mu}$, and $\mathcal{R}^{\mathbf{O}_\mathrm{h}}_{\mathrm{A_{1g}}:\mu}$, commute with the corresponding Hamiltonians and therefore reduce to elastic (Rayleigh) scattering. This is the case with $\mathcal{R}^{\mathbf{C}_\mathrm{6v}}_{\mathrm{A_1}:\mu}$ as well. Since $\mathcal{R}^{\mu\nu} = \mathcal{R}^{\nu\mu}$ within the LF scheme, all chiral terms such as

$$
\mathcal{R}^{\mathbf{C}_\mathrm{6v}}_{\mathrm{A_2}:1} = \frac{\mathcal{R}^{xy} - \mathcal{R}^{yx}}{\sqrt{2}},
\tag{4.7}
$$

are apparently disappears.

Since the ground state (2.10) is invariant under every symmetry operation of $\mathbf{P}$, every expectation value between Raman vertices of different symmetry species for it goes to zero [63, 65, 66],

$$
\begin{aligned}
&\frac{1}{2\pi\hbar L}\int_{-\infty}^{\infty}\langle 0|e^{\frac{i\mathscr{H}t}{\hbar}}\mathcal{R}^{\mathbf{P}}_{\Xi_i:\mu}e^{-\frac{i\mathscr{H}t}{\hbar}}\mathcal{R}^{\mathbf{P}}_{\Xi_j:\nu}|0\rangle e^{i\omega t}dt\\
&= \frac{\delta_{ij}\delta_{\mu\nu}}{2\pi\hbar L}\int_{-\infty}^{\infty}\langle 0|e^{\frac{i\mathscr{H}t}{\hbar}}\mathcal{R}^{\mathbf{P}}_{\Xi_i:\mu}e^{-\frac{i\mathscr{H}t}{\hbar}}\mathcal{R}^{\mathbf{P}}_{\Xi_i:\mu}|0\rangle e^{i\omega t}dt\\
&\equiv \delta_{ij}\delta_{\mu\nu}I^{\mathbf{P}}_{\Xi_i:\mu}(\omega),
\end{aligned}
\tag{4.8}
$$

and $I^{\mathbf{P}}_{\Xi_i:\mu}(\omega)\,(\mu=1,\cdots,d^{\mathbf{P}}_{\Xi_i})$ no longer depend on μ [24, 29, 64, 65]. While the Raman spectra of gauge-ground Kitaev polyhedra are analyzable with direct-product representations of their projective symmetry groups $\widetilde{\mathbf{P}}$, they can be classified by irreducible representations of the corresponding point symmetry groups $\mathbf{P}$. Substituting the irreducible decomposition of the Raman operator $\mathscr{R}$ (4.4) into the LF expression of the Raman intensity (4.1) and taking account of the spectral degeneracy within each multidimensional irreducible representation, we have

$$\begin{aligned} I(\omega) &= \sum_i{}' \sum_j{}' \sum_{\mu=1}^{d^{\mathbf{P}}_{\Xi_i}} \sum_{\nu=1}^{d^{\mathbf{P}}_{\Xi_j}} E^{\mathbf{P}}_{\Xi_i:\mu} E^{\mathbf{P}}_{\Xi_j:\nu} \int_{-\infty}^{\infty} \frac{dt\, e^{i\omega t}}{2\pi\hbar L} \langle 0| e^{\frac{i\mathscr{H}t}{\hbar}} \mathcal{R}^{\mathbf{P}}_{\Xi_i:\mu} e^{-\frac{i\mathscr{H}t}{\hbar}} \mathcal{R}^{\mathbf{P}}_{\Xi_j:\nu} |0\rangle \\ &= \sum_i{}' \sum_{\mu=1}^{d^{\mathbf{P}}_{\Xi_i}} \left(E^{\mathbf{P}}_{\Xi_i:\mu}\right)^2 \int_{-\infty}^{\infty} \frac{dt\, e^{i\omega t}}{2\pi\hbar L} \langle 0| e^{\frac{i\mathscr{H}t}{\hbar}} \mathcal{R}^{\mathbf{P}}_{\Xi_i:\mu} e^{-\frac{i\mathscr{H}t}{\hbar}} \mathcal{R}^{\mathbf{P}}_{\Xi_i:\mu} |0\rangle \\ &= \sum_i{}' \sum_{\mu=1}^{d^{\mathbf{P}}_{\Xi_i}} \left(E^{\mathbf{P}}_{\Xi_i:\mu}\right)^2 I^{\mathbf{P}}_{\Xi_i:\mu}(\omega). \end{aligned} \tag{4.9}$$

We write the Raman vertices in Cartesian coordinates (4.5) and then in terms of spinon operators (4.3). Having in mind that $\alpha_k|0\rangle = 0$ and discarding Rayleigh terms, we can express $I(\omega)$ by Fermi's golden rule,

$$\begin{aligned} I(\omega) &= \sum_i{}' \sum_{\mu=1}^{d^{\mathbf{P}}_{\Xi_i}} \left(E^{\mathbf{P}}_{\Xi_i:\mu}\right)^2 \int_{-\infty}^{\infty} \frac{dt\, e^{i\omega t}}{2\pi\hbar L} \sum_{q=0}^{2^{\frac{L}{2}+1}-1} \sum_{\kappa=0}^{2^{\frac{L}{2}-1}-1} \langle 0| e^{\frac{i\mathscr{H}t}{\hbar}} \mathcal{R}^{\mathbf{P}}_{\Xi_i:\mu} e^{-\frac{i\mathscr{H}t}{\hbar}} |\{n_k\}\rangle_\kappa \otimes |\{W_p\}\rangle_q \\ &\quad \times {}_q\langle\{W_p\}| \otimes {}_\kappa\langle\{n_k\}| \mathcal{R}^{\mathbf{P}}_{\Xi_i:\mu}|0\rangle \\ &= \frac{1}{L} \sum_i{}' \sum_{\mu=1}^{d^{\mathbf{P}}_{\Xi_i}} \left(E^{\mathbf{P}}_{\Xi_i:\mu}\right)^2 \frac{1}{2\pi\hbar} \sum_{1=k<k'=\frac{L}{2}} \int_{-\infty}^{\infty} e^{i\left(\omega - \frac{\epsilon_k}{\hbar} - \frac{\epsilon_{k'}}{\hbar}\right)t} dt \\ &\quad \times \sum_{q=0}^{2^{\frac{L}{2}+1}-1} {}_0\langle\{W_p\}|\{W_p\}\rangle_q {}_q\langle\{W_p\}|\{W_p\}\rangle_0 \\ &\quad \times {}_0\langle\{n_k\}| \mathcal{R}^{\mathbf{P}}_{\Xi_i:\mu}\big|_{\{u_{<m,n>_\lambda}\}_{0(r)}} \alpha^\dagger_{k'}\alpha^\dagger_k |\{n_k\}\rangle_0 {}_0\langle\{n_k\}|\alpha_k\alpha_{k'} \mathcal{R}^{\mathbf{P}}_{\Xi_i:\mu}\big|_{\{u_{<m,n>_\lambda}\}_{0(r)}} |\{n_k\}\rangle_0 \\ &= \frac{1}{L} \sum_i{}' \sum_{\mu=1}^{d^{\mathbf{P}}_{\Xi_i}} \left(E^{\mathbf{P}}_{\Xi_i:\mu}\right)^2 \sum_{1=k<k'=\frac{L}{2}} \left|\langle 0|\alpha_k\alpha_{k'} \mathcal{R}^{\mathbf{P}}_{\Xi_i:\mu}|0\rangle\right|^2 \delta(\hbar\omega - \varepsilon_k - \varepsilon_{k'}), \end{aligned} \tag{4.10}$$

where $\mathcal{R}^{\mathbf{P}}_{\Xi_i:\mu}\big|_{\{u_{<m,n>_\lambda}\}_{0(r)}}$ are the *gauge-ground* LF vertices.

We may be reminded that the above is not the case with any single spin operator. Unlike the Raman

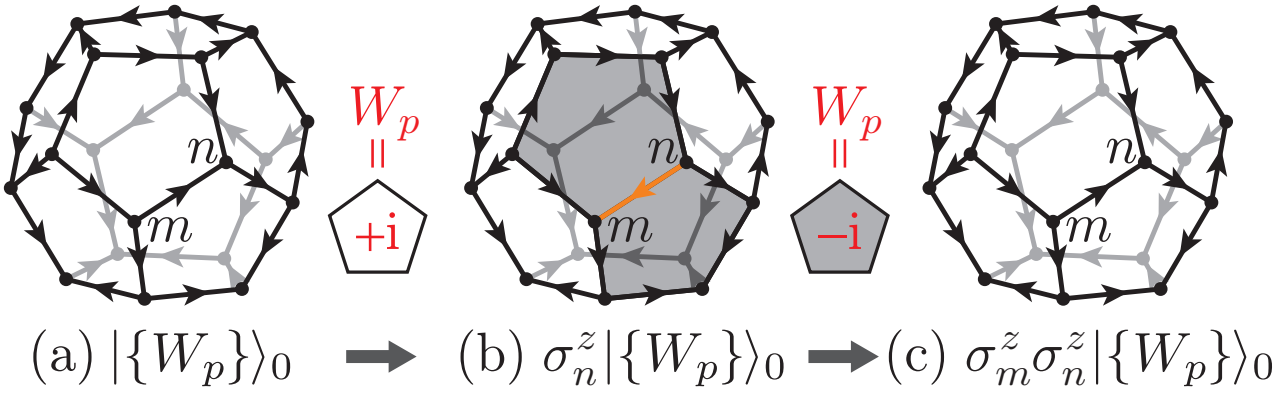

Fig. 7: Actions of the spin operators $\sigma_n^z = ic_n\eta_n^z$ (b) and $\sigma_m^z\sigma_n^z = -i\hat{u}_{<m,n>_z}c_mc_n$ (c) on the gauge-ground Kitaev dodecahedron $|\{W_p\}\rangle_0$ (a) in the context of calculating the dynamic structure factor (4.11) and Raman scattering intensity (4.10).

response, visons (Fig. 7) as well as spinons are involved in the dynamic spin response [68, 69]

$$\begin{aligned}
S^{\lambda\lambda}(\boldsymbol{q},\omega) &= \frac{1}{2\pi\hbar L}\int_{-\infty}^{\infty}\sum_{m,n=1}^{L} e^{-i\boldsymbol{q}\cdot(\boldsymbol{r}_m-\boldsymbol{r}_n)}\langle 0|e^{\frac{i\mathscr{H}t}{\hbar}}\sigma_m^\lambda e^{-\frac{i\mathscr{H}t}{\hbar}}\sigma_n^\lambda|0\rangle e^{i\omega t}dt \\
&= \int_{-\infty}^{\infty}\frac{dt\,e^{i\omega t}}{2\pi\hbar L}\sum_{m,n=1}^{L}\sum_{q=0}^{2^{\frac{L}{2}+1}-1}\sum_{\kappa=0}^{2^{\frac{L}{2}-1}-1} e^{-i\boldsymbol{q}\cdot(\boldsymbol{r}_m-\boldsymbol{r}_n)} \\
&\times {}_0\langle\{W_p\}|\otimes{}_0\langle\{n_k\}|e^{\frac{i\mathscr{H}t}{\hbar}}\sigma_m^\lambda e^{-\frac{i\mathscr{H}t}{\hbar}}|\{n_k'\}\rangle_\kappa\otimes|\{W_p\}\rangle_q \\
&\times {}_q\langle\{W_p\}|\otimes{}_\kappa\langle\{n_k'\}|\sigma_n^\lambda|\{n_k\}\rangle_0\otimes|\{W_p\}\rangle_0.
\end{aligned} \tag{4.11}$$

Indeed ${}_0\langle\{n_k\}|\alpha_k^\dagger\alpha_k|\{n_k\}\rangle_0 = 0$ $(k = 1,\cdots,\frac{L}{2})$, but the spinon operator α_k and therefore vacuum state $|\{n_k\}\rangle_0$ depend on the background flux configuration $|\{W_p\}\rangle_q$. We denote those against an excited flux configuration $|\{W_p\}\rangle_{q\neq 0}$ by α_k' and $|\{n_k'\}\rangle_0$ distinguishably from α_k and $|\{n_k\}\rangle_0$ against $|\{W_p\}\rangle_0$ in Eq. (4.11). Since spinons in an excited flux sector reads a linear combination of spinons in the ground flux sector, $\alpha_{k'}' = \sum_{k=1}^{L/2}(\chi_{k',k}\alpha_k + \upsilon_{k',k}\alpha_k^\dagger)$ $(k' = 1,\cdots,\frac{L}{2})$, and their vacuum $|\{n_k'\}\rangle_0$ reads a linear combination of the ground-flux-sector spinon vacuum and/or excited states, i.e. either a linear combination of $|\{n_k\}\rangle_0$, $\alpha_{k_1}^\dagger\alpha_{k_2}^\dagger|\{n_k\}\rangle_0$, $\alpha_{k_1}^\dagger\alpha_{k_2}^\dagger\alpha_{k_3}^\dagger\alpha_{k_4}^\dagger|\{n_k\}\rangle_0$, $\cdots$ or that of $\alpha_{k_1}^\dagger|\{n_k\}\rangle_0$, $\alpha_{k_1}^\dagger\alpha_{k_2}^\dagger\alpha_{k_3}^\dagger|\{n_k\}\rangle_0$, $\cdots$, we can exactly calculate the dynamic structure factor (4.11) as well [69]. In higher dimensions, Eq. (4.11) is hard to calculate for sufficiently large systems, with excited flux configurations $|\{W_p\}\rangle_{q\neq 0}$ being no longer invariant under the primitive translation, but we can employ a Dyson equation instead to accomplish the thermodynamic-limit calculation [68, 69].

Figure 8 shows the polarized Raman spectra of gauge-ground Kitaev spin balls with light polarization vectors varying within the xy plane. The polarization dependence of the intensity is very weak in the dodecahedron but significant and individual in the truncated tetrahedron and octahedron. The former observations are similar to the case with the honeycomb Kitaev QSL [24].

The spectral degeneracy within each multidimensional irreducible representation [65] is the case with Kitaev spin balls as well. Considering the QSL ground state (2.10) is invariant under every

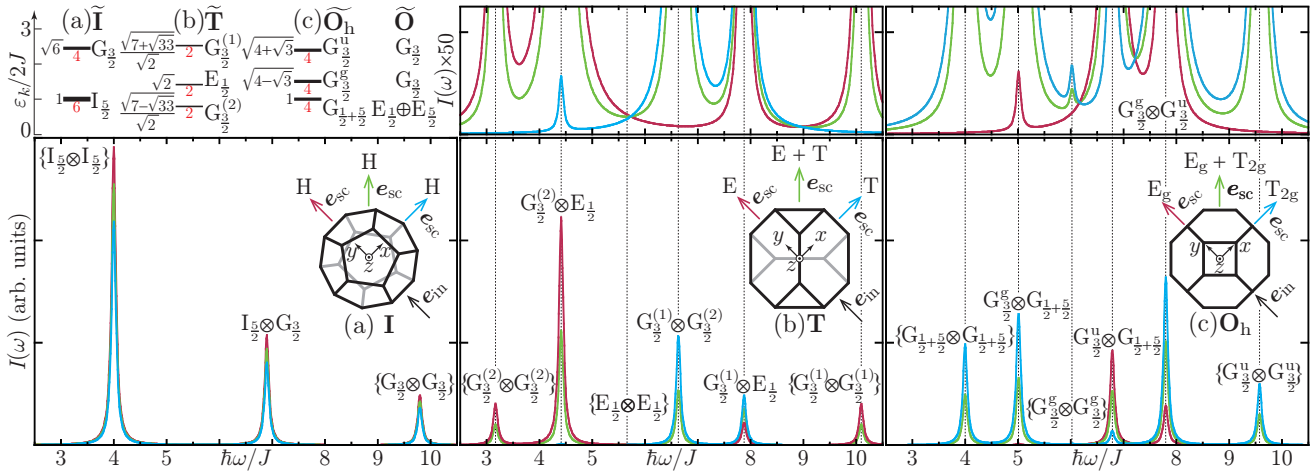

Fig. 8: Spinon excitation energies ε_k and Raman intensities $I(\omega)$ of Kitaev spin balls consisting of dodecahedral (a), truncated-tetrahedral (b), and truncated-octahedral (c) lattices in their ground flux configurations, where δ-function peaks are Lorentzian-broadened by $0.05J$ [59]. For the incident polarization $(\frac{\pi}{2},\frac{\pi}{2})$, we observe various scattered polarizations $(\frac{\pi}{2},\frac{l\pi}{4})$ $(l=0,1,2)$, each consisting of peaks attributable to direct-product representations of the projective symmetry groups $\widetilde{\mathbf{I}}$, $\widetilde{\mathbf{T}}$, and $\widetilde{\mathbf{O}}_{\rm h}$ ($\widetilde{\Xi}_i\otimes\widetilde{\Xi}_j$ in Table 9) on one hand and containing one or more irreducible representations of the point symmetry groups $\mathbf{I}$, $\mathbf{T}$, and $\mathbf{O}_{\rm h}$ ($\bigoplus_k \Xi_k$ in Table 9) on the other hand.

symmetry operation $P\in\mathbf{P}$, the Raman response with $\mathcal{P}\boldsymbol{e}_{\rm in}\equiv\tilde{\boldsymbol{e}}_{\rm in}$ and $\mathcal{P}\boldsymbol{e}_{\rm sc}\equiv\tilde{\boldsymbol{e}}_{\rm sc}$, which we shall denote by $\tilde{I}(\omega)$, should remain the same as $I(\omega)$ with $\boldsymbol{e}_{\rm in}$ and $\boldsymbol{e}_{\rm sc}$, where we denote the matrix representation in Cartesian coordinates for a point symmetry operation P by $\mathcal{P}$. With Eq. (4.1) in mind, a point symmetry operation of the Raman operator reads

$$\begin{aligned}{}^{\rm t}\tilde{\boldsymbol{e}}_{\rm in}\mathcal{R}\tilde{\boldsymbol{e}}_{\rm sc}\equiv\widetilde{\mathscr{R}}&=\sum_{\mu,\nu=x,y,z}\sum_{\mu',\nu'=x,y,z}e^{\mu}_{\rm in}\,{}^{\rm t}\mathcal{P}^{\mu\mu'}\mathcal{R}^{\mu'\nu'}\mathcal{P}^{\nu'\nu}e^{\nu}_{\rm sc}\\&\equiv\sum_{\mu,\nu=x,y,z}e^{\mu}_{\rm in}\widetilde{\mathcal{R}}^{\mu\nu}(P)e^{\nu}_{\rm sc}\equiv{}^{\rm t}\boldsymbol{e}_{\rm in}\widetilde{\mathcal{R}}(P)\boldsymbol{e}_{\rm sc},\end{aligned}\tag{4.12}$$

and therefore, we have an intensity

$$\begin{aligned}\tilde{I}(\omega)&=\int_{-\infty}^{\infty}\frac{dt\,e^{i\omega t}}{2\pi\hbar L}\langle 0|e^{\frac{i\mathscr{H}t}{\hbar}}\widetilde{\mathscr{R}}e^{-\frac{i\mathscr{H}t}{\hbar}}\widetilde{\mathscr{R}}|0\rangle\\&=\sum_{i}{}'\sum_{\mu=1}^{d^{\mathbf{P}}_{\Xi_i}}\left(E^{\mathbf{P}}_{\Xi_i:\mu}\right)^2\int_{-\infty}^{\infty}\frac{dt\,e^{i\omega t}}{2\pi\hbar L}\langle 0|e^{\frac{i\mathscr{H}t}{\hbar}}\widetilde{\mathcal{R}}^{\mathbf{P}}_{\Xi_i:\mu}(P)e^{-\frac{i\mathscr{H}t}{\hbar}}\widetilde{\mathcal{R}}^{\mathbf{P}}_{\Xi_i:\mu}(P)|0\rangle\\&\equiv\sum_{i}{}'\sum_{\mu=1}^{d^{\mathbf{P}}_{\Xi_i}}\left(E^{\mathbf{P}}_{\Xi_i:\mu}\right)^2\tilde{I}^{\mathbf{P}}_{\Xi_i:\mu}(\omega)=\sum_{i}{}'\sum_{\mu=1}^{d^{\mathbf{P}}_{\Xi_i}}\left(E^{\mathbf{P}}_{\Xi_i:\mu}\right)^2 I^{\mathbf{P}}_{\Xi_i:\mu}(\omega).\end{aligned}\tag{4.13}$$

Arbitrary polarization vectors $\boldsymbol{e}_{\rm in}$ and $\boldsymbol{e}_{\rm sc}$ yield arbitrary coefficients $\left(E^{\mathbf{P}}_{\Xi_i:\mu}\right)^2$ and therefore demand that $\tilde{I}^{\mathbf{P}}_{\Xi_i:\mu}(\omega)=I^{\mathbf{P}}_{\Xi_i:\mu}(\omega)$ for every Raman-active mode $\Xi_i:\mu$. It is instructive to review the Raman-active E_2 symmetry species of the $\mathbf{C}_{6\rm v}$ honeycomb lattice [65] on the xy plane. The threefold rotation

about the z axis of the polarization vectors reads converting the Raman operator into

$$C_{3(z)}\mathcal{R} \equiv \widetilde{\mathcal{R}}(C_{3(z)}) = \begin{bmatrix} \widetilde{\mathcal{R}}^{xx}(C_{3(z)}) & \widetilde{\mathcal{R}}^{xy}(C_{3(z)}) \\ \widetilde{\mathcal{R}}^{yx}(C_{3(z)}) & \widetilde{\mathcal{R}}^{zz}(C_{3(z)}) \end{bmatrix} = \begin{bmatrix} -\frac{1}{2} & \frac{\sqrt{3}}{2} \\ -\frac{\sqrt{3}}{2} & -\frac{1}{2} \end{bmatrix} \begin{bmatrix} \mathcal{R}^{xx} & \mathcal{R}^{xy} \\ \mathcal{R}^{yx} & \mathcal{R}^{zz} \end{bmatrix} \begin{bmatrix} -\frac{1}{2} & -\frac{\sqrt{3}}{2} \\ \frac{\sqrt{3}}{2} & -\frac{1}{2} \end{bmatrix}. \tag{4.14}$$

Then the Raman vertices of E_2 symmetry species behave as

$$C_{3(z)}\mathcal{R}^{\mathbf{C}_{6\mathrm{v}}}_{\mathrm{E}_2:1} \equiv \widetilde{\mathcal{R}}^{\mathbf{C}_{6\mathrm{v}}}_{\mathrm{E}_2:1}(C_{3(z)}) = \frac{\widetilde{\mathcal{R}}^{xx}(C_{3(z)}) - \widetilde{\mathcal{R}}^{yy}(C_{3(z)})}{\sqrt{2}} = -\frac{1}{2}\mathcal{R}^{\mathbf{C}_{6\mathrm{v}}}_{\mathrm{E}_2:1} - \frac{\sqrt{3}}{2}\mathcal{R}^{\mathbf{C}_{6\mathrm{v}}}_{\mathrm{E}_2:2}. \tag{4.15}$$

The Raman response of the Kitaev honeycomb QSL remains unchanged against the symmetry operation $C_{3(z)} \in \mathbf{C}_{6\mathrm{v}}$,

$$\begin{aligned} I^{\mathbf{C}_{6\mathrm{v}}}_{\mathrm{E}_2:1}(\omega) = C_{3(z)} I^{\mathbf{C}_{6\mathrm{v}}}_{\mathrm{E}_2:1}(\omega) &= \int_{-\infty}^{\infty} \frac{dt\, e^{i\omega t}}{2\pi\hbar L} \langle 0| e^{\frac{i\mathscr{H}t}{\hbar}} \widetilde{\mathcal{R}}^{\mathbf{C}_{6\mathrm{v}}}_{\mathrm{E}_2:1}(C_{3(z)}) e^{-\frac{i\mathscr{H}t}{\hbar}} \widetilde{\mathcal{R}}^{\mathbf{C}_{6\mathrm{v}}}_{\mathrm{E}_2:1}(C_{3(z)}) |0\rangle \\ &= \frac{1}{4} I^{\mathbf{C}_{6\mathrm{v}}}_{\mathrm{E}_2:1}(\omega) + \frac{3}{4} I^{\mathbf{C}_{6\mathrm{v}}}_{\mathrm{E}_2:2}(\omega), \end{aligned} \tag{4.16}$$

and therefore, we find that $I^{\mathbf{C}_{6\mathrm{v}}}_{\mathrm{E}_2:1}(\omega) = I^{\mathbf{C}_{6\mathrm{v}}}_{\mathrm{E}_2:2}(\omega)$. Next we consider rotating the $\mathbf{T}$ and $\mathbf{O}_{\mathrm{h}}$ polyhedra by $\frac{2\pi}{3}$ about the $[111]$ axis, which reads converting the Raman operator into

$$\begin{aligned} C_{3(111)}\mathcal{R} &\equiv \begin{bmatrix} \widetilde{\mathcal{R}}^{xx}(C_{3(111)}) & \widetilde{\mathcal{R}}^{xy}(C_{3(111)}) & \widetilde{\mathcal{R}}^{xz}(C_{3(111)}) \\ \widetilde{\mathcal{R}}^{yx}(C_{3(111)}) & \widetilde{\mathcal{R}}^{yy}(C_{3(111)}) & \widetilde{\mathcal{R}}^{yz}(C_{3(111)}) \\ \widetilde{\mathcal{R}}^{zx}(C_{3(111)}) & \widetilde{\mathcal{R}}^{zy}(C_{3(111)}) & \widetilde{\mathcal{R}}^{zz}(C_{3(111)}) \end{bmatrix} \\ &= \begin{bmatrix} 0 & 1 & 0 \\ 0 & 0 & 1 \\ 1 & 0 & 0 \end{bmatrix} \begin{bmatrix} \mathcal{R}^{xx} & \mathcal{R}^{xy} & \mathcal{R}^{xz} \\ \mathcal{R}^{yx} & \mathcal{R}^{yy} & \mathcal{R}^{yz} \\ \mathcal{R}^{zx} & \mathcal{R}^{zy} & \mathcal{R}^{zz} \end{bmatrix} \begin{bmatrix} 0 & 0 & 1 \\ 1 & 0 & 0 \\ 0 & 1 & 0 \end{bmatrix}. \end{aligned} \tag{4.17}$$

They each have the two Raman-active symmetry species $\mathrm{E}/\mathrm{E}_{\mathrm{g}}$ and $\mathrm{T}/\mathrm{T}_{2\mathrm{g}}$ and the corresponding Raman vertices behave under the threefold rotation as

$$\begin{aligned} C_{3(111)}\mathcal{R}^{\mathbf{T}/\mathbf{O}_{\mathrm{h}}}_{\mathrm{E}/\mathrm{E}_{\mathrm{g}}:1} &\equiv \widetilde{\mathcal{R}}^{\mathbf{T}/\mathbf{O}_{\mathrm{h}}}_{\mathrm{E}/\mathrm{E}_{\mathrm{g}}:1}(C_{3(111)}) = \frac{2\widetilde{\mathcal{R}}^{zz}(C_{3(111)}) - \widetilde{\mathcal{R}}^{xx}(C_{3(111)}) - \widetilde{\mathcal{R}}^{yy}(C_{3(111)})}{\sqrt{6}} \\ &= -\frac{1}{2}\mathcal{R}^{\mathbf{T}/\mathbf{O}_{\mathrm{h}}}_{\mathrm{E}/\mathrm{E}_{\mathrm{g}}:1} + \frac{\sqrt{3}}{2}\mathcal{R}^{\mathbf{T}/\mathbf{O}_{\mathrm{h}}}_{\mathrm{E}/\mathrm{E}_{\mathrm{g}}:2}, \\ C_{3(111)}\mathcal{R}^{\mathbf{T}/\mathbf{O}_{\mathrm{h}}}_{\mathrm{T}/\mathrm{T}_{2\mathrm{g}}:1} &\equiv \widetilde{\mathcal{R}}^{\mathbf{T}/\mathbf{O}_{\mathrm{h}}}_{\mathrm{T}/\mathrm{T}_{2\mathrm{g}}:1}(C_{3(111)}) = \frac{\widetilde{\mathcal{R}}^{xy}(C_{3(111)}) + \widetilde{\mathcal{R}}^{yx}(C_{3(111)})}{\sqrt{2}} = \mathcal{R}^{\mathbf{T}/\mathbf{O}_{\mathrm{h}}}_{\mathrm{T}/\mathrm{T}_{2\mathrm{g}}:2}, \\ C_{3(111)}\mathcal{R}^{\mathbf{T}/\mathbf{O}_{\mathrm{h}}}_{\mathrm{T}/\mathrm{T}_{2\mathrm{g}}:2} &\equiv \widetilde{\mathcal{R}}^{\mathbf{T}/\mathbf{O}_{\mathrm{h}}}_{\mathrm{T}/\mathrm{T}_{2\mathrm{g}}:2}(C_{3(111)}) = \frac{\widetilde{\mathcal{R}}^{yz}(C_{3(111)}) + \widetilde{\mathcal{R}}^{zy}(C_{3(111)})}{\sqrt{2}} = \mathcal{R}^{\mathbf{T}/\mathbf{O}_{\mathrm{h}}}_{\mathrm{T}/\mathrm{T}_{2\mathrm{g}}:3}, \\ C_{3(111)}\mathcal{R}^{\mathbf{T}/\mathbf{O}_{\mathrm{h}}}_{\mathrm{T}/\mathrm{T}_{2\mathrm{g}}:3} &\equiv \widetilde{\mathcal{R}}^{\mathbf{T}/\mathbf{O}_{\mathrm{h}}}_{\mathrm{T}/\mathrm{T}_{2\mathrm{g}}:3}(C_{3(111)}) = \frac{\widetilde{\mathcal{R}}^{zx}(C_{3(111)}) + \widetilde{\mathcal{R}}^{xz}(C_{3(111)})}{\sqrt{2}} = \mathcal{R}^{\mathbf{T}/\mathbf{O}_{\mathrm{h}}}_{\mathrm{T}/\mathrm{T}_{2\mathrm{g}}:1}. \end{aligned} \tag{4.18}$$

The Raman responses of these Kitaev polyhedral QSLs are invariant under their common symmetry operation $C_{3(111)}$,

$$I^{\mathbf{T}/\mathbf{O}_{\mathrm{h}}}_{\mathrm{E}/\mathrm{E}_{\mathrm{g}}:1}(\omega) = C_{3(111)} I^{\mathbf{T}/\mathbf{O}_{\mathrm{h}}}_{\mathrm{E}/\mathrm{E}_{\mathrm{g}}:1}(\omega) = \frac{1}{4} I^{\mathbf{T}/\mathbf{O}_{\mathrm{h}}}_{\mathrm{E}/\mathrm{E}_{\mathrm{g}}:1}(\omega) + \frac{3}{4} I^{\mathbf{T}/\mathbf{O}_{\mathrm{h}}}_{\mathrm{E}/\mathrm{E}_{\mathrm{g}}:2}(\omega),$$

$$
\begin{aligned}
I^{\mathbf{T}/\mathbf{O}_\mathrm{h}}_{\mathrm{T}/\mathrm{T}_{2\mathrm{g}}:1}(\omega) &= C_{3(111)} I^{\mathbf{T}/\mathbf{O}_\mathrm{h}}_{\mathrm{T}/\mathrm{T}_{2\mathrm{g}}:1}(\omega) = I^{\mathbf{T}/\mathbf{O}_\mathrm{h}}_{\mathrm{T}/\mathrm{T}_{2\mathrm{g}}:2}(\omega), \\
I^{\mathbf{T}/\mathbf{O}_\mathrm{h}}_{\mathrm{T}/\mathrm{T}_{2\mathrm{g}}:2}(\omega) &= C_{3(111)} I^{\mathbf{T}/\mathbf{O}_\mathrm{h}}_{\mathrm{T}/\mathrm{T}_{2\mathrm{g}}:2}(\omega) = I^{\mathbf{T}/\mathbf{O}_\mathrm{h}}_{\mathrm{T}/\mathrm{T}_{2\mathrm{g}}:3}(\omega), \\
I^{\mathbf{T}/\mathbf{O}_\mathrm{h}}_{\mathrm{T}/\mathrm{T}_{2\mathrm{g}}:3}(\omega) &= C_{3(111)} I^{\mathbf{T}/\mathbf{O}_\mathrm{h}}_{\mathrm{T}/\mathrm{T}_{2\mathrm{g}}:3}(\omega) = I^{\mathbf{T}/\mathbf{O}_\mathrm{h}}_{\mathrm{T}/\mathrm{T}_{2\mathrm{g}}:1}(\omega),
\end{aligned} \tag{4.19}
$$

and therefore, we find that $I^{\mathbf{T}/\mathbf{O}_\mathrm{h}}_{\mathrm{E}/\mathrm{E}_\mathrm{g}:1}(\omega) = I^{\mathbf{T}/\mathbf{O}_\mathrm{h}}_{\mathrm{E}/\mathrm{E}_\mathrm{g}:2}(\omega)$ and $I^{\mathbf{T}/\mathbf{O}_\mathrm{h}}_{\mathrm{T}/\mathrm{T}_{2\mathrm{g}}:1}(\omega) = I^{\mathbf{T}/\mathbf{O}_\mathrm{h}}_{\mathrm{T}/\mathrm{T}_{2\mathrm{g}}:2}(\omega) = I^{\mathbf{T}/\mathbf{O}_\mathrm{h}}_{\mathrm{T}/\mathrm{T}_{2\mathrm{g}}:3}(\omega)$. For the Raman-active H symmetry species of the Kitaev dodecahedral QSL as well, we can similarly find the spectral degeneracy $I^{\mathbf{I}}_{\mathrm{H}:1}(\omega) = I^{\mathbf{I}}_{\mathrm{H}:2}(\omega) = I^{\mathbf{I}}_{\mathrm{H}:3}(\omega) = I^{\mathbf{I}}_{\mathrm{H}:4}(\omega) = I^{\mathbf{I}}_{\mathrm{H}:5}(\omega)$.

Now that Eq. (4.9) reduces to

$$
I(\omega) = {\sum_i}' \sum_{\mu=1}^{d^{\mathbf{P}}_{\Xi_i}} \left(E^{\mathbf{P}}_{\Xi_i:\mu}\right)^2 I^{\mathbf{P}}_{\Xi_i:\mu}(\omega) = {\sum_i}' I^{\mathbf{P}}_{\Xi_i:1}(\omega) \sum_{\mu=1}^{d^{\mathbf{P}}_{\Xi_i}} \left(E^{\mathbf{P}}_{\Xi_i:\mu}\right)^2, \tag{4.20}
$$

how many Raman-active modes are possible in the lattice geometry is most decisive of whether and how the scattering intensity depends on the light polarization.

For polarization vectors in the xy plain, $\vartheta_\mathrm{in} = \vartheta_\mathrm{sc} = \frac{\pi}{2}$ with varying φ_in and φ_sc, we have

$$
\begin{aligned}
&\sum_{\mu=1}^{2} \left(E^{\mathbf{C}_{6\mathrm{v}}}_{\mathrm{E}_2:\mu}\right)^2 = \frac{1}{2}; \\
&\sum_{\mu=1}^{5} \left(E^{\mathbf{I}}_{\mathrm{H}:\mu}\right)^2 = \frac{\cos^2(\varphi_\mathrm{in} - \varphi_\mathrm{sc})}{6} + \frac{1}{2}; \\
&\sum_{\mu=1}^{2} \left(E^{\mathbf{T}}_{\mathrm{E}:\mu}\right)^2 = \sum_{\mu=1}^{2} \left(E^{\mathbf{O}_\mathrm{h}}_{\mathrm{E}_\mathrm{g}:\mu}\right)^2 \\
&\qquad\qquad = \frac{\cos^2(\varphi_\mathrm{in} - \varphi_\mathrm{sc})}{6} + \frac{\cos^2(\varphi_\mathrm{in} + \varphi_\mathrm{sc})}{2}, \\
&\sum_{\mu=1}^{3} \left(E^{\mathbf{T}}_{\mathrm{T}:\mu}\right)^2 = \sum_{\mu=1}^{3} \left(E^{\mathbf{O}_\mathrm{h}}_{\mathrm{T}_{2\mathrm{g}}:\mu}\right)^2 = \frac{\sin^2(\varphi_\mathrm{in} + \varphi_\mathrm{sc})}{2};
\end{aligned} \tag{4.21}
$$

hence the perfect depolarization of Raman scattering in a honeycomb QSL. While the $\widetilde{\mathbf{I}}$ gauged dodecahedron also has one and only Raman-active multidimensional irreducible representation and all the three relevant direct-product representations of $\widetilde{\mathbf{I}}$ contain this H mode, the sum of its five basis functions no longer reduces to a constant, resulting in similar shapes peaked at the three fixed frequencies $\hbar\omega/2J = 2,\ 1+\sqrt{6},\ 2\sqrt{6}$ but different weights varying as Eq. (4.21) of the polarized spectra. The $\widetilde{\mathbf{T}}$ and $\widetilde{\mathbf{O}_\mathrm{h}}$ gauged polyhedra each have two Raman-active modes to yield spectra peaking and weighing differently according to the light polarization. Such observations are also the case with $\widetilde{\mathbf{D}_{2\mathrm{h}}}$ harmonic honeycomb Kitaev QSLs in three dimensions [42, 65].

In Eq. (4.20), we have

$$
\sum_{\mu=1}^{2} \left(E^{\mathbf{C}_{6\mathrm{v}}}_{\mathrm{E}_2:\mu}\right)^2 = \frac{1}{2} \sin^2\vartheta_\mathrm{in} \sin^2\vartheta_\mathrm{sc} \tag{4.22}
$$

for the two-dimensional honeycomb lattice,

$$\begin{aligned}\sum_{\mu=1}^{5}\left(E^{\mathbf{I}}_{\mathrm{H}:\mu}\right)^2 &= \frac{1}{6}\left[2\cos\vartheta_{\mathrm{in}}\cos\vartheta_{\mathrm{sc}}-\sin\vartheta_{\mathrm{in}}\sin\vartheta_{\mathrm{sc}}\cos(\varphi_{\mathrm{in}}-\varphi_{\mathrm{sc}})\right]^2\\ &+\frac{1}{2}[\sin\vartheta_{\mathrm{in}}\sin\vartheta_{\mathrm{sc}}\cos(\varphi_{\mathrm{in}}+\varphi_{\mathrm{sc}})]^2\\ &+\frac{1}{2}\left[\sin\vartheta_{\mathrm{in}}\sin\vartheta_{\mathrm{sc}}\sin(\varphi_{\mathrm{in}}+\varphi_{\mathrm{sc}})\right]^2\\ &+\frac{1}{2}(\sin\vartheta_{\mathrm{in}}\sin\varphi_{\mathrm{in}}\cos\vartheta_{\mathrm{sc}}+\cos\vartheta_{\mathrm{in}}\sin\vartheta_{\mathrm{sc}}\sin\varphi_{\mathrm{sc}})^2\\ &+\frac{1}{2}(\cos\vartheta_{\mathrm{in}}\sin\vartheta_{\mathrm{sc}}\cos\varphi_{\mathrm{sc}}+\sin\vartheta_{\mathrm{in}}\cos\varphi_{\mathrm{in}}\cos\vartheta_{\mathrm{sc}})^2\end{aligned}\tag{4.23}$$

for the dodecahedral lattice, and

$$\begin{aligned}\sum_{\mu=1}^{2}\left(E^{\mathbf{T}}_{\mathrm{E}:\mu}\right)^2=\sum_{\mu=1}^{2}\left(E^{\mathbf{O}_{\mathrm{h}}}_{\mathrm{E_g}:\mu}\right)^2 &= \frac{1}{6}\left[2\cos\vartheta_{\mathrm{in}}\cos\vartheta_{\mathrm{sc}}-\sin\vartheta_{\mathrm{in}}\sin\vartheta_{\mathrm{sc}}\cos(\varphi_{\mathrm{in}}-\varphi_{\mathrm{sc}})\right]^2\\ &+\frac{1}{2}\left[\sin\vartheta_{\mathrm{in}}\sin\vartheta_{\mathrm{sc}}\cos(\varphi_{\mathrm{in}}+\varphi_{\mathrm{sc}})\right]^2,\\ \sum_{\mu=1}^{3}\left(E^{\mathbf{T}}_{\mathrm{T}:\mu}\right)^2=\sum_{\mu=1}^{3}\left(E^{\mathbf{O}_{\mathrm{h}}}_{\mathrm{T_{2g}}:\mu}\right)^2 &= \frac{1}{2}\left[\sin\vartheta_{\mathrm{in}}\sin\vartheta_{\mathrm{sc}}\sin(\varphi_{\mathrm{in}}+\varphi_{\mathrm{sc}})\right]^2\\ &+\frac{1}{2}(\sin\vartheta_{\mathrm{in}}\sin\varphi_{\mathrm{in}}\cos\vartheta_{\mathrm{sc}}+\cos\vartheta_{\mathrm{in}}\sin\vartheta_{\mathrm{sc}}\sin\varphi_{\mathrm{sc}})^2\\ &+\frac{1}{2}(\cos\vartheta_{\mathrm{in}}\sin\vartheta_{\mathrm{sc}}\cos\varphi_{\mathrm{sc}}+\sin\vartheta_{\mathrm{in}}\cos\varphi_{\mathrm{in}}\cos\vartheta_{\mathrm{sc}})^2\end{aligned}\tag{4.24}$$

for the truncated tetrahedral and octahedral lattices. For the honeycomb lattice, we take interest only in the polarization vectors parallel to the plain,

$$\sum_{\mu=1}^{2}\left(E^{\mathbf{C}_{6\mathrm{v}}}_{\mathrm{E_2}:\mu}\right)^2\Bigg|_{\vartheta_{\mathrm{in}}=\vartheta_{\mathrm{sc}}=\frac{\pi}{2}}=\frac{1}{2},\tag{4.25}$$

and find no polarization dependence of the Raman response within the LF scheme. For the dodecahedral lattice, even if we restrict the polarization vectors to the xy plain, the Raman response still exhibits weak polarization dependence even within the LF scheme,

$$\sum_{\mu=1}^{5}\left(E^{\mathbf{I}}_{\mathrm{H}:\mu}\right)^2\Bigg|_{\vartheta_{\mathrm{in}}=\vartheta_{\mathrm{sc}}=\frac{\pi}{2}}=\frac{1}{6}\cos^2(\varphi_{\mathrm{in}}-\varphi_{\mathrm{sc}})+\frac{1}{2},\tag{4.26}$$

i.e., the spectra peak exactly the same but weigh differently according to the light polarization. For the truncated tetrahedral and octahedral lattices, even if we consider the Raman scattering within the LF scheme and restrict the polarization vectors to the xy plain, we have two Raman-active symmetry species to find strong polarization dependence of the spectra,

$$\sum_{\mu=1}^{2}\left(E^{\mathbf{T}}_{\mathrm{E}:\mu}\right)^2\Bigg|_{\vartheta_{\mathrm{in}}=\vartheta_{\mathrm{sc}}=\frac{\pi}{2}}=\sum_{\mu=1}^{2}\left(E^{\mathbf{O}_{\mathrm{h}}}_{\mathrm{E_g}:\mu}\right)^2\Bigg|_{\vartheta_{\mathrm{in}}=\vartheta_{\mathrm{sc}}=\frac{\pi}{2}}=\frac{1}{6}\cos^2(\varphi_{\mathrm{in}}-\varphi_{\mathrm{sc}})+\frac{1}{2}\cos^2(\varphi_{\mathrm{in}}+\varphi_{\mathrm{sc}}),$$

$$\sum_{\mu=1}^{3}\left(E^{\mathbf{T}}_{\mathrm{T}:\mu}\right)^2\Bigg|_{\vartheta_{\mathrm{in}}=\vartheta_{\mathrm{sc}}=\frac{\pi}{2}}=\sum_{\mu=1}^{3}\left(E^{\mathbf{O}_{\mathrm{h}}}_{\mathrm{T}_{2\mathrm{g}}:\mu}\right)^2\Bigg|_{\vartheta_{\mathrm{in}}=\vartheta_{\mathrm{sc}}=\frac{\pi}{2}}=\frac{1}{2}\sin^2(\varphi_{\mathrm{in}}+\varphi_{\mathrm{sc}}),\tag{4.27}$$

i.e., spectra peak and weigh differently according to the light polarization. Note in this context that we do not have any accidental degeneracy, i.e., neither $I^{\mathbf{T}}_{\mathrm{E}:1}(\omega)$ equals $I^{\mathbf{T}}_{\mathrm{T}:1}(\omega)$ nor $I^{\mathbf{O}_{\mathrm{h}}}_{\mathrm{E}_{\mathrm{g}}:1}(\omega)$ equals $I^{\mathbf{O}_{\mathrm{h}}}_{\mathrm{T}_{2\mathrm{g}}:1}(\omega)$.

4.3 Raman intensity at absolute zero: projective-symmetry argument

The $\widetilde{\mathbf{T}}$ and $\widetilde{\mathbf{O}_{\mathrm{h}}}$ gauged polyhedra each have three spinon modes to yield geminate excitations of $3 +_3 \mathrm{C}_2$ types. There are 6 pair-spinon-resonant frequencies in them each. In the case of $\widetilde{\mathbf{T}}$, one of them, $\{\mathrm{E}_{\frac{1}{2}} \otimes \mathrm{E}_{\frac{1}{2}}\}$ ($\hbar\omega/2J = 2\sqrt{2}$), is a Rayleigh channel, while all the rest contain the Raman-active E (detectable with $\varphi_{\mathrm{in}} \pm \varphi_{\mathrm{sc}} \neq \frac{\pi}{2}$) and/or T (detectable with $\varphi_{\mathrm{in}} + \varphi_{\mathrm{sc}} \neq 0, \pi$) modes, where the two-dimensional real irreducible representation $\mathrm{E} \equiv \mathrm{E}^{(1)} \oplus \mathrm{E}^{(2)}$ splits into two one-dimensional complex ones, $\mathrm{E}^{(1)}$ and $\mathrm{E}^{(2)}$, bringing nonvanishing Raman intensities at all the six frequencies but $\hbar\omega/2J = 2\sqrt{2}$. In the case of $\widetilde{\mathbf{O}_{\mathrm{h}}}$, all the direct-product representations contain the Raman-active $\mathrm{T}_{2\mathrm{g}}$ mode (detectable with $\varphi_{\mathrm{in}} + \varphi_{\mathrm{sc}} \neq 0, \pi$), bringing nonvanishing Raman intensities at all the six frequencies. On the other hand, only the three direct-product representations $\mathrm{G}^{\mathrm{g}}_{\frac{3}{2}} \otimes \mathrm{G}_{\frac{1}{2}+\frac{5}{2}}$ ($\hbar\omega/2J = 1+\sqrt{4-\sqrt{3}}$), $\mathrm{G}^{\mathrm{u}}_{\frac{3}{2}} \otimes \mathrm{G}_{\frac{1}{2}+\frac{5}{2}}$ ($\hbar\omega/2J = 1+\sqrt{4+\sqrt{3}}$), and $\mathrm{G}^{\mathrm{g}}_{\frac{3}{2}} \otimes \mathrm{G}^{\mathrm{u}}_{\frac{3}{2}}$ ($\hbar\omega/2J = \sqrt{4-\sqrt{3}}+\sqrt{4+\sqrt{3}}$) contain another Raman-active mode E_{g} (detectable with $\varphi_{\mathrm{in}} \pm \varphi_{\mathrm{sc}} \neq \frac{\pi}{2}$). In this context, we should pay special attention to the geminate excitations labeled $\{\mathrm{G}^{\mathrm{g}}_{\frac{3}{2}} \otimes \mathrm{G}^{\mathrm{g}}_{\frac{3}{2}}\}$ ($\hbar\omega/2J = 2\sqrt{4-\sqrt{3}}$) and $\{\mathrm{G}^{\mathrm{u}}_{\frac{3}{2}} \otimes \mathrm{G}^{\mathrm{u}}_{\frac{3}{2}}\}$ ($\hbar\omega/2J = 2\sqrt{4+\sqrt{3}}$). If we describe this gauged polyhedron in terms of $\widetilde{\mathbf{O}}$, rather than $\widetilde{\mathbf{O}_{\mathrm{h}}}$, these two direct-product representations degenerate into $\{\mathrm{G}_{\frac{3}{2}} \otimes \mathrm{G}_{\frac{3}{2}}\} = \{\underline{\mathrm{A}_1}\} \oplus \{\underline{\underline{\mathrm{E}}}\} \oplus \{\underline{\underline{\mathrm{T}_2}}\}$ (see Table 9) to cause misunderstanding as if outgoing photons of $\varphi_{\mathrm{sc}} = \varphi_{\mathrm{in}}$ brought nonvanishing Raman intensities at the two frequencies $\hbar\omega/2J = 2\sqrt{4 \mp \sqrt{3}}$ as well. Under the pertinent $\widetilde{\mathbf{O}_{\mathrm{h}}}$ description, the Raman intensities at the two frequencies $\hbar\omega/2J = 2\sqrt{4 \mp \sqrt{3}}$ in the gauged truncated octahedron purely belongs to the $\mathrm{T}_{2\mathrm{g}}$ symmetry species, because they are mediated by spinon geminate excitations belonging to the direct-product representations $\{\mathrm{G}^{\mathrm{g}}_{\frac{3}{2}} \otimes \mathrm{G}^{\mathrm{g}}_{\frac{3}{2}}\}$ and $\{\mathrm{G}^{\mathrm{u}}_{\frac{3}{2}} \otimes \mathrm{G}^{\mathrm{u}}_{\frac{3}{2}}\}$, both of which decompose into $\{\underline{\mathrm{A}_{1\mathrm{g}}}\} \oplus \{\mathrm{E}_{\mathrm{u}}\} \oplus \{\underline{\underline{\mathrm{T}_{2\mathrm{g}}}}\}$, i.e., the Raman-active $\mathrm{T}_{2\mathrm{g}}$, LF-Raman-inactive $\mathrm{A}_{1\mathrm{g}}$, and Raman-inactive E_{u} (instead of Raman-active E_{g}) symmetry species (see Table 9).

In an attempt to describe partons in Kitaev truncated octahedron, MPT [49] restrict their symmetry argument to gauged rotations $\widetilde{\mathbf{R}} \subset \mathrm{SU}(2) \cong \mathrm{Spin}(3)$, i.e. double covers of pure rotation groups $\mathbf{R} \subset \mathrm{SO}(3)$, because they employ projective symmetry groups with the aim to characterize an itinerant parton as a charged particle in quantized orbital motion, and therefore need the isomorphism $\mathrm{SU}(2)/\mathbb{Z}_2 \cong \mathrm{SO}(3)$. For partons emergent in a gauged truncated octahedron, they consider gauging the subgroup $\mathbf{O}$ of the full octahedral group $\mathbf{O}_{\mathrm{h}}$. On the other hand, in order to describe spinon geminate, rather than single, excitations in the context of Raman scattering, we construct and have to construct the double cover of $\mathbf{O}_{\mathrm{h}} \subset \mathrm{O}(3)$ [70] instead of that of $\mathbf{O} \subset \mathrm{SO}(3)$. It is not until we analyze the projective symmetry of Majorana spinons to the fullest extent that we can correctly understand Raman scattering in a time-reversal-invariant gauged polyhedron.

4.4 Raman intensity at finite temperatures

Taking the Kitaev dodecahedron as an example, we see the effect of Raman scattering intensity at finite temperature. The Raman scattering intensity at finite temperature reads [25, 35]

$$I(\omega)=\frac{1}{2\pi\hbar L}\int_{-\infty}^{\infty}\langle e^{\frac{i\mathscr{H}t}{\hbar}}\mathscr{R}e^{-\frac{i\mathscr{H}t}{\hbar}}\mathscr{R}\rangle_T e^{i\omega t}dt, \tag{4.28}$$

where $\langle\hat{A}\rangle_T$ is a thermal expectation value of operator $\hat{A}$. If we fix a bond configuration and diagonalize Majorana Hamiltonian, we can express Raman operator in terms of quasi-particles:

$$c_l=\sum_{k=1}^{L/2}\left[(\psi_{l,2k-1}-\mathrm{i}\psi_{l,2k})\alpha_k+(\psi_{l,2k-1}+\mathrm{i}\psi_{l,2k})\alpha_k^\dagger\right], \tag{4.29}$$

$$\begin{aligned}\mathscr{R}&=\frac{1}{2}\sum_{m,n=1}^{L}iJ(\boldsymbol{e}_{\mathrm{in}}\cdot\boldsymbol{d}_{mn})(\boldsymbol{e}_{\mathrm{sc}}\cdot\boldsymbol{d}_{mn})u_{<m,n>_\lambda}\\&\quad\times\sum_{k=1}^{N}\left[(\psi_{m,2k-1}-\mathrm{i}\psi_{m,2k})\alpha_k+(\psi_{m,2k-1}+\mathrm{i}\psi_{m,2k})\alpha_k^\dagger\right]\\&\quad\times\sum_{k=1}^{N}\left[(\psi_{n,2k'-1}-\mathrm{i}\psi_{n,2k'})\alpha_{k'}+(\psi_{n,2k'-1}+\mathrm{i}\psi_{n,2k'})\alpha_{k'}^\dagger\right]\\&=\frac{1}{2}\sum_{k,l=1}^{N}\left[C_{k,k'}\left(2\alpha_k^\dagger\alpha_{k'}-\delta_{k,k'}\right)+D_{k',k}^*\alpha_k\alpha_{k'}+D_{k,k'}\alpha_k^\dagger\alpha_{k'}^\dagger\right];\end{aligned} \tag{4.30}$$

$$C_{k,k'}\equiv\sum_{m,n=1}^{L}iJ(\boldsymbol{e}_{\mathrm{in}}\cdot\boldsymbol{d}_{mn})(\boldsymbol{e}_{\mathrm{sc}}\cdot\boldsymbol{d}_{mn})(\psi_{m,2k-1}-\mathrm{i}\psi_{m,2k})(\psi_{n,2k'-1}+\mathrm{i}\psi_{n,2k'}), \tag{4.31}$$

$$D_{k,k'}\equiv\sum_{m,n=1}^{L}iJ(\boldsymbol{e}_{\mathrm{in}}\cdot\boldsymbol{d}_{mn})(\boldsymbol{e}_{\mathrm{sc}}\cdot\boldsymbol{d}_{mn})(\psi_{m,2k-1}+\mathrm{i}\psi_{m,2k})(\psi_{n,2k'-1}+\mathrm{i}\psi_{n,2k'}). \tag{4.32}$$

Using Bloch-de Dominicis theorem for fermion operator

$$\langle\hat{A}\hat{B}\hat{C}\hat{D}\rangle_T=\langle\hat{A}\hat{B}\rangle_T\langle\hat{C}\hat{D}\rangle_T-\langle\hat{A}\hat{C}\rangle_T\langle\hat{B}\hat{D}\rangle_T+\langle\hat{A}\hat{D}\rangle_T\langle\hat{B}\hat{C}\rangle_T, \tag{4.33}$$

then,

$$\begin{aligned}I(\omega)=\frac{1}{8\pi\hbar L}\sum_{k,k',k'',k'''=1}^{L/2}\int_{-\infty}^{\infty}dt\,e^{i\omega t}\Big[&4C_{k,k''}C_{k',k'''}\langle e^{\frac{i\mathscr{H}t}{\hbar}}\alpha_k^\dagger e^{-\frac{i\mathscr{H}t}{\hbar}}e^{\frac{i\mathscr{H}t}{\hbar}}\alpha_{k''}e^{-\frac{i\mathscr{H}t}{\hbar}}\alpha_{k'}^\dagger\alpha_{k'''}\rangle_T\\&+D_{k'',k}^*D_{k',k'''}\langle e^{\frac{i\mathscr{H}t}{\hbar}}\alpha_k e^{-\frac{i\mathscr{H}t}{\hbar}}e^{\frac{i\mathscr{H}t}{\hbar}}\alpha_{k''}e^{-\frac{i\mathscr{H}t}{\hbar}}\alpha_{k'}^\dagger\alpha_{k'''}^\dagger\rangle\\&+D_{k,k''}D_{k''',k'}^*\langle e^{\frac{i\mathscr{H}t}{\hbar}}\alpha_k^\dagger e^{-\frac{i\mathscr{H}t}{\hbar}}e^{\frac{i\mathscr{H}t}{\hbar}}\alpha_{k''}^\dagger e^{-\frac{i\mathscr{H}t}{\hbar}}\alpha_{k'}\alpha_{l'}\rangle_T\Big]\end{aligned}$$

$$
\begin{aligned}
&= \frac{1}{8\pi\hbar L}\sum_{k,k',k'',k'''=1}^{L/2}\int_{-\infty}^{\infty} dt\, e^{i\omega t} \\
&\quad\times\Big[4C_{k,k}C_{k',k'}\delta_{k,k''}\delta_{k,k'''}\langle e^{\frac{i\mathscr{H}t}{\hbar}}\alpha_k^\dagger e^{-\frac{i\mathscr{H}t}{\hbar}}e^{\frac{i\mathscr{H}t}{\hbar}}\alpha_k e^{-\frac{i\mathscr{H}t}{\hbar}}\rangle_T\langle\alpha_{k'}^\dagger\alpha_{k'}\rangle_T \\
&\qquad+4C_{k,k''}C_{k'',k}\delta_{k,k'''}\delta_{k''',k'}\langle e^{\frac{i\mathscr{H}t}{\hbar}}\alpha_k^\dagger e^{-\frac{i\mathscr{H}t}{\hbar}}\alpha_k\rangle_T\langle e^{\frac{i\mathscr{H}t}{\hbar}}\alpha_{k''}e^{-\frac{i\mathscr{H}t}{\hbar}}\alpha_{k''}^\dagger\rangle_T \\
&\qquad+D_{k'',k}^*D_{k',k'''}\big(-\delta_{k,k'}\delta_{k'',k'''}\langle e^{\frac{i\mathscr{H}t}{\hbar}}\alpha_k e^{-\frac{i\mathscr{H}t}{\hbar}}\alpha_k^\dagger\rangle_T\langle e^{\frac{i\mathscr{H}t}{\hbar}}\alpha_{k''}e^{-\frac{i\mathscr{H}t}{\hbar}}\alpha_{k''}^\dagger\rangle_T \\
&\qquad\qquad+\delta_{k,k'''}\delta_{k'',k'}\langle e^{\frac{i\mathscr{H}t}{\hbar}}\alpha_k e^{-\frac{i\mathscr{H}t}{\hbar}}\alpha_k^\dagger\rangle_T\langle e^{\frac{i\mathscr{H}t}{\hbar}}\alpha_{k''}e^{-\frac{i\mathscr{H}t}{\hbar}}\alpha_{k''}^\dagger\rangle_T\big) \\
&\qquad+D_{k,k''}D_{k''',k'}^*\big(-\delta_{k,k'}\delta_{k'',k'''}\langle e^{\frac{i\mathscr{H}t}{\hbar}}\alpha_k^\dagger e^{-\frac{i\mathscr{H}t}{\hbar}}\alpha_k\rangle_T\langle\alpha_{k''}^\dagger(t)\alpha_{k''}\rangle_T \\
&\qquad\qquad+\delta_{k,k'''}\delta_{k'',k'}\langle e^{\frac{i\mathscr{H}t}{\hbar}}\alpha_k^\dagger e^{-\frac{i\mathscr{H}t}{\hbar}}\alpha_k\rangle_T\langle e^{\frac{i\mathscr{H}t}{\hbar}}\alpha_{k''}^\dagger e^{-\frac{i\mathscr{H}t}{\hbar}}\alpha_{k''}\rangle_T\big)\Big] \\
&=\frac{1}{2L}\sum_{k,k'=1}^{L/2}\Big[2\underbrace{C_{k,k}C_{k',k'}\left\langle\alpha_k^\dagger\alpha_k\right\rangle_T\left\langle\alpha_{k'}^\dagger\alpha_{k'}\right\rangle_T\delta(\hbar\omega)}_{\text{Rayleigh term}} \\
&\qquad+2|C_{k,k'}|^2\left\langle\alpha_k^\dagger\alpha_k\right\rangle_T(1-\left\langle\alpha_{k'}^\dagger\alpha_{k'}\right\rangle_T)\delta(\hbar\omega+\varepsilon_k-\varepsilon_{k'}) \\
&\qquad+|D_{k,k'}|^2\left\langle\alpha_k^\dagger\alpha_k\right\rangle_T\left\langle\alpha_{k'}^\dagger\alpha_{k'}\right\rangle_T\delta(\hbar\omega+\varepsilon_k+\varepsilon_{k'}) \\
&\qquad+|D_{k,k'}|^2(1-\left\langle\alpha_k^\dagger\alpha_k\right\rangle_T)(1-\left\langle\alpha_{k'}^\dagger\alpha_{k'}\right\rangle_T)\delta(\hbar\omega-\varepsilon_k-\varepsilon_{k'})\Big]. \qquad (4.34)
\end{aligned}
$$

First term of Eq. (4.34) is the Rayleigh term and thus don't contribute Raman scattering process. Since $\langle 0|\alpha_k^\dagger\alpha_k|0\rangle = 0$, Raman scattering intensity at absolute zero only comes from the last term of Eq. (4.34), that is, Majorana-geminate excitation modes. In contrast, at finite temperatures, Raman intensity reflects Majorana creation and annihilation process occurs in addition to pair-creation process. This creation and annihilation process can be detectable in *fermionic* T independence of integrated Raman intensity process [25].

Figure 9(a) shows $I(\omega)$ as a function of temperature. As soon as visons are thermally excited, $\hat{W}_p$ configurations breaks the symmetry of $\mathbf{I}$ and the Majorana Hamiltonian is no longer belongs to $\widetilde{\mathbf{I}}$. However, The flux state in which the symmetry is broken is degenerated so that the symmetry $\mathbf{I}$ is restored. Therefore, as a result of taking the thermal average, the polarization dependence of the Raman scattering intensity of group $\mathbf{P}$ is maintained.

Figure 9(b) shows $I(\omega)$ of various polarization vectors at $k_{\mathrm{B}}T = 0.2J$. The peak structure seen at absolute zero has almost disappeared, but the polarization dependence of $\mathbf{I}$ in Eq. (4.26) is maintained, i.e., the spectra peak exactly the same but weigh differently according to the light polarization.

Vison excitations can be measured by the parameter [39, 71]

$$
w_{\mathrm{P}} = \frac{1}{Z}\sum_{q=0}^{2^{\frac{L}{2}+1}-1}\sum_{\kappa=0}^{2^{\frac{L}{2}-1}-1} {}_q\langle\{W_p\}|\otimes{}_\kappa\langle\{n_k\}|\mathrm{e}^{-\beta\mathscr{H}}\hat{w}_{\mathrm{P}}|\{n_k\}\rangle_\kappa\otimes|\{W_p\}\rangle_q; \qquad (4.35)
$$

$$
Z = \sum_{q=0}^{2^{\frac{L}{2}+1}-1}\sum_{\kappa=0}^{2^{\frac{L}{2}-1}-1} {}_q\langle\{W_p\}|\otimes{}_\kappa\langle\{n_k\}|\mathrm{e}^{-\beta\mathscr{H}}|\{n_k\}\rangle_\kappa\otimes|\{W_p\}\rangle_q, \qquad (4.36)
$$

$$
\hat{w}_{\mathrm{P}} \equiv \frac{5}{3L}\left|\sum_{p=1}^{3L/5}\hat{W}_p\right| \qquad (4.37)
$$

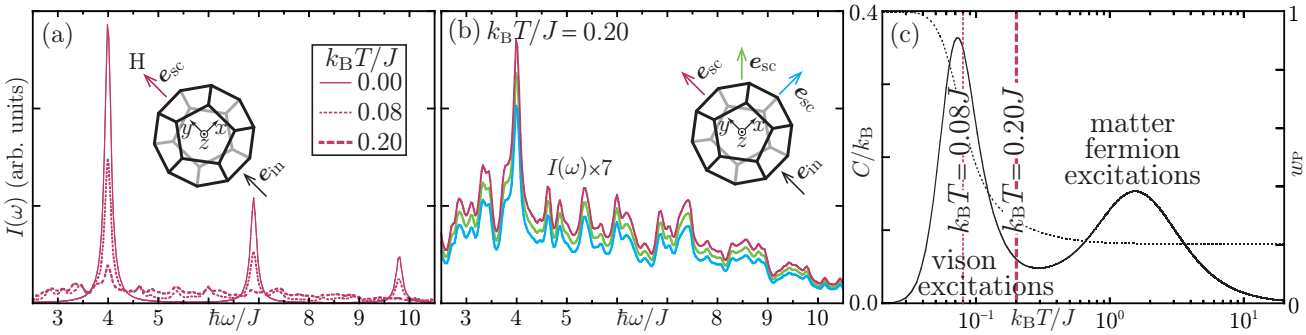

Fig. 9: Thermodynamic quantities of the Kitaev dodecahedron. (a) $I(\omega)$ at various T with $(\vartheta_{\rm in}, \varphi_{\rm in}) = (\frac{\pi}{4}, 0)$ and $(\vartheta_{\rm sc}, \varphi_{\rm sc}) = (\frac{3\pi}{4}, \pi)$; where $\boldsymbol{e}_{\rm in} \equiv (1, \vartheta_{\rm in}, \varphi_{\rm in})$ and $\boldsymbol{e}_{\rm sc} \equiv (1, \vartheta_{\rm sc}, \varphi_{\rm sc})$; (b) $I(\omega)$ at $k_{\rm B}T = 0.2J$ with $(\vartheta_{\rm in}, \varphi_{\rm in}) = (\frac{\pi}{2}, 0)$ and $\vartheta_{\rm sc} = \frac{\pi}{2}$, $\varphi_{\rm sc} = \frac{\pi}{4}, \frac{\pi}{2}, \pi$. (c) Specific heat C and the flux-sum magnitude $w_{\rm P}$ as functions of T.

and observed through specific heat. Figure 9(c) shows their temperature dependences. $w_{\rm P} = 1$ without any vison at absolute zero, while $w_{\rm P} = 5040/2048/12 = 0.205078125$ with visons emerging at random in the $T \to \infty$ limit. At $k_{\rm B}T = 0.2J$, visons are almost fully excited and therefore the symmetry-definite Raman scattering intensity peaks melt away. Matter fermions are excited at much higher temperatures. Specific heat is thus doubly peaked with increasing temperature.

5 Summary and Discussion

We have analyzed the Raman scattering intensity in the Kitaev quantum spin liquid from two viewpoints, point symmetry group and projective symmetry group. Vanishing polarization dependence seen in the Kitaev honeycomb model and the Kagome antiferromagnet is due to the two-dimensional three-fold rotational symmetry. Point symmetry group analysis shows that the polarization dependence in the quantum spin liquid depends on their lattice (cf. Table 10). Vanishing light polarization dependence of Raman scattering is not necessarily for quantum spin liquids. Quantum spin liquids on lattices with multiple Raman active modes can have strong polarization dependence.

Table. 10: Projective symmetry group and polarization dependence of the Kitaev honeycomb model and Kitaev spin balls

model	projective symmetry group	polarization dependence
honeycomb	$\widetilde{\mathbf{C}_{6\mathrm{v}}}$	*no*
dodecahedron	$\widetilde{\mathbf{I}}$	*little*
truncated tetrahedron	$\widetilde{\mathbf{T}}$	*strong*
truncated octahedron	$\widetilde{\mathbf{O}_{\mathrm{h}}}$	*strong*

If a Kitaev quantum spin liquid has strong polarization dependence, the projective symmetry of spinons can be seen in the Raman scattering process through the selection rule. Two spinons excited states is characterized by the direct-product representation of projective symmetry group of Majorana spinons. The direct-product representation consists of single-valued irreducible representations of the $\mathbb{Z}_2$ gauge extension of the point symmetry group. This single-valued irreducible representations correspond to those of original point symmetry group. If the intermediate state consists Raman inactive mode only, the state is Raman inactive. In addition, for Kitaev models with even-sided polygons only, it is necessary to consider the gauge expansion of point symmetry groups $\subset \mathrm{O}(3)$ to determine whether it is Raman activity or not. In the Kitaev truncated octahedron, the Raman scattering intensity actually reflects the $\widetilde{\mathbf{O}_{\mathrm{h}}}$. This result indicates that the symmetry of Majorana spinon may be highlighted by analysing the polarization dependence.

Our approach to Raman observations of QSLs is feasible regardless of whatever geometry and dimension. For instance, let us discuss about two-dimensional Kitaev diamond-square lattice [72]. The diamond-square lattice is of $\mathbf{P}_{\mathrm{org}} = \mathbf{C}_{4\mathrm{v}}$ point symmetry [see Figs. 10(a) and (b)]. Since diamond-square lattice consists only of even-sided polygons, the gauge-ground Kitaev diamond-square lattice belong to gauged point group $\widetilde{\mathbf{C}_{4\mathrm{v}}}$ as well as the case of Kitaev truncated octahedron. The isotropy group of $\boldsymbol{k}$ in the first Brillouin zone $\mathbf{P}_{\boldsymbol{k}}$ consists of symmetry operations $P_{\boldsymbol{k}}$ such that

$$P_{\boldsymbol{k}}\boldsymbol{k} = \boldsymbol{k} + \boldsymbol{K} \cong \boldsymbol{k} \tag{5.1}$$

with $\boldsymbol{K}$ being $\mathbf{0}$ or a reciprocal lattice vector. The $\mathbb{Z}_2$-gauged $\boldsymbol{k}$-point symmetry group $\widetilde{\mathbf{P}'_{\boldsymbol{k}}}$ keeps the $\boldsymbol{k}_\kappa$ block of the gauge-ground Majorana Hamiltonian invariant. Under the Fourier transformation for primitive translation of the lattice, $\widetilde{\mathbf{P}'_{\boldsymbol{k}}}$ should consist of *primitive-translation-invariant* gauged point symmetry operations, i.e., $\widetilde{\mathbf{P}'_{\boldsymbol{k}}}$ may be written as $\widetilde{\mathbf{P}'_{\mathbf{0}}}$ with $\mathbf{P}'_{\mathbf{0}} \subseteq \mathbf{P}_{\mathbf{0}}$. $\mathbf{P}_{\mathbf{0}}$ equals the full point symmetry group of the background lattice $\mathbf{P}_{\rm org}$ and reads $\mathbf{C}_{4\rm v}$. Figure 10(b) shows that the gauge transformations $\Lambda(C_4)$ recover the initial ground gauge configuration but break the primitive translation symmetry. Thus, every $\mathbf{P}'_{\mathbf{0}}$ is limited to a proper subset of $\mathbf{P}_{\mathbf{0}}$, $\mathbf{P}'_{\mathbf{0}} \subset \mathbf{P}_{\mathbf{0}}$, for the diamond-square lattice. We show in Fig. 10(c) how $\mathbf{P}_{\boldsymbol{k}}$ and $\widetilde{\mathbf{P}'_{\mathbf{0}}}$ read at high symmetry points of the diamond-square reciprocal lattice. $\widetilde{\mathbf{P}'_{\mathbf{0}}}$ becomes $\widetilde{\mathbf{C}_{2\rm v}}$ even at the highest symmetry points Γ and M. The thus-defined

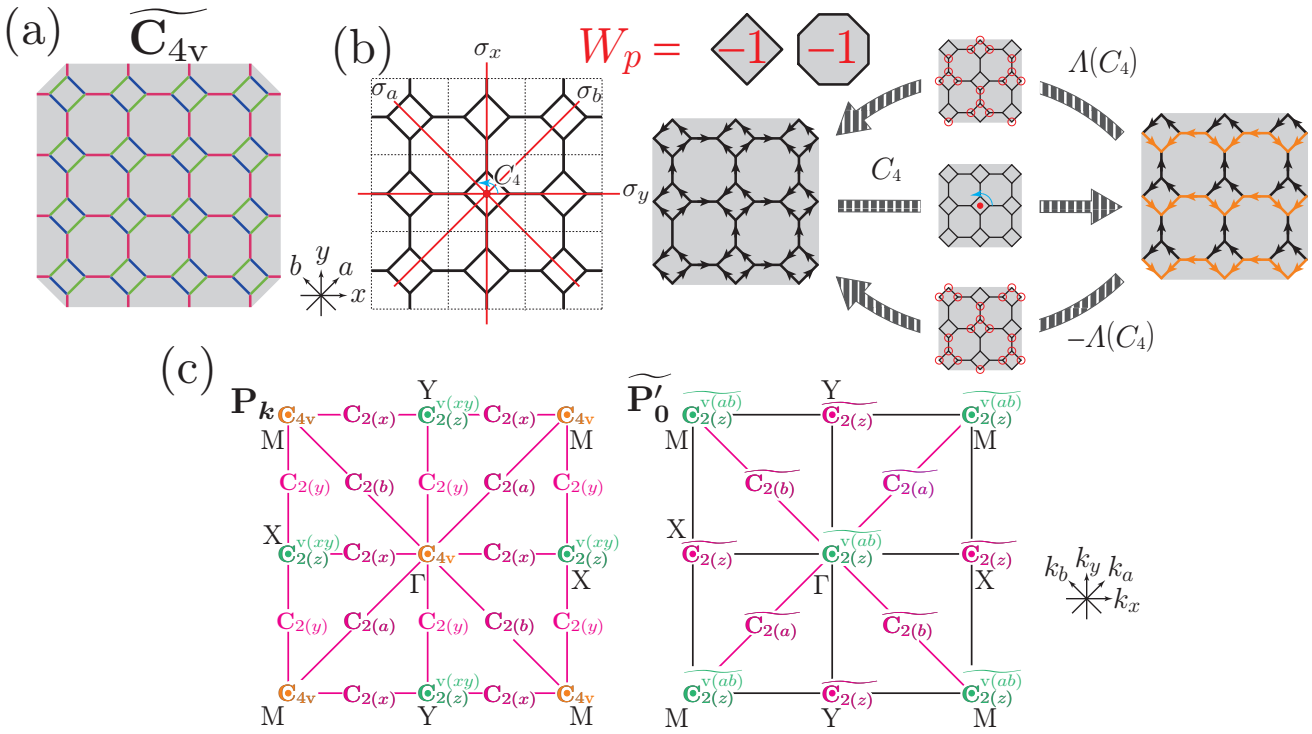

Fig. 10: (a) Kitaev diamond-square lattice of ground flux configurations. The diamond-square lattice of $\mathbf{C}_{4\rm v}$ point symmetry with primitive cells enriched by dotted lines. Gauge-ground Kitaev diamond-square is characterized by $\widetilde{\mathbf{C}_{4\rm v}}$. (b) Gauged rotations of gauge-ground Kitaev diamond-square lattice. C_4 can be followed by no such gauge transformation as to recover the initial bond configuration with the primitive translation vectors remaining unchanged. (c) $\boldsymbol{k}$-point symmetry groups (isotropy groups of $\boldsymbol{k}$) $\mathbf{P}_{\boldsymbol{k}}$ at high symmetry points $\boldsymbol{k}$ of the diamond-square reciprocal lattice, each consisting of symmetry operations $\mathbf{P}_{\boldsymbol{k}}$. $\mathbb{Z}_2$-gauged $\boldsymbol{k}$-point symmetry groups $\widetilde{\mathbf{P}'_{\boldsymbol{k}}}$ under the Fourier transformation for primitive translation of the lattice, i.e. $\widetilde{\mathbf{P}'_{\mathbf{0}}}$, at high symmetry points $\boldsymbol{k}_\kappa$ of the diamond-square reciprocal lattice, each keeping the $\boldsymbol{k}_\kappa$ block of the Fourier-transformed gauge-ground Majorana Hamiltonian invariant. We specify the principal axis τ for n-fold rotations and/or the normal vector σ for mirror operations and replace the usual Schönflies notation $\mathbf{C}_{n(\tau)\rm v(\sigma)}$ by $\mathbf{C}^{\rm v(\sigma)}_{n(\tau)}$ for the sake of saving space.

projective symmetry group of the $\mathbb{Z}_2$-gauged diamond-square lattice reads $\mathbf{L} \wedge \widetilde{\mathbf{C}_{2\mathrm{v}}}$, where $\mathbf{L}$ is a two-dimensional translation group. Eigenspectra of the gauge-ground Kitaev diamond-square lattice are no longer discrete but consist of continuous bands. The “momentum-locked" spinon geminate excitations are distinguished and identified by light polarizations and direct-product representations of $\mathbf{L} \wedge \widetilde{\mathbf{P}}$ [73]. We can identify emergent spinons singly by combining a standard point-symmetry-group analysis of the Raman vertex in the real space and an elaborate projective-symmetry-group analysis of Raman-scattering-mediating Majorana spinons in the reciprocal space. A more detailed analysis of the Raman scattering response of the planar Kitaev model is discussed in Ref. 72.

Another extension of our approach is going beyond the LF vertices [26, 27]. In the $\widetilde{\mathbf{T}}$ Kitaev spin ball, the direct-product representation $\{\mathrm{E}_{\frac{1}{2}} \otimes \mathrm{E}_{\frac{1}{2}}\}$ is Raman-inactive within the LF scheme (cf. Table 9), but an $\mathrm{E}_{\frac{1}{2}}$ multiple direct-product representation may become Raman active in higher-order scatterings to visualize the Majorana spinon spectrum in a wider range. Optical observation of partons in QSLs will be even more attractive with the language of projective symmetry.

Appendix A Time Reversal Symmetry for Kitaev Model

We define time-reversal operator Θ for Majorana fermions. Spin operator is antisymmetric with respect to Θ:

$$\Theta \boldsymbol{\sigma}_l \Theta^{-1} = -\boldsymbol{\sigma}_l. \tag{A.1}$$

Then, time-reversal operation for Majorana fermions and bond operators are expressed by

$$\Theta c_l \Theta^{-1} = c_l, \quad \Theta \eta_l^\lambda \Theta^{-1} = \eta_l^\lambda, \tag{A.2}$$

$$\Theta \hat{u}_{<l,l'>_\lambda} \Theta^{-1} = \Theta i \eta_l^\lambda \eta_{l'}^\lambda \Theta^{-1} = -i \eta_l^\lambda \eta_{l'}^\lambda = -\hat{u}_{<l,l'>_\lambda}. \tag{A.3}$$

On the other hand,

$$\Theta \hat{W}_p \Theta^{-1} = \begin{cases} \hat{W}_p & : \text{for even-sided polygons,} \\ -\hat{W}_p & : \text{for odd-sided polygons.} \end{cases} \tag{A.4}$$

U(1) gauge fluxes $\hat{W}_p \equiv e^{i\Phi_p}$ of odd-sided polygons inverse under time reversal operation. Although the spin Hamiltonian is time-reversal symmetric, that is,

$$\begin{aligned} \Theta \mathscr{H} \Theta^{-1} &= \sum_{\lambda=x,y,z} \sum_{<m,n>_\lambda} J_\lambda \Theta \sigma_m^\lambda \sigma_n^\lambda \Theta^{-1} = \sum_{\lambda=x,y,z} \sum_{<m,n>_\lambda} J_\lambda \Theta \sigma_m^\lambda \Theta^{-1} \Theta \sigma_n^\lambda \Theta^{-1} \\ &= \sum_{\lambda=x,y,z} \sum_{<m,n>_\lambda} J_\lambda (-\sigma_m^\lambda)(-\sigma_n^\lambda) = \sum_{\lambda=x,y,z} \sum_{<m,n>_\lambda} J_\lambda \sigma_m^\lambda \sigma_n^\lambda = \mathscr{H}, \end{aligned} \tag{A.5}$$

flux states may be changes under the time-reversal operation.

Including the empty set, let $\{W_p\}_{(\mathrm{e})}$ and $\{W_p\}_{(\mathrm{o})}$ be the set of eigenvalues of even-sided and odd-sided polygons, respectively. Assuming $|\{W_p\}\rangle = |\{W_p\}_{(\mathrm{e})}, \{W_p\}_{(\mathrm{o})}\rangle$ and $E(\{W_p\}) = E(\{W_p\}_{(\mathrm{e})}, \{W_p\}_{(\mathrm{o})})$ are the eigenvectors and eigenvalues of spin Hamiltonian, respectively,

$$\langle \{W_p\} | \mathscr{H} | \{W_p\} \rangle = \langle \{W_p\} | E(\{W_p\}) | \{W_p\} \rangle = E(\{W_p\}). \tag{A.6}$$

Considering time-reversal symmetry of spin Hamiltonian [Eq. (A.5)],

$$\begin{aligned} E(\{W_p\}) = \langle \{W_p\} | \mathscr{H} | \{W_p\} \rangle &= \langle \{W_p\} | \Theta^{-1} \overbrace{\Theta \mathscr{H} \Theta^{-1}}^{=\mathscr{H}} \Theta | \{W_p\} \rangle = \langle \{W_p\}^{\mathrm{T}} | \mathscr{H} | \{W_p\}^{\mathrm{T}} \rangle \\ &= \langle \{W_p\}^{\mathrm{T}} | E(\{W_p\}^{\mathrm{T}}) | \{W_p\}^{\mathrm{T}} \rangle = E(\{W_p\}^{\mathrm{T}}), \end{aligned} \tag{A.7}$$

$$\therefore \quad E(\{W_p\}_{(\mathrm{e})}, \{W_p\}_{(\mathrm{o})}) = E(\{W_p\}_{(\mathrm{e})}^{\mathrm{T}}, \{W_p\}_{(\mathrm{o})}^{\mathrm{T}}). \tag{A.8}$$

Therefore, the Kitaev model with odd-sided polygons are degenerate with $\{-W_p\}_{(\mathrm{o})}$ for a certain $\{W_p\}_{(\mathrm{o})}$. This degeneracy comes from the spontaneous time-reversal symmetry breaking of the system.

Appendix B Projection Operator Eliminating Unphysical States

We consider $\mathscr{P}_0$ in projection operator. Take a linear combination of original Majorana fermions c_l so that the Hamiltonian is a 2×2 block diagonalized. Using the real symmetric matrix $\mathbf{\Psi}$, c_l and resulting $\tilde{c}_l$ is expressed as follows:

$$[\tilde{c}_1, \tilde{c}_2, \ldots, \tilde{c}_L] = [c_1, c_2, \ldots, c_L]\mathbf{\Psi}, \tag{B.1}$$

$$\tilde{c}_l = \sum_{l'=1}^{L} \psi_{l',l} c_{l'}, \quad c_{l'} = \sum_{l=1}^{L} \psi_{l',l} \tilde{c}_l. \tag{B.2}$$

Considering the $L!$ permutations of c_l,

$$\prod_{l=1}^{L} c_l = \frac{1}{L!} \sum_{P} (-)^P \prod_{l'=1}^{L} c_{P(l')}; \tag{B.3}$$
$$(-)^P = \begin{cases} 1 & \text{even permutation,} \\ -1 & \text{odd permutation.} \end{cases}$$

Assuming L is an even number,

$$\begin{aligned}
\prod_{l=1}^{L} c_l &= \frac{1}{L!} \sum_{P} (-)^P \prod_{l'=1}^{L} c_{P(1)} c_{P(2)} \cdots c_{P(L)} \\
&= \frac{1}{L!} \sum_{P} (-)^P \sum_{l_{P(1)}, l_{P(2)}, \ldots, l_{P(L)}=1}^{L} \psi_{P(1),l_{P(1)}} \psi_{P(2),l_{P(2)}} \cdots \psi_{P(L),l_{P(L)}} \tilde{c}_{l_{P(1)}} \tilde{c}_{l_{P(2)}} \cdots \tilde{c}_{l_{P(L)}} \\
&= \frac{1}{L!} \sum_{P} (-)^P \sum_{l_1, l_2, \ldots, l_L=1}^{L} \psi_{P(1),l_{P(1)}} \psi_{P(2),l_{P(2)}} \cdots \psi_{P(L),l_{P(L)}} \tilde{c}_{l_{P(1)}} \tilde{c}_{l_{P(2)}} \cdots \tilde{c}_{l_{P(L)}} \\
&= \frac{1}{L!} \sum_{P} \epsilon (-)^P \sum_{l_1, l_2, \ldots, l_L=1}^{L} \psi_{1,l_1} \psi_{2,l_2} \cdots \psi_{L,l_L} \tilde{c}_{l_{P(1)}} \tilde{c}_{l_{P(2)}} \cdots \tilde{c}_{l_{P(L)}} \\
&= \frac{1}{L!} \sum_{l_1, l_2, \ldots, l_L=1}^{L} \prod_{m=1}^{L} \psi_{m,l_m} \sum_{P} (-)^P \tilde{c}_{l_{P(1)}} \tilde{c}_{l_{P(2)}} \cdots \tilde{c}_{l_{P(L)}} \\
&= \frac{1}{L!} \sum_{P'} \prod_{k=1}^{L} \psi_{k,P'(k)} \sum_{P} (-)^P \tilde{c}_{P'[P(1)]} \tilde{c}_{P'[P(2)]} \cdots \tilde{c}_{P'[P(L)]} \\
&= \frac{1}{L!} \sum_{P} \sum_{P'} \prod_{k=1}^{L} \psi_{k,P'(k)} (-)^{P'} \tilde{c}_1 \tilde{c}_2 \cdots \tilde{c}_L \\
&= \sum_{P'} (-)^{P'} \prod_{k=1}^{L} \psi_{k,P'(k)} \tilde{c}_1 \tilde{c}_2 \cdots \tilde{c}_L = \det(\mathbf{\Psi}) \prod_{l=1}^{L} \tilde{c}_l = \det(\mathbf{\Psi}) \prod_{k=1}^{L/2} \tilde{c}_{2k-1} \tilde{c}_{2k}.
\end{aligned} \tag{B.4}$$

We rewrite $\tilde{c}_l$ to quasi-particle α_k,

$$\alpha_k = \frac{1}{2}\left(\tilde{c}_{2k-1} + i\tilde{c}_{2k}\right), \quad \alpha_k^\dagger = \frac{1}{2}\left(\tilde{c}_{2k-1} - i\tilde{c}_{2k}\right), \tag{B.5}$$

$$\tilde{c}_{2k-1} = \alpha_k + \alpha_k^\dagger, \quad \tilde{c}_{2k} = -i(\alpha_k - i\alpha_k^\dagger), \tag{B.6}$$

$$\tilde{c}_{2k-1}\tilde{c}_{2k} = -i(\alpha_k + \alpha_k^\dagger)(\alpha_k - i\alpha_k^\dagger) = i(1 - 2\alpha_k^\dagger\alpha_k), \tag{B.7}$$

and then,

$$\prod_{l=1}^{L} c_l = \det(\mathbf{\Psi}) i^{L/2} \prod_{k=1}^{N}(1 - 2\alpha_k^\dagger\alpha_k). \tag{B.8}$$

Next, we consider

$$\prod_{l=1}^{L} \hat{D}_l = \eta_1^x\eta_1^y\eta_1^z c_1 \eta_2^x\eta_2^y\eta_2^z c_2 \cdots \eta_L^x\eta_L^y\eta_L^z c_L. \tag{B.9}$$

We first move c_l to the right,

$$\begin{aligned}
&\eta_1^x\eta_1^y\eta_1^z c_1 \cdots \eta_{L-2}^x\eta_{L-2}^y\eta_{L-2}^z c_{L-2}\eta_{L-1}^x\eta_{L-1}^y\eta_{L-1}^z c_{L-1}\eta_L^x\eta_L^y\eta_L^z c_L \\
&\quad = (-1)^3\eta_1^x\eta_1^y\eta_1^z c_1 \cdots \eta_{L-2}^x\eta_{L-2}^y\eta_{L-2}^z c_{L-2}\eta_{L-1}^x\eta_{L-1}^y\eta_{L-1}^z\eta_L^x\eta_L^y\eta_L^z c_{L-1}c_L \\
&\quad = (-1)^{3+3}\eta_1^x\eta_1^y\eta_1^z c_1 \cdots \eta_{L-2}^x\eta_{L-2}^y\eta_{L-2}^z\eta_{L-1}^x\eta_{L-1}^y\eta_{L-1}^z\eta_L^x\eta_L^y\eta_L^z c_{L-2}c_{L-1}c_L \\
&\quad = \cdots = (-1)^{\phi_1}\eta_1^x\eta_1^y\eta_1^z \cdots \eta_{L-2}^x\eta_{L-2}^y\eta_{L-2}^z\eta_{L-1}^x\eta_{L-1}^y\eta_{L-1}^z\eta_L^x\eta_L^y\eta_L^z \prod_{l=1}^{L} c_l \\
&\quad = (-1)^{\phi_1}\prod_{l'=1}^{L}\eta_{l'}^x\eta_1^y\eta_1^z \cdots \eta_{L-2}^y\eta_{L-2}^z\eta_{L-1}^y\eta_{L-1}^z\eta_L^y\eta_L^z \prod_{l=1}^{L} c_l \\
&\quad = (-1)^{\phi_1+1}\prod_{l'=1}^{L}\eta_{l'}^x\eta_1^y\eta_1^z \cdots \eta_{L-2}^y\eta_{L-2}^z\eta_{L-1}^y\eta_L^y\eta_{L-1}^z\eta_L^z \prod_{l=1}^{L} c_l \\
&\quad = (-1)^{\phi_1+1+2}\prod_{l'=1}^{L}\eta_l^x\eta_1^y\eta_1^z \cdots \eta_{L-2}^y\eta_{L-1}^y\eta_L^y\eta_{L-2}^z\eta_{L-1}^z\eta_L^z \prod_{l=1}^{L} c_l \\
&\quad = \cdots = (-1)^{\phi_1+\phi_2}\prod_{l'=1}^{L}\eta_{l'}^x \prod_{l''=1}^{L}\eta_{l''}^y \prod_{l'''=1}^{L}\eta_{l'''}^z \prod_{l=1}^{L} c_l,
\end{aligned} \tag{B.10}$$

$$\phi_1 \equiv \sum_{n=1}^{L-1} 3n = \frac{3}{2}L(L-1), \quad \phi_2 \equiv \sum_{n=1}^{L-1} n = \frac{1}{2}L(L-1) \tag{B.11}$$

$$\therefore \quad \prod_{l=1}^{L}\hat{D}_l = \prod_{l'=1}^{L}\eta_{l'}^x \prod_{l''=1}^{L}\eta_{l''}^y \prod_{l'''=1}^{L}\eta_{l'''}^z \prod_{l=1}^{L} c_l \qquad (\because \phi_1 + \phi_2 = 2m, m \in \mathbb{Z}). \tag{B.12}$$

We sort η_l^λ so that η_l^λ forms $\hat{u}_{<m,n>_\lambda}$. Then, the phase factor $\theta = \pm 1$ is generated depending on the geometric structure of the system. Therefore, $\mathscr{P}_0$ is expressed as follows:

$$\mathscr{P}_0 = \frac{1 + \prod_{l=1}^{L}\hat{D}_l}{2} = \frac{1}{2}\Big[1 + (-)^\theta \det(\mathbf{\Psi}) \prod_{<m,n>_\lambda} \hat{u}_{<m,n>_\lambda} \prod_{k=1}^{N}(1 - 2\alpha_k^\dagger\alpha_k)\Big].$$

The state in which the eigenvalue of $\mathscr{P}_0$ is 0 is a completely unphysical state. The terms $\alpha_k^\dagger \alpha_k$ exclude either even or odd particle excited states as physical states and the other as unphysical states.

We show that the physical Majorana fermion excitation number does not change under the local gauge transformation. Let $\mathbf{\Psi}$ be the matrix that 2×2-block diagonalizes the Hamiltonian:

$$\mathscr{H} = \frac{i}{2} {}^{\mathrm{t}}\boldsymbol{c}\mathcal{H}\boldsymbol{c} = \frac{i}{2} {}^{\mathrm{t}}\boldsymbol{c}\mathbf{\Psi}\,{}^{\mathrm{t}}\mathbf{\Psi}\mathcal{H}\mathbf{\Psi}\,{}^{\mathrm{t}}\mathbf{\Psi}\boldsymbol{c} = \frac{i}{2} {}^{\mathrm{t}}\widetilde{\boldsymbol{c}}\mathcal{E}\widetilde{\boldsymbol{c}}, \tag{B.13}$$

$${}^{\mathrm{t}}\boldsymbol{c} \equiv [c_1, c_2, \ldots, c_{L-1}, c_L]\,, \; {}^{\mathrm{t}}\widetilde{\boldsymbol{c}} \equiv [\tilde{c}_1, \tilde{c}_2, \ldots, \tilde{c}_{L-1}, \tilde{c}_L]\,,$$

$$\mathcal{E} = {}^{\mathrm{t}}\mathbf{\Psi}\mathcal{H}\mathbf{\Psi} = \frac{1}{2}\begin{bmatrix} 0 & \varepsilon_1 & & & \\ -\varepsilon_1 & 0 & & & \\ & & \ddots & & \\ & & & 0 & \varepsilon_{\frac{L}{2}} \\ & & & -\varepsilon_{\frac{L}{2}} & 0 \end{bmatrix} \tag{B.14}$$

If the adjacent sites of site l site are l_1, l_2, l_3, the gauge transformation to the l site is expressed as

$$\Lambda_l = \begin{array}{c} \\ \vdots \\ c_l \\ \vdots \\ c_{l_1} \\ \vdots \\ c_{l_2} \\ \vdots \\ c_{l_3} \\ \vdots \end{array} \begin{array}{c} \begin{array}{ccccccccc} \cdots & c_l & \cdots & c_{l_1} & \cdots & c_{l_2} & \cdots & c_{l_3} & \cdots \end{array} \\ \begin{pmatrix} \cdots & & \cdots & & \cdots & & \cdots & & \cdots \\ \cdots & -1 & \cdots & 0 & \cdots & 0 & \cdots & 0 & \cdots \\ \cdots & 0 & \ddots & 0 & \cdots & 0 & \cdots & 0 & \cdots \\ \cdots & 0 & \cdots & 1 & \cdots & 0 & \cdots & 0 & \cdots \\ \cdots & 0 & \cdots & 0 & \ddots & 0 & \cdots & 0 & \cdots \\ \cdots & 0 & \cdots & 0 & \cdots & 1 & \cdots & 0 & \cdots \\ \cdots & & \cdots & & \cdots & & \ddots & & \cdots \\ \cdots & 0 & \cdots & 0 & \cdots & 0 & \cdots & 1 & \cdots \\ \cdots & & \cdots & & \cdots & & \cdots & & \cdots \end{pmatrix} \end{array} ; {}^{\mathrm{t}}\Lambda_l = \Lambda_l,\ \Lambda_l^2 = \mathbb{1}, \tag{B.15}$$

$$\mathcal{H}' = \Lambda_l \mathcal{H} \Lambda_l, \tag{B.16}$$

$$\mathcal{H} = \begin{array}{c} \\ \vdots \\ c_l \\ \vdots \\ c_{l_1} \\ \vdots \\ c_{l_2} \\ \vdots \\ c_{l_3} \\ \vdots \end{array} \begin{array}{c} \begin{array}{ccccccccc} \cdots & c_l & \cdots & c_{l_1} & \cdots & c_{l_2} & \cdots & c_{l_3} & \cdots \end{array} \\ \begin{pmatrix} \cdots & & \cdots & & \cdots & & \cdots & & \cdots \\ \cdots & 0 & \cdots & H_1 & \cdots & H_2 & \cdots & H_3 & \cdots \\ \cdots & & \cdots & & \cdots & & \cdots & & \cdots \\ \cdots & -H_1 & \cdots & 0 & \cdots & & \cdots & & \cdots \\ \cdots & & \cdots & & \cdots & & \cdots & & \cdots \\ \cdots & -H_2 & \cdots & & \cdots & 0 & \cdots & & \cdots \\ \cdots & & \cdots & & \cdots & & \cdots & & \cdots \\ \cdots & -H_3 & \cdots & & \cdots & & \cdots & 0 & \cdots \\ \cdots & & \cdots & & \cdots & & \cdots & & \cdots \end{pmatrix} \end{array}, \tag{B.17}$$

$$\mathcal{H}' = \begin{array}{c} \\ \vdots \\ c_l \\ \vdots \\ c_{l_1} \\ \vdots \\ c_{l_2} \\ \vdots \\ c_{l_3} \\ \vdots \end{array} \begin{array}{c} \begin{array}{ccccccccc} \cdots & c_l & \cdots & c_{l_1} & \cdots & c_{l_2} & \cdots & c_{l_3} & \cdots \end{array} \\ \begin{pmatrix} \cdots & & \cdots & & \cdots & & \cdots & & \cdots \\ \cdots & 0 & \cdots & -H_1 & \cdots & -H_2 & \cdots & -H_3 & \cdots \\ \cdots & & \cdots & & \cdots & & \cdots & & \cdots \\ \cdots & H_1 & \cdots & 0 & \cdots & & \cdots & & \cdots \\ \cdots & & \cdots & & \cdots & & \cdots & & \cdots \\ \cdots & H_2 & \cdots & & \cdots & 0 & \cdots & & \cdots \\ \cdots & & \cdots & & \cdots & & \cdots & & \cdots \\ \cdots & H_3 & \cdots & & \cdots & & \cdots & 0 & \cdots \\ \cdots & & \cdots & & \cdots & & \cdots & & \cdots \end{pmatrix} \end{array}. \tag{B.18}$$

$\mathcal{H}'$ can be diagonalized by $\mathbf{\Psi}' \equiv \Lambda_l \mathbf{\Psi}$:

$$\begin{aligned}\mathscr{H}' &= \frac{i}{2}{}^{\mathrm{t}}\boldsymbol{c}\mathcal{H}'\boldsymbol{c} = \frac{i}{2}{}^{\mathrm{t}}\boldsymbol{c}\Lambda_l\mathcal{H}\Lambda_l\boldsymbol{c} = \frac{i}{2}\underbrace{{}^{\mathrm{t}}\boldsymbol{c}\mathbf{\Psi}'}_{\equiv{}^{\mathrm{t}}\widetilde{\boldsymbol{c}}'}{}^{\mathrm{t}}\mathbf{\Psi}'\Lambda_l\mathcal{H}\Lambda_l\mathbf{\Psi}'\underbrace{{}^{\mathrm{t}}\mathbf{\Psi}'\boldsymbol{c}}_{\equiv\widetilde{\boldsymbol{c}}'} \\ &= \frac{i}{2}{}^{\mathrm{t}}\widetilde{\boldsymbol{c}}'{}^{\mathrm{t}}\mathbf{\Psi}\underbrace{\Lambda_l\Lambda_l}_{=\mathbb{1}}\mathcal{H}\underbrace{\Lambda_l\Lambda_l}_{=\mathbb{1}}\mathbf{\Psi} = \frac{i}{2}{}^{\mathrm{t}}\widetilde{\boldsymbol{c}}'\underbrace{{}^{\mathrm{t}}\mathbf{\Psi}\mathcal{H}\mathbf{\Psi}}_{=\mathcal{E}}\widetilde{\boldsymbol{c}}' = \frac{i}{2}{}^{\mathrm{t}}\widetilde{\boldsymbol{c}}'\mathcal{E}\widetilde{\boldsymbol{c}}'. \end{aligned} \tag{B.19}$$

Having in mind

$$\det(\mathbf{\Psi}) = -\det(\mathbf{\Psi}'), \tag{B.20}$$

the projection operator changes as follows by the local gauge transformations:

$$\begin{aligned}\mathscr{P}_0 &= \frac{1}{2}\left[1+(-1)^{\theta}\det(\mathbf{\Psi})\prod_{<m,n>_\lambda}u_{<m,n>_\lambda}\prod_{k=1}^{N}(1-2\alpha_k^\dagger\alpha_k)\right] \\ &\overset{\text{local gauge trasformation}}{\longrightarrow} \frac{1}{2}\left[1+(-1)^{\theta}\det(\mathbf{\Psi}')\prod_{<m,n>_\lambda}u'_{<m,n>_\lambda}\prod_{k=1}^{N}(1-2\alpha_k^\dagger\alpha_k)\right] \\ &= \frac{1}{2}\left[1+(-1)^{\theta}(-1)\det(\mathbf{\Psi})(-1)\prod_{<m,n>_\lambda}u_{<m,n>_\lambda}\prod_{k=1}^{N}(1-2\alpha_k^\dagger\alpha_k)\right] \\ &= \frac{1}{2}\left[1+(-1)^{\theta}\det(\mathbf{\Psi})\prod_{<m,n>_\lambda}u_{<m,n>_\lambda}\prod_{k=1}^{N}(1-2\alpha_k^\dagger\alpha_k)\right] = \mathscr{P}_0. \end{aligned} \tag{B.21}$$

Therefore, the projection operator does not change under the gauge transformation, and the number of excited fermions that is unphysical does not change either.

References

[1] A. Kitaev, Ann. Phys. **321**, 2 (2006).

[2] L. Savary and L. Balents, Rep. Prog. Phys. **80**, 016502 (2016).

[3] Y. Zhou, K. Kanoda, and T.-K. Ng, Rev. Mod. Phys. **89**, 025003 (2017).

[4] J. Knolle and R. Moessner, Annu. Rev. Condens. Matter Phys. **10**, 451 (2019).

[5] Y. Motome and J. Nasu, J. Phys. Soc. Jpn. **89**, 012002 (2020).

[6] G. Jackeli and G. Khaliullin, Phys. Rev. Lett. **102**, 017205 (2009).

[7] Y. Singh and P. Gegenwart, Phys. Rev. B **82**, 064412 (2010).

[8] Y. Singh, S. Manni, J. Reuther, T. Berlijn, R. Thomale, W. Ku, S. Trebst, and P. Gegenwart, Phys. Rev. Lett. **108**, 127203 (2012).

[9] K. Kitagawa, T. Takayama, Y. Matsumoto, R. Kato, A. Takano, Y. Kishimoto, S. Bette, R. Dinnebier, G. Jackeli, and H. Takagi, Nature **554**, 341 (2018).

[10] K. W. Plumb, J. P. Clancy, L. J. Sandilands, V. V. Shankar, Y. F. Hu, K. S. Burch, H.-Y. Kee, and Y.-J. Kim, Phys. Rev. B **90**, 041112 (2014).

[11] J. Chaloupka, G. Jackeli, and G. Khaliullin, Phys. Rev. Lett. **105**, 027204 (2010).

[12] J. Chaloupka, G. Jackeli, and G. Khaliullin, Phys. Rev. Lett. **110**, 097204 (2013).

[13] K. Slagle, W. Choi, L. E. Chern, and Y. B. Kim, Phys. Rev. B **97**, 115159 (2018).

[14] H. Tomishige, J. Nasu, and A. Koga, Phys. Rev. B **97**, 094403 (2018).

[15] U. F. P. Seifert, J. Gritsch, E. Wagner, D. G. Joshi, W. Brenig, M. Vojta, and K. P. Schmidt, Phys. Rev. B **98**, 155101 (2018).

[16] H. Tomishige, J. Nasu, and A. Koga, Phys. Rev. B **99**, 174424 (2019).

[17] J. G. Rau, E. K.-H. Lee, and H.-Y. Kee, Phys. Rev. Lett. **112**, 077204 (2014).

[18] V. M. Katukuri, S. Nishimoto, V. Yushankhai, A. Stoyanova, H. Kandpal, S. Choi, R. Coldea, I. Rousochatzakis, L. Hozoi, and J. van den Brink, New Journal of Physics **16**, 013056 (2014).

[19] Y. Yamaji, Y. Nomura, M. Kurita, R. Arita, and M. Imada, Phys. Rev. Lett. **113**, 107201 (2014).

[20] T. Suzuki, T. Yamada, Y. Yamaji, and S. Suga, Phys. Rev. B **92**, 184411 (2015).

[21] Y. Yamaji, T. Suzuki, T. Yamada, S. Suga, N. Kawashima, and M. Imada, Phys. Rev. B **93**, 174425 (2016).

[22] M. Gohlke, G. Wachtel, Y. Yamaji, F. Pollmann, and Y. B. Kim, Phys. Rev. B **97**, 075126 (2018).

[23] J. Knolle, S. Bhattacharjee, and R. Moessner, Phys. Rev. B **97**, 134432 (2018).

[24] J. Knolle, G.-W. Chern, D. L. Kovrizhin, R. Moessner, and N. B. Perkins, Phys. Rev. Lett. **113**, 187201 (2014).

[25] J. Nasu, J. Knolle, D. Kovrizhin, Y. Motome, and R. Moessner, Nat. Phys. **12**, 912 (2016).

[26] B. Perreault, J. Knolle, N. B. Perkins, and F. J. Burnell, Phys. Rev. B **94**, 060408 (2016).

[27] B. Perreault, J. Knolle, N. B. Perkins, and F. J. Burnell, Phys. Rev. B **94**, 104427 (2016).

[28] B. Perreault, S. Rachel, F. J. Burnell, and J. Knolle, Phys. Rev. B **95**, 184429 (2017).

[29] I. Rousochatzakis, S. Kourtis, J. Knolle, R. Moessner, and N. B. Perkins, Phys. Rev. B **100**, 045117 (2019).

[30] S. K. Choi, R. Coldea, A. N. Kolmogorov, T. Lancaster, I. I. Mazin, S. J. Blundell, P. G. Radaelli, Y. Singh, P. Gegenwart, K. R. Choi, S.-W. Cheong, P. J. Baker, C. Stock, and J. Taylor, Phys. Rev. Lett. **108**, 127204 (2012).

[31] A. Banerjee, C. A. Bridges, J.-Q. Yan, A. A. Aczel, L. Li, M. B. Stone, G. E. Granroth, M. D. Lumsden, Y. Yiu, J. Knolle, S. Bhattacharjee, D. L. Kovrizhin, R. Moessner, D. A. Tennant, D. G. Mandrus, and S. E. Nagler, Nat. Mater. **15**, 733 (2016).

[32] A. Banerjee, J. Yan, J. Knolle, C. A. Bridges, M. B. Stone, M. D. Lumsden, D. G. Mandrus, D. A. Tennant, R. Moessner, and S. E. Nagler, Science **356**, 1055 (2017).

[33] S.-H. Do, S.-Y. Park, J. Yoshitake, J. Nasu, Y. Motome, Y. Kwon, D. T. Adroja, D. J. Voneshen, K. Kim, T.-H. Jang, J.-H. Park, K.-Y. Choi, and S. Ji, Nat. Phys. **13**, 1079 (2017).

[34] L. J. Sandilands, Y. Tian, K. W. Plumb, Y.-J. Kim, and K. S. Burch, Phys. Rev. Lett. **114**, 147201 (2015).

[35] S. Yamamoto and T. Kimura, Journal of Physics: Conference Series **1220**, 012003 (2019).

[36] T. Takayama, A. Kato, R. Dinnebier, J. Nuss, H. Kono, L. S. I. Veiga, G. Fabbris, D. Haskel, and H. Takagi, Phys. Rev. Lett. **114**, 077202 (2015).

[37] K. A. Modic, T. E. Smidt, I. Kimchi, N. P. Breznay, A. Biffin, S. Choi, R. D. Johnson, R. Coldea, P. Watkins-Curry, G. T. McCandless, J. Y. Chan, F. Gandara, Z. Islam, A. Vishwanath, A. Shekhter, R. D. McDonald, and J. G. Analytis, Nat. Commun **5**, 4203 (2014).

[38] S. Mandal and N. Surendran, Phys. Rev. B **79**, 024426 (2009).

[39] J. Nasu, M. Udagawa, and Y. Motome, Phys. Rev. Lett. **113**, 197205 (2014).

[40] I. Kimchi, J. G. Analytis, and A. Vishwanath, Phys. Rev. B **90**, 205126 (2014).

[41] M. Hermanns and S. Trebst, Phys. Rev. B **89**, 235102 (2014).

[42] K. O'Brien, M. Hermanns, and S. Trebst, Phys. Rev. B **93**, 085101 (2016).

[43] Y. Kato, Y. Kamiya, J. Nasu, and Y. Motome, Phys. Rev. B **96**, 174409 (2017).

[44] A. Smith, J. Knolle, D. L. Kovrizhin, J. T. Chalker, and R. Moessner, Phys. Rev. B **93**, 235146 (2016).

[45] K. Suzuki and S. Yamamoto, Journal of Physics: Conference Series **1220**, 012046 (2019).

[46] M. Thakurathi, K. Sengupta, and D. Sen, Phys. Rev. B **89**, 235434 (2014).

[47] W. DeGottardi, D. Sen, and S. Vishveshwara, New Journal of Physics **13**, 065028 (2011).

[48] F. L. Pedrocchi, S. Chesi, S. Gangadharaiah, and D. Loss, Phys. Rev. B **86**, 205412 (2012).

[49] P. Mellado, O. Petrova, and O. Tchernyshyov, Phys. Rev. B **91**, 041103(R) (2015).

[50] X.-G. Wen, Phys. Rev. B **65**, 165113 (2002).

[51] F. Wang and A. Vishwanath, Phys. Rev. B **74**, 174423 (2006).

[52] P. A. Fleury and R. Loudon, Phys. Rev. **166**, 514 (1968).

[53] B. S. Shastry and B. I. Shraiman, Phys. Rev. Lett. **65**, 1068 (1990).

[54] B. S. Shastry and B. I. Shraiman, Int. J. Mod. Phys. B **05**, 365 (1991).

[55] H. Yao and S. A. Kivelson, Phys. Rev. Lett. **99**, 247203 (2007).

[56] O. Petrova, P. Mellado, and O. Tchernyshyov, Phys. Rev. B **90**, 134404 (2014).

[57] H. Yao, S.-C. Zhang, and S. A. Kivelson, Phys. Rev. Lett. **102**, 217202 (2009).

[58] F. L. Pedrocchi, S. Chesi, and D. Loss, Phys. Rev. B **84**, 165414 (2011).

[59] F. Zschocke and M. Vojta, Phys. Rev. B **92**, 014403 (2015).

[60] M. Udagawa, Phys. Rev. B **98**, 220404(R) (2018).

[61] H. Yao and X.-L. Qi, Phys. Rev. Lett. **105**, 080501 (2010).

[62] M. Dresselhaus, G. Dresselhaus, and A. Jorio, *Group Theory: Application to the Physics of Condensed Matter* (Springer Berlin Heidelberg, 2007).

[63] T. P. Devereaux and R. Hackl, Rev. Mod. Phys. **79**, 175 (2007).

[64] O. Cépas, J. O. Haerter, and C. Lhuillier, Phys. Rev. B **77**, 172406 (2008).

[65] B. Perreault, J. Knolle, N. B. Perkins, and F. J. Burnell, Phys. Rev. B **92**, 094439 (2015).

[66] W.-H. Ko, Z.-X. Liu, T.-K. Ng, and P. A. Lee, Phys. Rev. B **81**, 024414 (2010).

[67] N. Perkins and W. Brenig, Phys. Rev. B **77**, 174412 (2008).

[68] J. Knolle, D. L. Kovrizhin, J. T. Chalker, and R. Moessner, Phys. Rev. Lett. **112**, 207203 (2014).

[69] J. Knolle, D. L. Kovrizhin, J. T. Chalker, and R. Moessner, Phys. Rev. B **92**, 115127 (2015).

[70] A. Trautman, *Clifford Analysis and Its Applications* (Springer Netherlands, 2001), Nato Science Series II.

[71] J. Nasu, M. Udagawa, and Y. Motome, Phys. Rev. B **92**, 115122 (2015).

[72] S. Yamamoto and T. Kimura, J. Phys. Soc. Jpn. **89**, 063701 (2020).

[73] S. Yamamoto, Phys. Rev. B **63**, 125124 (2001).